TÉCNICO LISBOA

Optimisation of Ground Stations Location in Aeronautical Multilateration Systems

Ana Cláudia Miranda Ferreira de Castro

Thesis to obtain the Master of Science Degree in

Electrical and Computer Engineering

Supervisor: Prof. Luís Manuel de Jesus Sousa Correia

Examination Committee

Chairperson: Prof. José Eduardo Charters Ribeiro da Cunha Sanguino

Supervisor: Prof. Luís Manuel de Jesus Sousa Correia

Members of Committee: Prof. António Manuel Restani Graça Alves Moreira

Eng. André Maia

April 2016

To my family

Acknowledgements

First of all, I would like to thank Prof. Luís M. Correia, my thesis supervisor, for the opportunity to write this thesis and also for all the advices and shared knowledge in our weekly meetings. His supervision had a substantial role in the work developed in this thesis, because without it I would not had acquired the work ethics, the work methods and the discipline necessary to complete this thesis.

To the engineers from NAV Portugal, namely Eng. Luís Pissarro, Eng. Carlos Alves and Eng. André Maia, a special thank you to all. From the regular meetings to the emails exchanged, their input and feedback were valuable to the developing of this thesis.

I would also like to thank all the GROW members, particularly my master´s thesis colleagues and friends Carlos Martins, João Pires, Miguel Sá and Ricardo Gameiro for all the support they showed during this journey. They all contribute to make this a one of a kind experience.

To all my friends that follow me on this journey, that listen to my problems and were a part of my everyday doubts, a very special thank you, for all the support that you all gave me during this time.

And finally, I would want to thank my family, for their emotional support, understanding and patience, because there were times when I just needed to shift things and look at a problem in a new perspective and my father, my mother, my brother and my sister were all there to make me stop thinking so hard and light things up.

Thank you all for believing in me.

Abstract

The main goal of this thesis is to analyse the performance of the current multilateration systems installed in Portugal, by NAV Portugal, and to establish a set of recommendations for the future multilateration systems implementations. These goals were accomplished by the development and implementation of a set of models and algorithms: difference between WAM and ADS-B routes, analysis and dimensioning algorithm and selection algorithm. In order to achieve the intended analysis several simulations on different scenarios were performed, which were the Lisbon, Azores and Porto airports. From the analysis of the simulation results, it is possible to conclude that the WAM systems installed in the Lisbon and Azores regions perform according to the parameters set by the system´s manufactures, that is, for example when analysing the difference between WAM and ADS-B routes, for the Lisbon scenario under a 30 NM radius, the error is under 100 m and for the Azores scenario under a 100 NM radius the error is under 300 m. And finally, that the airplane´s position error decreases as the airplane navigates towards the ground stations.

Keywords

Surveillance, Multilateration, WAM System, ADS-B System, Ground Stations.

Resumo

O principal objetivo desta tese passa por analisar o desempenho dos sistemas de Multilateração atualmente instalados em Portugal, pela NAV Portugal, e por estabelecer um conjunto de recomendações para os futuros sistemas a serem implementados. Estes objetivos foram alcançados através do desenvolvimento e implementação de um conjunto de vários modelos e algoritmos: diferença existente entre as rotas WAM e ADS-B, algoritmo de análise e dimensionamento e algoritmo de seleção. A fim de alcançar a análise pretendida, várias simulações foram realizadas em diferentes cenários, dos quais fazem parte os aeroportos de Lisboa, Açores e Porto. A partir da análise dos resultados das simulações, foi possível concluir que os sistemas WAM instalados nas regiões de Lisboa e Açores cumprem os parâmetros que os fabricantes do sistema impuseram, ou seja, por exemplo quando se analisa a diferença entre as rotas WAM e ADS-B, da região de Lisboa num raio de 30 m.n. o erro do sistema assume valores abaixo de 100 m e quando se realiza a mesma análise, mas para a região dos Açores, num raio de 100 m.n. o erro do sistema é abaixo de 300m. E finalmente, é possível concluir também que à medida que o avião se aproxima dos sensores, o erro associado à posição do avião diminui.

Palavras-chave

Vigilância, Multilateração, Sistema WAM, Sistema ADS-B, Sensores.

Table of Contents

Acknowledgements v

Abstract vii

Resumo viii

Table of Contents ix

List of Figures xi

List of Tables xiii

List of Acronyms xiv

List of Symbols xvi

List of Software xviii

1 Introduction 1

1.1 Overview 2

1.2 Motivation and Contents 6

2 Basic Concepts 7

2.1 Radars 8

2.2 Multilateration system 11

2.3 Spatial and temporal resolution 14

2.4 State of the art 17

3 Model Development and Implementation 21

3.1. Model Development 22

3.1.1 Determination of the airplane´s position 22

3.1.2 Error in the determination of the airplane´s position 22

3.1.3 Difference between WAM and ADS-B routes 25

3.2 Algorithm Development 26

3.2.1 Initial considerations 26

3.2.2 Difference between WAM and ADS-B routes 28

3.2.3 Analysis and System Dimensioning Algorithm 28
3.2.4 Selection Algorithm 31
3.3 Model Implementation 31
3.3.1Main Simulator Structure 31
3.3.2 Maximum error of an airplane position simulator 33
3.4 Model Assessment 36
4 Analysis of Results 39
4.1 Scenarios Description 40
4.1.1 Initial Considerations 40
4.1.2 Lisbon Region Scenario 40
4.1.3 Azores Region Scenario 42
4.1.4 Porto Region Scenario 44
4.2 Difference between WAM and ADS-B routes analysis 44
4.3 Set of ground stations 51
4.4 Error analysis 54
4.5 Porto analysis 61
5 Conclusions 65
References 69

List of Figures

Figure 1.1 - Flight evolution (extracted from [Euro13]). 2
Figure 1.2 - Surveillance systems evolution (extracted from [Euro07]). 3
Figure 1.3 - MLAT presence worldwide (extracted from [Era10]). 4
Figure 1.4 - Cost benefit assessment (extracted from [Era10]). 4
Figure 1.5 - MLAT versus radar on accuracy (extracted from [Era10]). 5
Figure 1.6 - MLAT and radar coverage comparison (extracted from [Era10]). 5
Figure 2.1 - Primary surveillance radar (extracted from [ICAO07a]). 8
Figure 2.2 - Secondary surveillance radar (extracted from [ICAO07a]). 9
Figure 2.3 - ADS-B (extracted from [ICAO07a]). 10
Figure 2.4 - TOA data flow (extracted from [Nev05]). 12
Figure 2.5 - MLAT hyperbola intersection (extracted from [Air07]). 13
Figure 2.6 - Common clock system architecture (extracted from [Nev05]). 14
Figure 2.7 - Distributed clock system architecture (extracted from [Nev05]). 15
Figure 2.8 - Baseline and line of sight (extracted from [Nev05]). 15
Figure 3.1 - TDOA algorithm (extracted from [Sie07]). 23
Figure 3.2 – Airplane inside the uncertainty area (extracted from [Gav15]). 26
Figure 3.3 – Distance between a line and a point. 27
Figure 3.4 – Main structure of Scenario 1 analysis. 27
Figure 3.5 – Main structure of Scenario 2 analysis. 27
Figure 3.6 – Difference between WAM and ADS-B routes. 28
Figure 3.7 – Analysis – information loading. 29
Figure 3.8 – System dimensioning – hyperbola building. 30
Figure 3.9 – Selection of the ground stations. 32
Figure 3.10 – Main structure of the simulator. 32
Figure 3.11 – Detailed main structure. 34
Figure 3.12 – Hyperbolas intersection in a 3 ground stations scenario (extracted from [Air07]). 35
Figure 4.1 – Lisbon WAM ground stations locations (extracted from [Google Earth]). 41
Figure 4.2 – WAM and ADS-B routes for Lisbon scenario. 41
Figure 4.3 - Azores WAM ground stations locations. 43
Figure 4.4 - WAM and ADS-B routes for Azores scenario. 44
Figure 4.5 – Porto WAM ground stations locations (extracted from [Google Earth]). 46
Figure 4.6 – Porto ADS-B route and ground stations. 46
Figure 4.7 – Difference between WAM (blue) and ADS-B (red) routes. 47
Figure 4.8 – Difference between WAM and ADS-B routes for Lisbon. 47
Figure 4.9 - Difference between WAM and ADS-B routes for Azores. 48
Figure 4.10 - Normalised number of measurements fitted with normal distribution for the Azores scenario. 49
Figure 4.11 – Normalised number of measurements fitted with an exponential distribution for the Lisbon scenario. 50
Figure 4.12 - Normalised number of measurements fitted with an exponential distribution for the Azores scenario. 51

Figure 4.13 – Number ground stations used throughout Lisbon route. 52
Figure 4.14 – Number of ground stations versus distance between airplane and reference ground station, Lisbon scenario. 53
Figure 4.15 - Number ground stations used throughout Azores route. 54
Figure 4.16 - Number of ground stations versus distance between airplane and reference ground station, Azores scenario. 55
Figure 4.17 – Selection of ground stations for one route position, Lisbon. 56
Figure 4.18 – Ground stations selected to determine the airplane's position, Lisbon. 56
Figure 4.19 – Hyperbolas intersection with error equal to zero. 57
Figure 4.20 – Uncertainty area. 57
Figure 4.21 – Comparison of results applying different error values, 25 m (blue) and 52 m (red), for the Lisbon scenario. 58
Figure 4.22 – Lisbon simulation results with error at 25 m. 59
Figure 4.23 - Azores simulation results with error at 25 m. 59
Figure 4.24 – Lisbon results with error equal 25 m. 60
Figure 4.25 - Azores results with error equal 25 m. 60
Figure 4.26 – Minimum error associated with each airplane's position. 62
Figure 4.27 – Number of ground stations that provide the minimum error. 63
Figure 4.28 – Comparison of results regarding the maximum and minimum error associated with each airplane's position. 63
Figure 4.29 - Number of ground stations that provide the maximum error. 64

List of Tables

Table 2.1 - Assumptions for WAM system (extracted from [Nev05]). 16
Table 2.2 - Requirements for en-route applications (extracted from [Nev05]). 16
Table 2.3 - Detection requirements (extracted from [Nev05]). 17
Table 2.4 - Quality requirements (extracted from [Nev05]). 17
Table 3.1 – Summary of the WAM errors (extracted from [Err06]). 24
Table 3.2 - Header for WAM routes. 36
Table 3.3 - Header for ADS-B route. 36
Table 3.4 - Header for ground stations. 36
Table 4.1 – Lisbon WAM ground stations description. 40
Table 4.2 - Azores WAM ground stations description. 42
Table 4.3 – Porto ground stations description. 45
Table 4.4 - Comparison between Normal and Exponential distributions. 48
Table 4.5 – Goodness-of-fit parameters for Lisbon and Azores. 50
Table 4.6 - Goodness-of-fit parameters for the error analysis with error equal to 25 m. 61
Table 4.7 – Combinations of ground stations chosen. 62

List of Acronyms

A-SMGCS	Advanced Surface Movement Guidance and Control Systems
ADS	Automatic Dependent Surveillance
ADS-B	Automatic Dependent Surveillance – Broadcast
ADS-C	Automatic Dependent Surveillance – Contract
ANSP	Air Navigation Service Provider
AoA	Angle of Arrival
ATC	Air Traffic Control
ATM	Air Traffic Management
CPS	Central Processing Station
CRLB	Cramer-Rao Lower Bound
ECAC	European Civil Aviation Conference
EU	European Union
Eurocontrol	European Organisation for Safety of Air Navigation
FDOA	Frequency Difference of Arrival
GDOP	Geometric Dilution of Precision
GNSS	Global Navigation Satellite System
GPS	Global Positioning System
GS	Ground Station
HDOP	Horizontal Dilution of Precision
HPA	Horizontal Position Accuracy
ICAO	International Civil Aviation Organisation
IFR	Instrument Flight Rules
LAM	Local Area Multilateration
LoS	Line of Sight
MLAT	Multilateration
NAV, Portugal	Navegação Aérea de Portugal
PDF	Probability Density Function
PoD	Probability of Detection
PSR	Primary Surveillance Radar
RMS	Root Mean Squared
RMSE	Root Mean Squared Error
RTD	Round-Trip Delay
RU	Remote Unit
SSR	Secondary Surveillance Radar

TDOA	Time Difference of Arrival
TDOP	Time Dilution of Precision
TOA	Time of Arrival
TLS	Target Level of Safety
UTM	Universal Transverse Mercator
VDOP	Vertical Dilution of Precision
WAM	Wide Area Multilateration

List of Symbols

γ_{GDOP}	Precision and accuracy MLAT system parameter
Δt_{time}	Maximum timing error
Δt_{clock}	Maximum clock jitter error
Δt_{quant}	Quantisation error
Δt_{dig}	Digitisation error
Δt_{sync}	Synchronisation error
$\sqrt{\overline{\varepsilon^2}}$	Root mean squared error
λ	Rate parameter
μ_y	Average of the observations of variable y
σ_{TDOA}	RMS TDOA accuracy
σ_{xyz}	RMS of the airplane position accuracy
c	Speed of light
d	Distance between a point and a line
D_i	Distance between the ground station and the airplane
i	Index of sensor
k	Number of distinct elements in a combination
m	Number of ground stations that are closer to the airplane
n	Number of observations
$n_{i,1}$	Quantified error

n_{gs}	Number of ground stations
N	Normalised number of measurements
$N_{intersect}$	Number of intersections
N_{choos}	Number of vertices
P_{targ}	Airplane position
Q_m	Coordinates of the point *m* from the ADS-B route that above the airplane position
Q_{m+1}	Coordinates of the point *m+1* from the ADS-B route that above the airplane position
R^2	Coefficient of Determination
S	Set of ground stations
t	Time when the airplane sent a signal
t_i	Time when the sensor receive the signal
T_m	New target position
x	Value of the samples
y_i	Observation i
$\widehat{y_i}$	Estimated or predicted value of y_i
(x, y, z)	Cartesian coordinate of the airplane position
(x_i, y_i, z_i)	Cartesian coordinate of the ground stations
(x_1, y_1)	Cartesian coordinate of point *P*
(x_n, y_n)	Cartesian coordinate of point Q_m
(x_{n+1}, y_{n+1})	Cartesian coordinate of point Q_{m+1}

List of Software

Google Earth	Geographical information system
Inkscape	Vector graphics and images editor
Matlab r2013b	Matlab development environment
Microsoft Excel 2010	Spreadsheet application
Microsoft Word 2010	Word processor
Microsoft Power Point 2010	Presentation application
Paint	Image editing software

Chapter 1

Introduction

This chapter gives a brief overview of the work. It includes the scope and motivations that make this work, and the subject in analysis. The structure and organisation of the work is presented at the end of this chapter.

1.1 Overview

The goal to any new project is to make it work, and then make it work well, meaning that the first concern is effectiveness and the second efficiency. And like any other airplanes' project, specifically airplanes' surveillance systems followed this same path/procedure. First airplanes were put in the air, and then airlines were created and after that, a giant business was generated, from luggage security control to air-ground surveillance.

Since the moment that Humankind put the first airplanes in the air the necessity of a system that could ensure the security of everything and everyone involved in this huge operation was created. From this situation arose the concept of monitoring the big areas (air-ground area) where airplanes circulate, the initial surveillance system came from this concept.

Airplanes are considered the safest mode of transportation. In 2013, 9.6 million flights were made in the air space of the European Organisation for Safety of Air Navigation (Eurocontrol), European Union (EU) & European Civil Aviation Conference (ECAC) member states [Euro13]. In Portugal, the average number of flights is 1 564 flights/day [Euro13]. These numbers combined with the information regarding the forecast on daily flights, in Figure 1.1, show that the air space traffic is increasing, and therefore the ANSPs (Air Navigation Service Providers), who are responsible for the safety in the skies, need to have surveillance systems that are capable of managing this growing trend. Even though the traffic of airplanes in the air is not like the one that exists on the ground with cars, there is a real need to know with precision the position of each airplane.

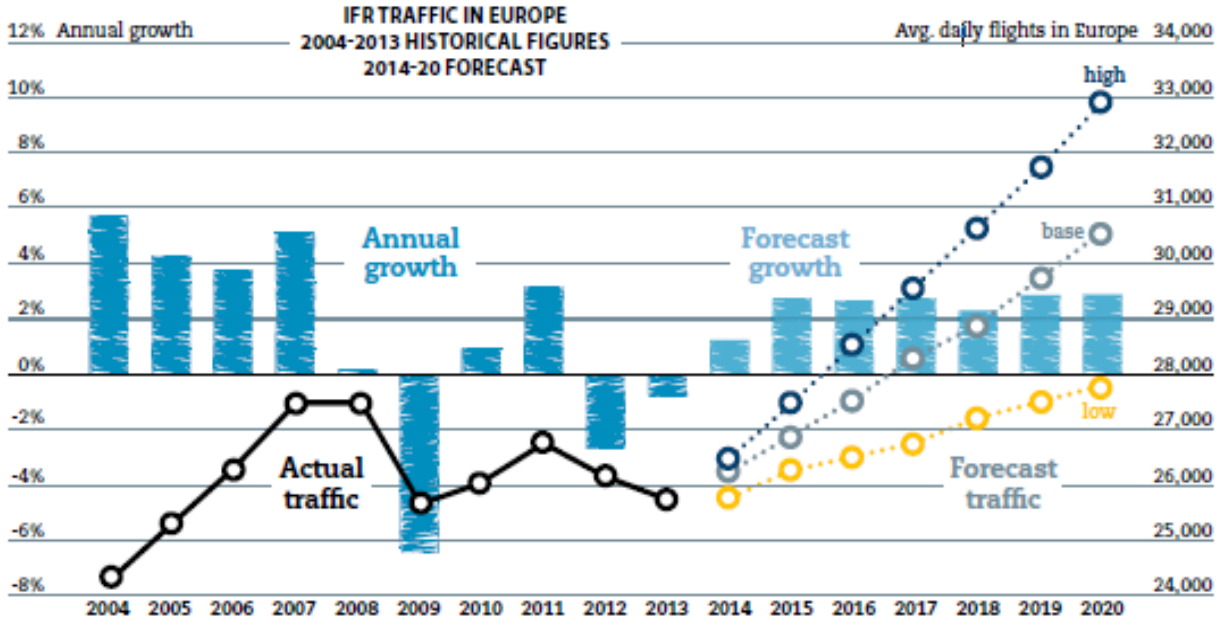

Figure 1.1 - Flight evolution (extracted from [Euro13]).

In Portugal, NAV is one of the responsible entities for ensuring the safety of each flight. NAV being the Portuguese air traffic controller, its main focus is to know the airplane position at every second, accurately, and with a minimum error.

To support the Air Traffic Control (ATC) work, there are several surveillance technologies available, which have been divided in categories by Eurocontrol [Euro07]:

- Independent non-cooperative surveillance: to track non-cooperative targets. This surveillance is provided by Primary Surveillance Radars (PSRs).
- Independent cooperative surveillance: to track cooperative targets. The first surveillance system of this category is the Secondary Surveillance Radar (SSR), which include Multilateration (MLAT), a recent technology. Both these systems work by sending messages and working in cooperation with ground stations, and through this calculate the airplane's position.
- Dependent cooperative surveillance: this category is based on Automatic Dependent Surveillance (ADS). In this type of systems, the airplane´s location is obtained without ground stations interaction.

In Figure 1.2, it is clear which are the surveillance systems that are currently used, or that will be used in the next years. This shows that even "old fashion" systems, like PSR, still work and are still relevant, and that an investment in new technologies, MLAT and ADS, is being done.

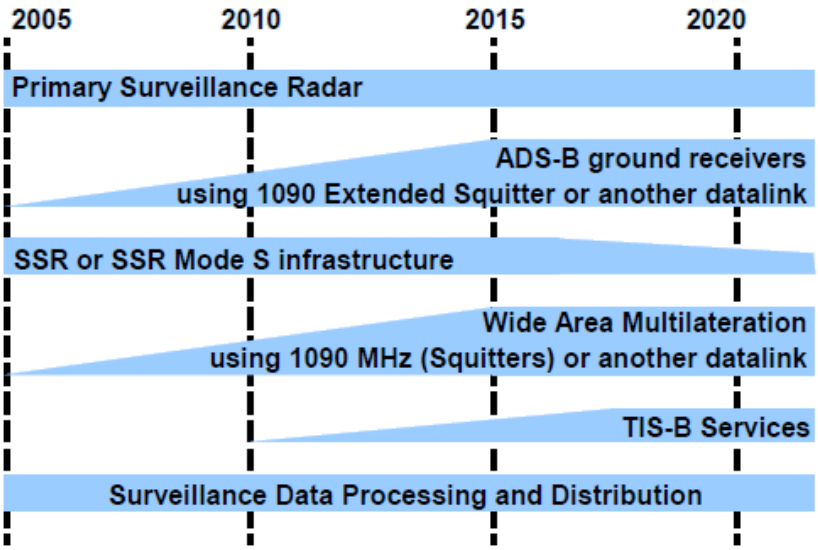

Figure 1.2 - Surveillance systems evolution (extracted from [Euro07]).

The focus of this thesis is on one specific type of surveillance system, the MLAT, which fits into the independent cooperative system category. MLAT, like all the others surveillance systems already mentioned, are discussed in detail in Chapter 2. With MLAT, it is possible to have an accurate 3D location of an airplane.

Nowadays, in order to be a relevant surveillance system, it is necessary to meet a set of requirements. The system has to provide an estimation of the position, altitude of the airplane, and identify it. An air-ground surveillance system is characterised by coverage volume, accuracy, integrity, update rate, reliability and availability [ICAO07]. According to Eurocontrol [Euro07], ANSPs should choose their surveillance systems based on operational requirements, cost benefit assessment, and safety assessment. The MLAT system is accurate, efficient, cheap (comparing with "common" radars), safe, and has a large coverage. With these set of characteristics, MLAT is nowadays the surveillance

system that is being used and implemented all over the world, Figure 1.3.

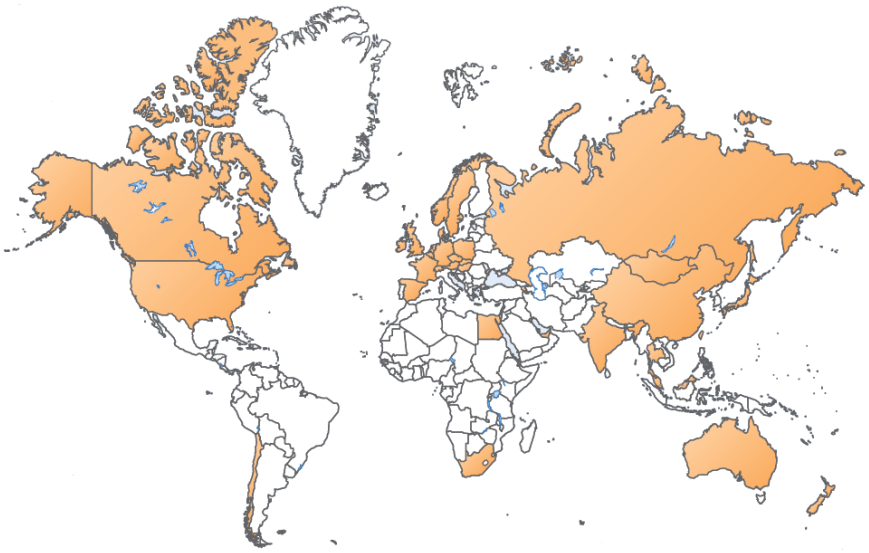

Figure 1.3 - MLAT presence worldwide (extracted from [Era10]).

According to Figure 1.3, Portugal is considered as non-user of MLAT, but in Lisbon and Santa Maria (Azores) airports, this technology has already been implemented, since 2010.

Initially, the MLAT system was developed for military purposes, but soon it became clear that it would be beneficial to adapt this technology to civil aviation applications, particularly to monitor the movements of the airplane at the airport's surface. In major airports spread all over the world, the use of MLAT technology in A-SMGCS (Advanced Surface Movement Guidance and Control Systems) installations is visible, Figure 1.3, because MLAT covers large areas, identifies airplanes and vehicles, and its system performance is not affected by weather changes.

MLAT is a very attractive system with various benefits. In terms of costs, it is safe to say that MLAT systems are a better solution. From a study provided by ERA [Era10] (ERA is a surveillance system manufacturer),when comparing radar with MLAT, the MLAT system has lower costs regarding equipment, power supply and backup, installation (planning and tests) and maintenance, in Figure 1.4.

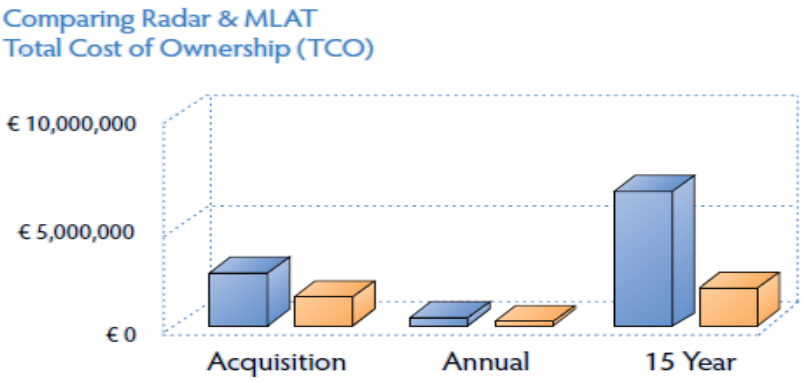

Radar	€ 2,500,000	€ 270,757	€ 6,561,355
MLAT	€ 1,250,000	€ 50,000	€ 2,000,000

Figure 1.4 - Cost benefit assessment (extracted from [Era10]).

Although the cost benefits assessment is relevant, MLAT also outperforms radars on range, accuracy, Figure 1.5, and coverage (aerial and horizontal) and safety, Figure 1.6. Even when one of the sites is non-working (i.e., site outage) the MLAT system is able to remain completely operational and without any coverage degradation.

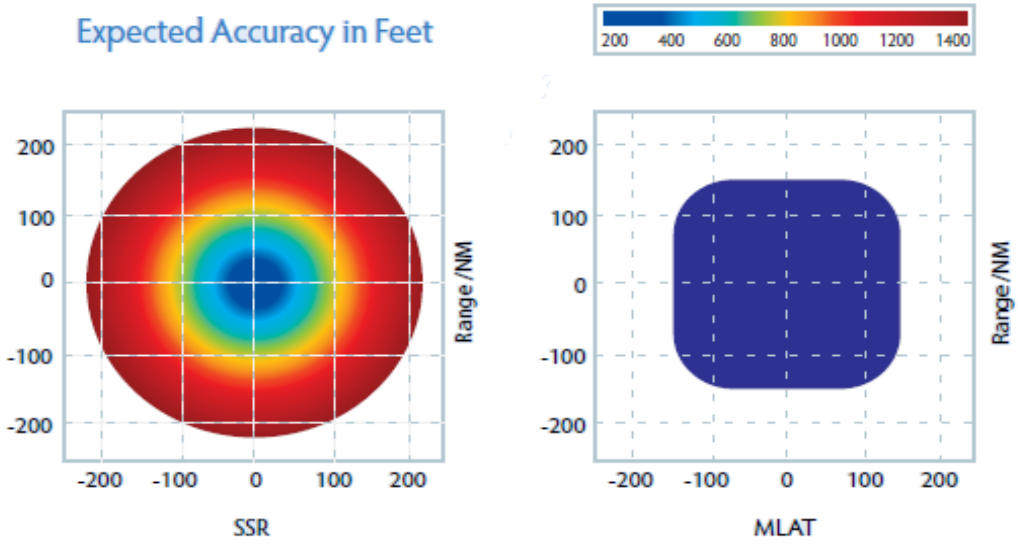

Figure 1.5 - MLAT versus radar on accuracy (extracted from [Era10]).

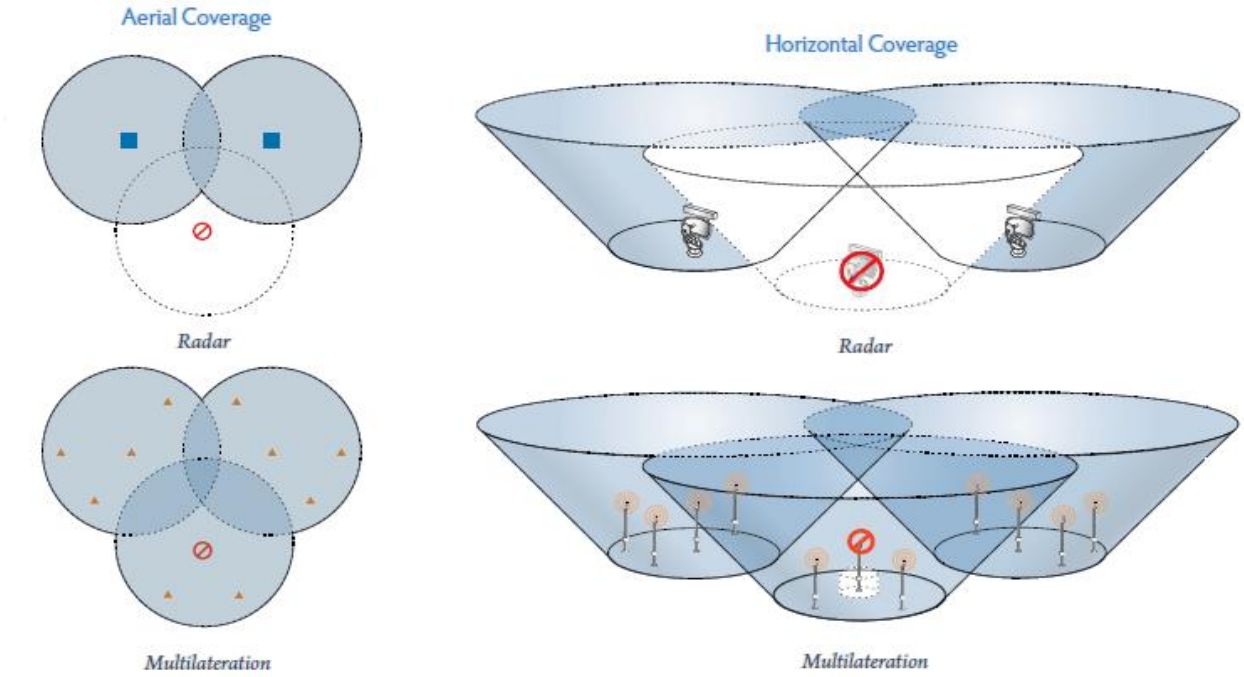

Figure 1.6 - MLAT and radar coverage comparison (extracted from [Era10]).

Multilateration systems enable the location of an airplane based on the TDOA (Time Difference of Arrival) method, which are the main focus of study in this thesis. In order to provide and calculate the airplane's location, ground stations (i.e., sensors) are spread throughout airport´s areas to enable total air traffic surveillance. The main goal of this thesis is to achieve the optimal number and location of

ground stations, in order to supply the angular and spatial resolution required to obtain the airplane's location. The work in this thesis aims to be relevant on future implementations of multilateration systems in Portugal.

1.2 Motivation and Contents

The idea of a safer and more reliable air surveillance system is behind the motivation for this thesis. The present work is focused on assessing the performance of the MLAT systems installed by NAV in Portugal. In order to achieve the goal of this thesis, several steps were taken. An assessment of the multilateration systems installed by NAV was done, implying a study of the basic aspects of MLAT systems, an analysis of the current systems performance, an optimisation of the ground stations' location, and recommendations for future implementations. These final recommendations result in a proposal that translates into the set of ground stations to be used in order to implement a WAM (Wide Area Multilateration) system and generate a minimum error associated with the airplane's position.

The work presented in this thesis is the result of a direct collaboration with NAV Portugal E.P.E., which resulted in providing all the information necessary to accomplish the goals of this thesis, and a close follow up of its progress.

This thesis is composed of 5 chapters being structured in the following way:

- Chapter 1 – Introduction.
- Chapter 2 – Basic concepts on the existing surveillance systems, description of the MLAT system, and state of the art in MLAT sensor location.
- Chapter 3 – The theoretical equations that are the basis of the TDOA algorithm are described, and the models and algorithms that were developed are presented. Algorithms were developed to calculate the difference between WAM and ADS-B (Automatic Dependent Surveillance – Broadcast) routes, to load all the information needed to build the hyperbolas, and to build the hyperbolas themselves. A detailed description of the developed simulator is presented. Finally an assessment of the simulator is done in order to validate the implemented models.
- Chapter 4 – The different scenarios under analysis are described, and the simulator output results are presented as well as their analysis. To conclude, recommendations for a future WAM installation are made.
- Chapter 5 – Conclusions of the thesis are presented, together with a summary of the results obtained in the simulations, followed by recommendations for future work on ground stations' location.

Chapter 2

Basic Concepts

This chapter presents an overview of the basic theoretical concepts to understand the surveillance systems used in traffic control, with focus on multilateration systems. To conclude, this chapter presents the state of the art on this technology.

2.1 Radars

Surveillance systems are necessary for air traffic control, being then possible to detect and send information about the airplane's position, identification, and altitude. Initially, these systems were mainly composed of primary and secondary radars, but now, with new technologies available, such as multilateration (MLAT), there are new and highly reliable systems, although complex and expensive [Era10].

The first air space surveillance system used basic radar, because it allows the detection of distant objects (i.e., airplanes), being named Primary Surveillance Radar (PSR), Figure 2.1. PSR is a radar that works with an echo, which simply detects objects, in our case airplanes, without any particular specificity. In terms of energy, these radars have very high levels of consumption, and there is a possibility that the received signal can be lost.

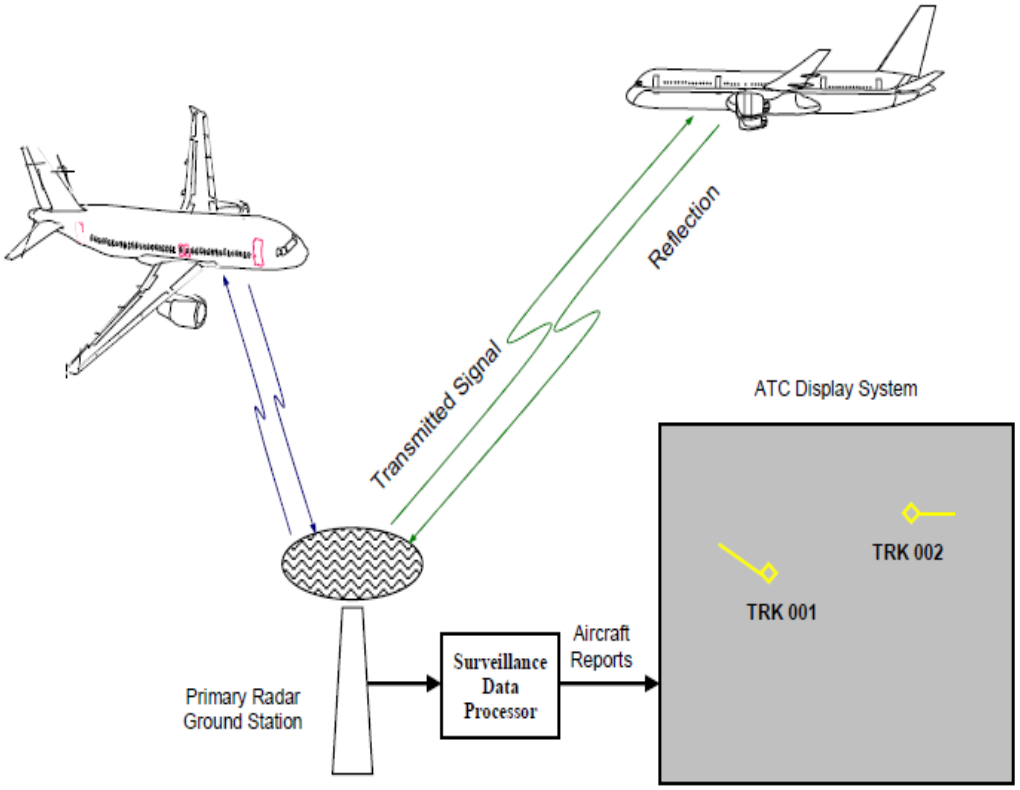

Figure 2.1 - Primary surveillance radar (extracted from [ICAO07a]).

The main goal of PSR systems is to ensure the airplane's landing and taking-off. These systems can only detect and position the airplane. Like any other system, the PSR has advantages and limitations. On the one hand, there is not one single object in the air space that can be invisible to the 'eyes' of air traffic controllers, and in addition no other equipment is necessary, hence, it is only needed one site per installation and the infrastructure costs are low. On the other hand, it has its cons, since it cannot

provide the airplane's identification, and because it uses an echo, it has a limited range and can only work in Line of Sight (LoS), so no installation in mountainous areas is possible.

In order to overcome the limitations of PSR, regarding costs, reliability and performance, the Secondary Surveillance Radar (SSR) was created, Figure 2.2. With the SSR it is possible to exchange information between the airplanes and the ground station in large surveillance areas, and to detect the position of a particular airplane (altitude and identification).

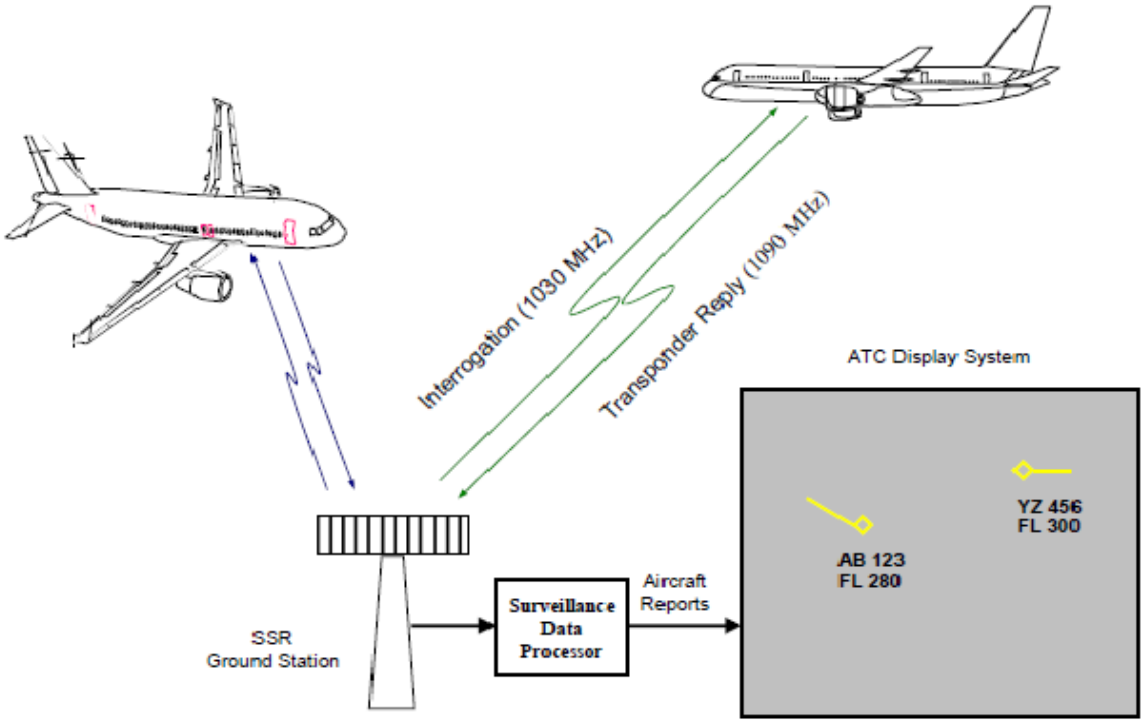

Figure 2.2 - Secondary surveillance radar (extracted from [ICAO07a]).

As PSR, the SSR provides airplanes' landing and taking-off surveillance, but also in en-route (in the air). One of the things that the PSR does not need, and that is vital to SSR, is a transponder on-board the airplane. The SSR system is composed by radar that operates on the ground and a transponder that goes on-board the airplane. The communication between radar (on the ground) and the transponder (at the airplane) works based on queries and replies that are coded. The radar interrogates the airplane's transponder at 1 030 MHz, which triggers the transponder on-board to reply at 1 090 MHz with the airplane's identification and altitude. It is important to refer that the airplane's position is not known by the same interrogation/reply process. This last information is obtained by the airplane itself by calculating the turnaround time from the radar to the airplane, in other words, by measuring the time difference between the interrogation and the transponder reply message. By knowing the airplane´s position, identification, and altitude, it is possible for the air traffic control system to have the airplane's position.

The transponder sends reply messages in 2 modes, A and C codes, depending on the coded signal. It is possible to extract the airplane's identification (from mode A) and pressure altitude information (from mode C) from the different replies received [Nev05].

Although modes A and C give different information about the airplane (identification and altitude, respectively), both modes have the same problem, i.e., they are replies to the radar interrogation. In other words, in order for the air traffic control system to know the airplane's position, the ground station (radar) has to send an interrogation message and the airplane has to reply.

In order to minimise this problem, the SSR mode S (Select) was developed, which can select interrogations. With mode S, one can detect and identify the airplane (already possible with modes A and C), but because its message is longer than modes A and C, one can have more information about the airplane, such as flight status, airplane's address and velocity.

Although not fully implemented (i.e., implementation expected between 2020 and 2025) the Automatic Dependent Surveillance (ADS) will be the surveillance system for the near future. In ADS, unlike the previous discussed methods, there is no need for interrogations and replies, because the airplane itself can determinate its position using the navigation system on-board. ADS is a satellite-based technology, and there are two different modes of using this type of surveillance, ADS-Contract (ADS-C) and ADS-Broadcast (ADS-B). ADS-C works by using the airplane´s navigation system and determines its position, velocity, and meteorological data, but as the name indicates, it works by contract. This technology is used in areas (e.g., mountainous or oceanic areas) where the use of radar is not possible, because it has no range. But it is the ADS-B that is used in complement to MLAT systems; in this case, the airplane has to have a Global Positioning System (GPS) receiver on-board, since it is used to obtain the airplane's position, Figure 2.3.

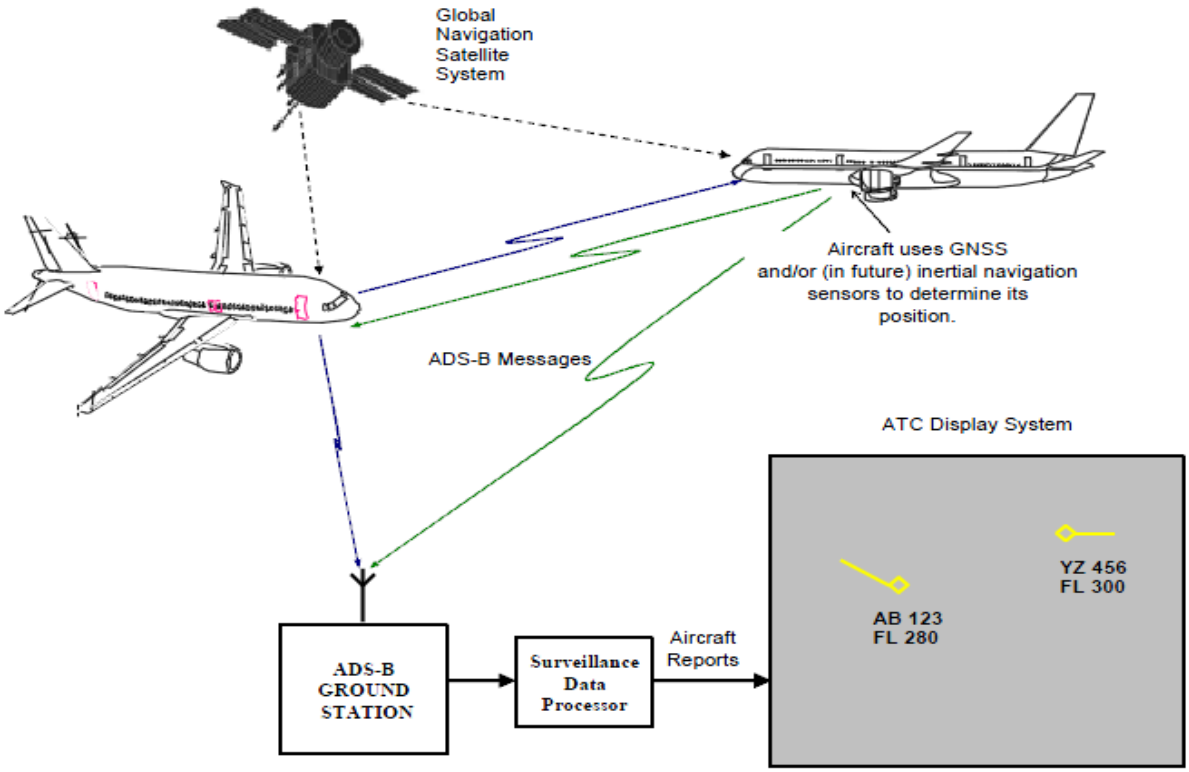

Figure 2.3 - ADS-B (extracted from [ICAO07a]).

The ADS-B has a very high update rate, good resolution, high accuracy, and overall low cost of installation.

To sum up, the SSR has a superior performance compared with PSR. With SSR, it is possible to have a very accurate location of the airplane, to cover bigger areas, and SSR is less sensitive to interferences [Air15]. Although SSR brings many advantages, it cannot provide ground surveillance and the requirements of latency and update rate need to be improved. Improvements have been done, and currently one uses Multilateration systems. The MLAT systems do everything that the SSR does with a plus, one can know the exact location of an airplane.

2.2 Multilateration system

MLAT is basically a set of sensors that are displaced in a certain way, in order to obtain an airplane's position and identification. This information is generated by the signals that are produced by the transponders and by the use of time difference of arrival (TDOA) techniques. This way, one can track airplanes in a very accurate form.

MLAT provides surveillance for modes A/C, mode S and ADS-B. There are two types of MLAT systems, LAM (local area multilateration) and WAM (wide area multilateration), which basically differ on the sensors coverage area. LAM is more appropriate to airplanes and vehicles surveillance at the airport area, while WAM has a wide area system, i.e., the sensors are widely spread in order to ensure the coverage area. They also differ in the number of antennas necessary to install and their location, which are consequences of the difference in the size of the coverage areas. Since the SSR has a wide coverage area, the most suitable choice to replace this one is the WAM system.

MLAT is based on TDOA, which analyses the airplane's received signal and the sensors' received signals. A different number of sensors lead to different accuracy results. The number of sensors cannot be less than 3, because with 3 sensors one has the object's two-dimensional location, i.e., the target would have to be on the ground. In order to have the target's three-dimensional location, one needs 4 or more sensors, enabling to know where the target is in the air. But with 4 sensors, one can only determine the location of one airplane at the same time (which in real life is unpractical, since one needs to know the position of various airplanes at the same time, and this makes the problem a very complex one), and it also creates a number of problems, such as synchronisation of the received times and precision of processed times. Hence, in real life, the number of sensors has to be larger than 4 in order to have a reliable system, a larger precision and the total coverage of the intended area.

There are different methods to calculate TDOA and to have the sensors synchronised. There are two options for these systems, cross correlation and Time of Arrival (TOA). The former can be used with any signal and the TDOA is calculated through the cross-correlation between signals; in the latter, the process is the same as the SSR transponder, the time of arrival being measured in waveforms

signals. TOA systems are the most used in multilateration, so only this method is described in what follows.

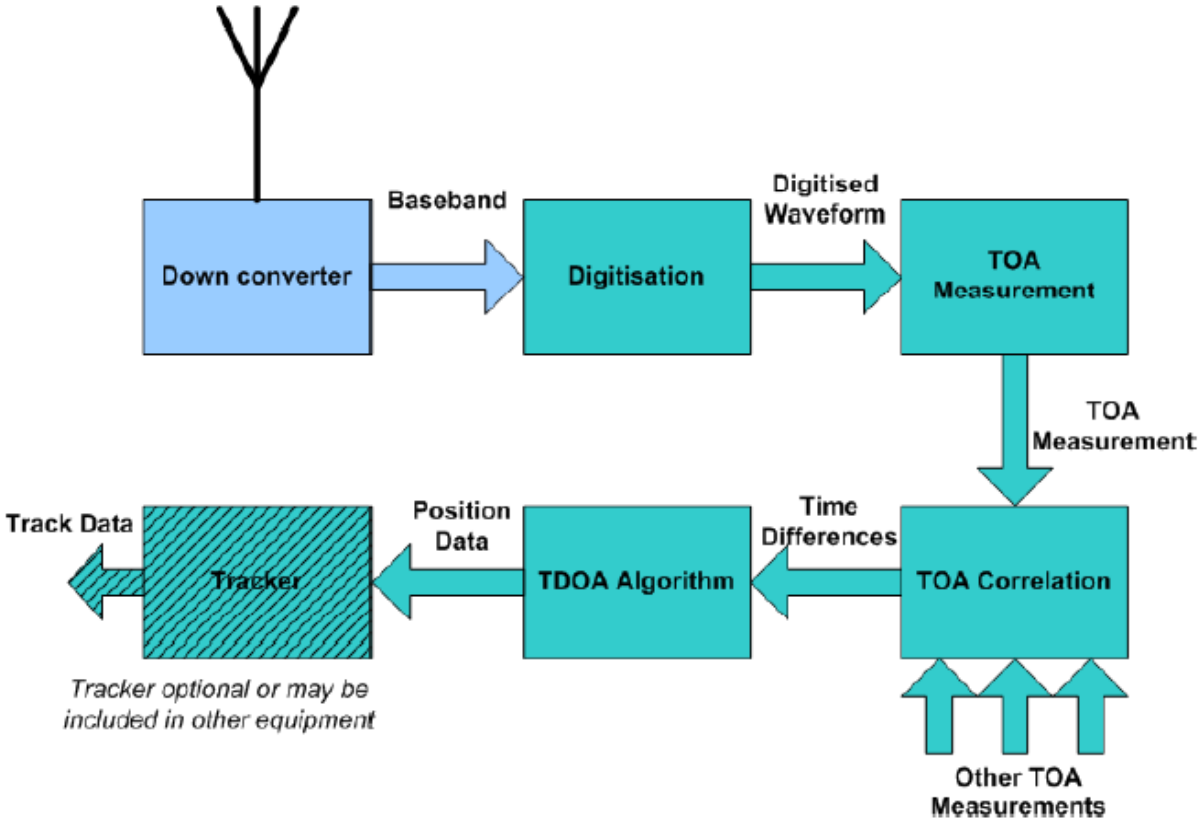

Figure 2.4 - TOA data flow (extracted from [Nev05]).

In Figure 2.4, the TOA process is explained, the different elements being:

- Down Converter: converts radio-frequency to a baseband signal.
- Digitisation: the baseband signal is digitised.
- TOA measurement: every message gets a time associated with it.
- TOA correlation: the time differences from the signals are calculated.
- TDOA algorithm: processing of the time differences to achieve the airplane's position.
- Tracker: provides to the ATC team the update on the airplane's position through *xyz* plots.

The concept behind the TDOA algorithm relies on knowing the time of arrival of a signal. The position of the airplane is calculated by measuring the TOA of the signal between the airplane´s transponder and the ground stations spread throughout the ground. Each of the signals is processed by the TDOA algorithm, being transformed into a hyperbola, and the intersection of all these hyperbolas provides the target's location, Figure 2.5.

There are different methods used on sensors' synchronisation, which can be common clock or distributed clock systems. This synchronisation is necessary, because when the signals arrive from the different sensors, and are then transformed into time differences, they are time stamped during the digitisation process. But in this process there are delays, which can compromise the accuracy of this technology, so to prevent this situation, synchronisation techniques are implemented.

In common clock systems, the digitisation occurs at the central site, which means that there is no need to synchronise each of the sensors. This technology uses a simple receiver, putting most of the complexity in the central multilateration processor, Figure 2.6. When there is an analogue link, as this link distance increases, the delay of the system also increases. So in order to minimise the link distances the multilateration processor is usually at the centre of the system.

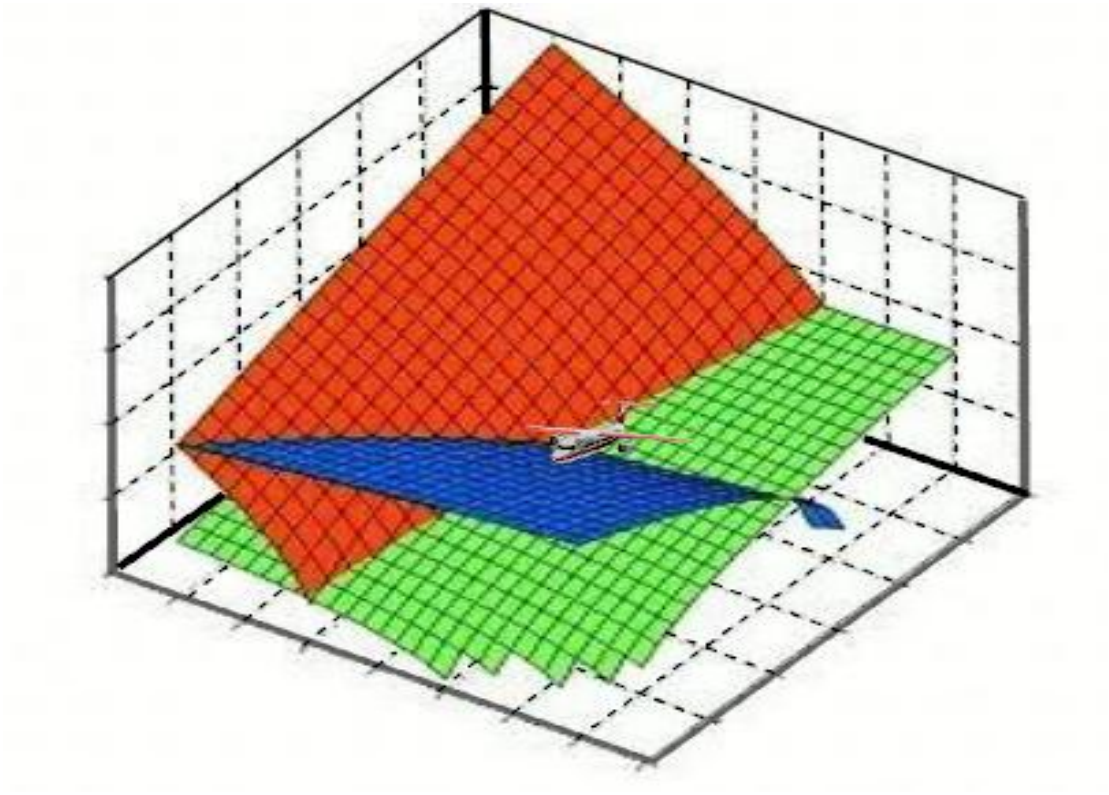

Figure 2.5 - MLAT hyperbola intersection (extracted from [Air07]).

Distributed clock systems have a different architecture, compared with common clock ones. In these systems, a local clock is applied to each of the digitisations, and the TOA measurement block increases the complexity of the system, Figure 2.7. The signal is converted to baseband, and then suffers a digitisation followed by the TOA measurement. This technique provides the needed flexibility in situations where there are high delay values. Each sensor has its own local clock, and its synchronisation is achieved by using the following methods:

- Transponder synchronised systems.
- GNSS (Global Navigation Satellite System) synchronised systems: standalone and common view GNSS synchronisation.

All these methods have their own characteristics regarding accuracy, baseline distances, link choices, and if they provide or not line of sight. Therefore, each of the existing manufacturers has deployed the method that best suits their needs.

2.3 Spatial and temporal resolution

In MLAT systems, the baseline (i.e., distance between adjacent sites) of sensors is directly related to the minimum height that enables the communications between airplane and ground stations. The maximum baseline between sensors is calculated by the sensors horizon reach. As said earlier, one needs 4 or more sensors [Air07].

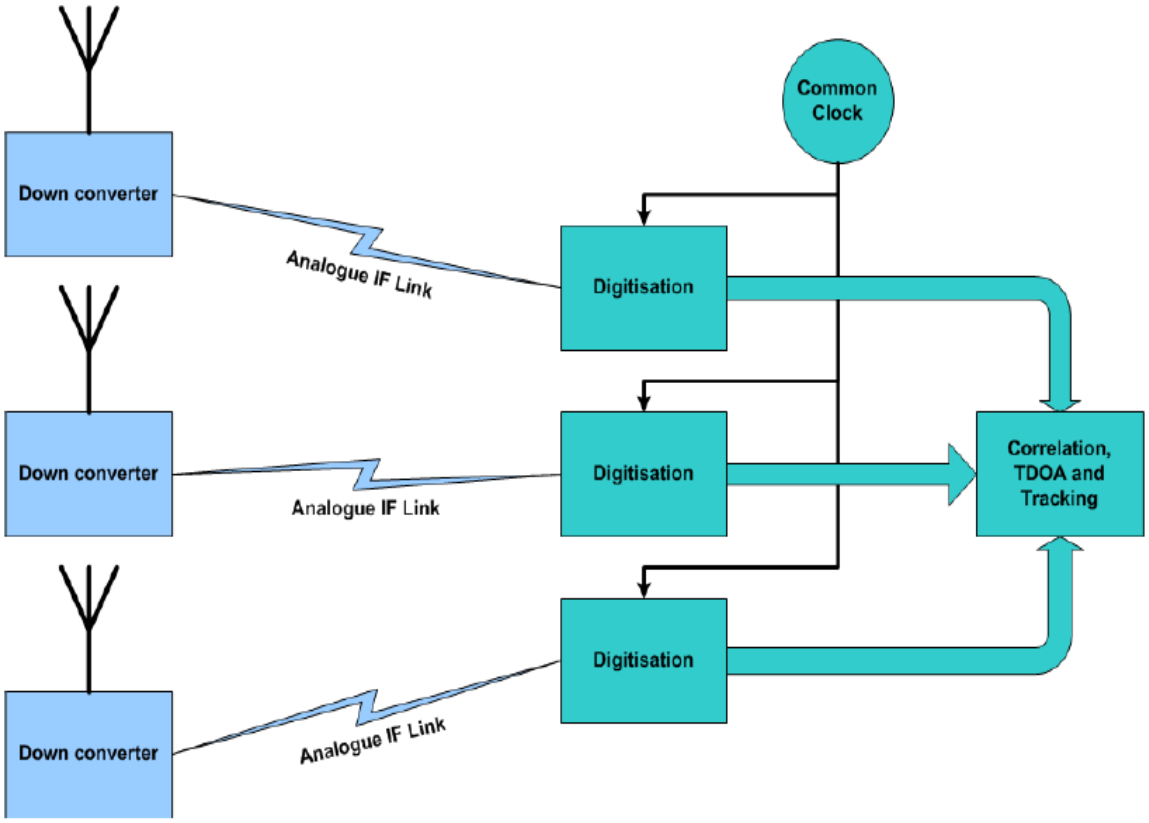

Figure 2.6 - Common clock system architecture (extracted from [Nev05]).

In Figure 2.8, one shows the impact that the Earth's curvature has on the target's visibility. It represents a scenario where the flat terrain model [Corr13] is considered, and, as expected, sensors are on the ground. This scenario represents a situation in which Rx0 and Rx2 are able to see the target, but Rx1 is not, from which it is possible to conclude that *"The wider the receiver baseline of a multilateration system, the worse the low level coverage of the system will be"* [Nev05].

In a 4 sensors configuration, the baselines are of 10 to 20 NM (1 NM = 1.852 km), but these values enable a low coverage level. One of the goals of this thesis is to cover large areas, so Geometric Dilution of Precision (GDOP), γ_{GDOP}, must be taken into account, which is a parameter that is related to precision and accuracy, being expressed by:

$$\sigma_{xyz} = \gamma_{GDOP} \cdot \sigma_{TDOA} \tag{2.1}$$

where:

- σ_{xyz}: RMS of the airplane's position accuracy.
- σ_{TDOA}: RMS TDOA accuracy.

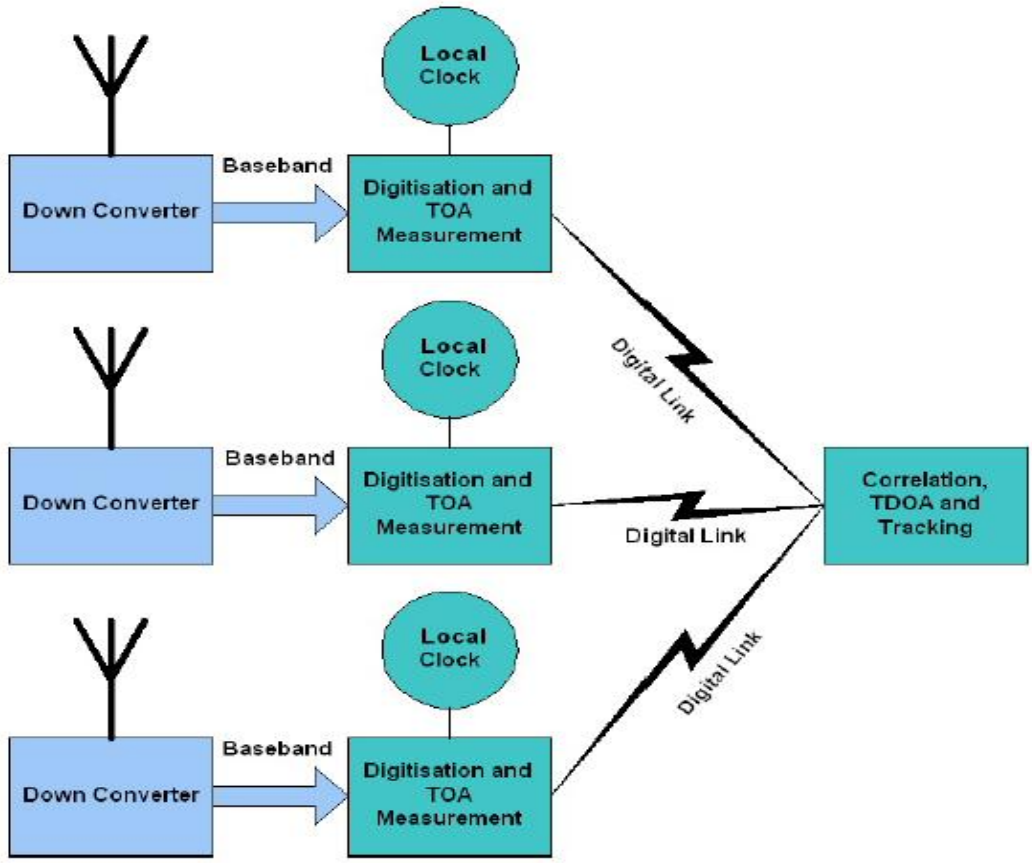

Figure 2.7 - Distributed clock system architecture (extracted from [Nev05]).

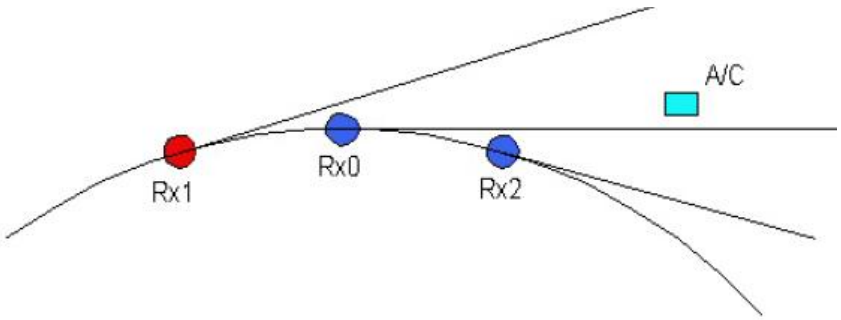

Figure 2.8 - Baseline and line of sight (extracted from [Nev05]).

GDOP is a complex parameter that varies with the target's position, being split into several components, [Nev05]:

- TDOP: Time dilution of precision.
- HDOP: Horizontal dilution of precision.
- VDOP: Vertical dilution of precision.

In WAM systems, accuracy varies with the airplane´s distance to the sensors, because the height impacts on the results, hence it is expected that for en-route and terminal area cases, system performance is different. This thesis addresses the requirements of an en-route scenario.

In Table 2.1, same assumptions for WAM systems performance are made. The presented parameters are used to calculate σ_{TDOA}, in order to determine accuracy. All these parameters, at same level, affect the performance (coverage and accuracy) of the system.

Table 2.1 - Assumptions for WAM system (extracted from [Nev05]).

Parameter	Value
Sensitivity	-85 dBm
Reply Rate Factor	2.5
Antenna	dB systems DME antenna with 3° squint
Bandwidth	22 MHz
Transmit Power	24 dBW
Synchronisation Accuracy	1 ns

In en-route applications, communications between airplane and sensor occur at more than 25 000 feet with large lateral and vertical accuracies, and the baseline of the sensors can vary between to 30 and 60 NM.

In order to provide en-route surveillance, like any other surveillance system, it is necessary to have the same basic requirements. These requirements are not static, and vary according to the Target Level of Safety (TLS), meaning that for a certain range of sensor separation, the error changes, Table 2.2. For example, for a 5 NM sensor separation, the position error standard deviation at 160 NM must be less than 344 m, and the mean of errors in the tail must be less than 836 m.

Table 2.2 - Requirements for en-route applications (extracted from [Nev05]).

Criterion	2 NM	3 NM	5 NM	10 NM
Less than 1% of errors may be greater than:	0.08°	0.12°	0.20°	0.40°
The tail is defined as starting at: (less than 0.03% of errors may be in the tail and they must have a negative exponential or faster-decaying form).	0.16°	0.24°	0.40°	0.80°
The mean of errors in the tail (see previous criterion) must be less than:	0.22°	0.33°	0.55°	1.10°

The requirements used on WAM have similarities to the ones used for the SSR surveillance radar. In order to have a reliable surveillance system, this has to follow a set of requirements that cover detection and quality. These requirements are in detailed in Tables 2.3 and 2.4, respectively.

In Table 2.3, the detection requirements are summarised. These requirements focus on target's

position detection, false target reports, code detection, and sources for multiple target reports (i.e., from reflection, sidelobes, and splits).

Table 2.3 - Detection requirements (extracted from [Nev05]).

Detection requirements	
Probability of detection	> 97%
False target report ratio	< 0.1%
Mode A probability of detection	> 98%
Mode C probability of detection	> 96%

In Table 2.4, the analysed requirements are regarding the quality of the system and certain related parameters, such as time stamp error and false codes ratio.

Table 2.4 - Quality requirements (extracted from [Nev05]).

Quality requirements					
Systematic errors		Random errors		False code information	
Slant range bias	< 100 m	Slant range	< 70 m	False mode A code	< 0.1%
Azimuth bias	< 0.1°	Azimuth	< 0.08°	False mode C code	< 0.1%
Slant range gain error	< 1 m/NM				
Time stamp error	< 100 ms				

2.4 State of the art

This last section presents the research and the state of the art in the subject of this thesis. Although Multilateration is a topic with several areas of study, this thesis focuses on sensors arrangement and on improving system accuracy, in order to reduce the uncertainty of the area in which the target can be in.

In [Sta13], methods were developed to test the implementation and results of a WAM system. The results addressed, mainly, the probability of target detection and data latency analysis. The work presents the dependencies of performance requirements when trying to optimise the system, such as, the minimisation of data latency may decrease the Probability of Target Detection (PoD) and/or Horizontal Position Accuracy (HPA), and the maximisation of PoD may increase the false target rate and/or decrease the HPA.

Another important factor when optimising a WAM system is the surrounding radio environment, due to the amount and type of traffic, and its distribution within the coverage volume. The amount and type of existing surveillance infrastructure, and the specific topography of the area, need to be considered to

accomplish a system that achieves the expected performance [Sta13]. Tests were made in order to evaluate data latency and the probability of target detection, and a dependency between these two requirements was found. Although the probability of target detection was above the required threshold of 97%, the authors strongly suggest that for future work in this type of testing, it is necessary to standardise the test approach for the WAM and ADS-B sensors, and to implement and qualify test tools for these sensors too.

In order to improve the accuracy of WAM systems, the authors in [Gal08] propose the analysis and application of the Cramer-Rao Lower Bound (CRLB) to determinate the theoretical system accuracy. In this analysis, a combination of different measurements is experimented, such as, differential Doppler frequency, elevation angle AOA (angle of arrival) and round-trip delay (RTD). CRLB is used as an analysis method for the accuracy of the position estimation using different measurements, and is used to calculate the theoretical system accuracy; with this method, it is possible to estimate the best case (or lower bound) when calculating the accuracy of the target position. CRLB is applied in the WAM configuration of the Malpensa airport, and it is evaluated for five different situations. After the different testing, the CRLB analysis enables the comparison of different MLAT algorithms combinations. The tests show good results and good performance for the combination TDOA + RTD at large distances (i.e., this was the combination that presented the lower percentage of error); because this combination is adaptable for large distances, it could be a good fit for the WAM system configuration. For future work, it is suggested to include evaluations with the FDOA (Frequency Difference of Arrival) and mitigation of conditioning problems.

In [Man11], the location problem in MLAT is explored. This study shows an improvement in the accuracy and convergence of the system by applying the Tikhonov method in the iterative procedure of the Taylor-series expansion.

In [Kon08], the authors analyse the multilateration system deployed at Boryspil Airport in Kiev, Ukraine. To achieve the most optimum sensor configuration, in order to obtain the maximum accuracy in localising the targets, several simulation schemes and different target positions were analysed. Three steps were taken into account in order to achieve the sensor configuration that will meet the system requirements: first, any MLAT system has to provide a high accuracy when targeting the airplane, independently of weather conditions and airport's location; second, the accuracy of measured coordinates depends on the MLAT system geometry; finally, factors such as multipath signal propagation, large buildings, and airport capacity, affect the number and the placement of receiver units (sensors). These three considerations are part of the pillars of the current thesis.

[Kon08] also studies the error associated with remote units (RUs) groups, allowing to exclude some RUs, because if an RU exceeds the threshold it can mean that the RU is not in line of sight to the target, and so this RU may produce corrupted results, hence, being excluded. It is concluded that the localisation of a target depends on the geometry of the MLAT system and on the target's position, meaning that the uncertainty of the target's position increases when the target moves outside the area covered by the sensor. The authors claim that these results allow installing an MLAT system in an optimal way in an airport area.

In [Aue14], the implementation of a WAM system is analysed, with a total 61 sensors spread throughout Austria. This paper describes the challenges found in the implementation of this system on an operational and technical level. Upon 2013, the Austrian WAM system configuration was one of the most complex in the world, having 61 sensors all connected to one single central processing station (CPS). Although this system brought many benefits, such as the reduction of surveillance costs and a type of surveillance that is adaptable to the type of topography existing in Austria, an overall better performance and a capability of expansion was necessary. This system was designed to have an accuracy of 50 m or a probability of detection of 99%, to process about 2 000 targets. The main focus of the paper is on the integration of the WAM system in the Austrian airspace, and the challenge behind this massive project was to work this new technology and protocols, mainly the lack of experience in projects like this one and in combining these sensors within operational ATM (Air Traffic Management) systems.

Most of the tests and improvements accomplished in the MLAT system, for LAM and WAM scenarios, were realised and achieved by MLAT manufactures (e.g., ERA and Sensis Corporation [Nev05]) and the Eurocontrol. Through the reports provided by these companies, it is possible to witness the evolution of this surveillance system, its advantages, disadvantages, challenges, setbacks and progress.

Chapter 3

Model Development and Implementation

This chapter presents a description of the models, followed by their implementation explained in detail. The development and implementation of the simulator, as well as the assessment of the presented models, can also be found at the end of this chapter.

3.1. Model Development

3.1.1 Determination of the airplane´s position

As previously seen, the MLAT system is based on the TDOA algorithm, enabling to determine the position of an airplane accurately. In order to do this, it is necessary to measure the TOA of the signals exchanged between the ground stations and the airplane. This technique can also be named hyperbolic positioning, because it is based on the intersection of the hyperbolas that are the direct result of the TDOA algorithm. Each hyperbola corresponds to the time difference of arrival between the signal transmitted by the airplane and received by one of the ground stations. After having all the hyperbolas, their intersection will provide the precise location of the airplane at that particular time.

The distance between the ground station and the airplane is calculated by [Gav15]:

$$D_{i\,[\mathrm{m}]} = \sqrt{(x_{[\mathrm{m}]} - x_{i_{[\mathrm{m}]}})^2 + (y_{[\mathrm{m}]} - y_{i_{[\mathrm{m}]}})^2 + (z_{[\mathrm{m}]} - z_{i_{[\mathrm{m}]}})^2}\ , i \in \{1,2,3,4 \dots, n_{gs}\} \qquad (3.1)$$

where:

- (x_i, y_i, z_i): Location of the ith ground station.
- (x, y, z): Position of the airplane.
- n_{gs} : Number of ground stations.

In order to achieve the hyperbolas intersection, Figure 3.1, it is necessary to have an equation for each of the hyperbolas [Gav15]:

$$\sqrt{\left(x_{[\mathrm{m}]} - x_{i_{[\mathrm{m}]}}\right)^2 + \left(y_{[\mathrm{m}]} - y_{i_{[\mathrm{m}]}}\right)^2 + \left(z_{[\mathrm{m}]} - z_{i_{[\mathrm{m}]}}\right)^2} - \sqrt{\left(x_{[\mathrm{m}]} - x_{1_{[\mathrm{m}]}}\right)^2 + \left(y_{[\mathrm{m}]} - y_{1_{[\mathrm{m}]}}\right)^2 + \left(z_{[\mathrm{m}]} - z_{1_{[\mathrm{m}]}}\right)^2}$$

$$= D_{i\,[\mathrm{m}]} - D_{1\,[\mathrm{m}]} = c_{[\mathrm{m/s}]} \cdot (t_{i[\mathrm{s}]} - t_{1[\mathrm{s}]}), i \in \{2,3,4 \dots, n_{gs}\} \qquad (3.2)$$

where:

- c : Speed of light.
- t : Time when the airplane sent a signal.
- t_i : Time when the sensor received the signal.

In Figure 3.1, one shows that, through the implementation of the TDOA algorithm, it is possible to create the hyperbolas that, in a perfect scenario, intersect in only one point, which is the position of the airplane.

3.1.2 Error in the determination of the airplane´s position

The perfect scenario consists of an ideal situation, in which there is an error equal to zero associated with the hyperbolas formation. According to [Err06], there are errors that occur throughout the multilateration process that can be identified and quantified. These errors have different sources

associated with them, Table 3.1. The errors can be considered random and systematic, being divided into:

- Timing errors.
- Propagation errors.
- Surveying errors.
- Reference errors.

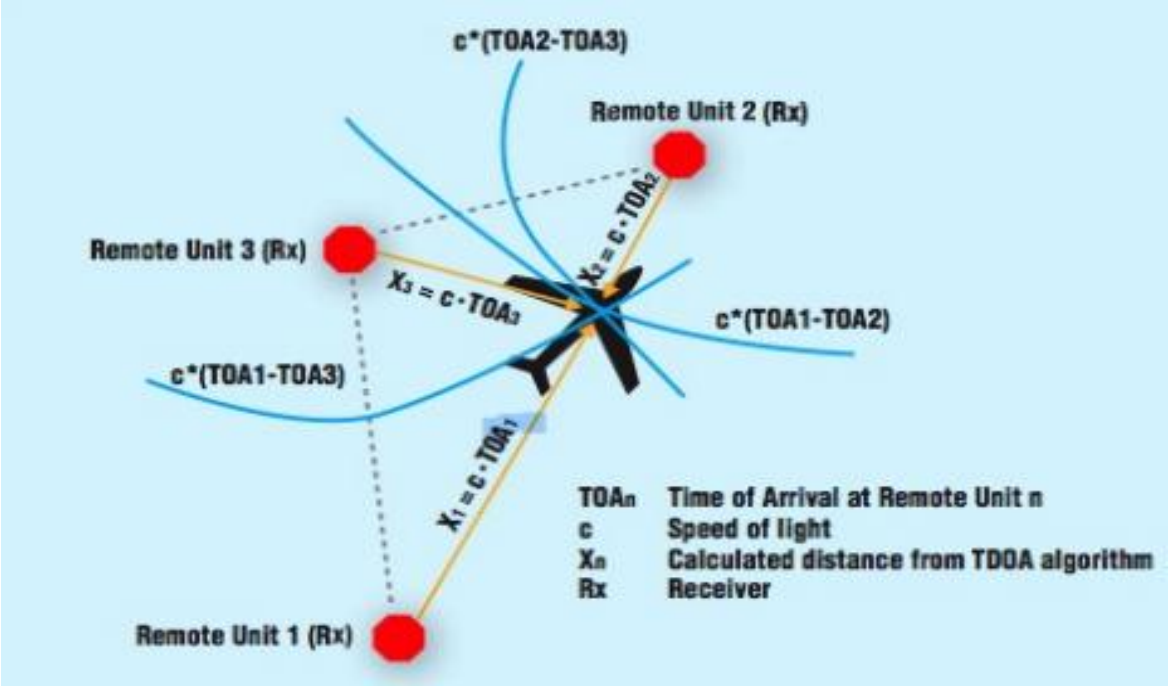

Figure 3.1 - TDOA algorithm (extracted from [Sie07]).

Timing errors are associated with the time of arrival measurements and TDOA calculations. From all errors, the timing ones are considered to be those that most contribute to the total error of the system [Err06]:

$$\Delta t_{time\,[\mathrm{ns}]} = \Delta t_{clock[\mathrm{ns}]} + \Delta t_{quant[\mathrm{ns}]} + \Delta t_{dig[\mathrm{ns}]} + \Delta t_{sync[\mathrm{ns}]} \quad (3.3)$$

where:

- Δt_{time} : Maximum timing error.
- Δt_{clock} : Maximum clock jitter error, varying according to the type of clock that is used.
- Δt_{quant}: Quantisation error.
- Δt_{dig} : Digitisation error.
- Δt_{sync} : Synchronisation error.

Table 3.1 provides information on the errors that are associated with the WAM system, regarding sources and the numerical contribution to the total error.

All these different sources that contribute to the timing error are related in one way or another to signal and time measurements.

Table 3.1 – Summary of the WAM errors (extracted from [Err06]).

Error Name	Notes	Typical Error Value	Uncertainty Contribution
Timing	Assumes region of good geometry.	50ns	50m
Clock Jitter	At limit of state-of-the-art crystal oscillators.		
Quantisation	Limit is determined by counting integer numbers of clock pulses – can be improved by increasing clock rate.		
Digitisation	Digitisation of the amplitude of the signal being measured introduces apparent phase shift and hence time delay. Reduced by increasing resolution of ADC.		
Synchronisation	Can be improved by reducing relative drift of clocks (such as temperature compensation, atomic reference clocks) and/or by better synchronisation (reference transponder, increase rate of synchronisation events).		
Propagation	Modelled maximum value.	23m	8m [a]
Speed	Can be reduced by introducing a higher fidelity atmospheric model and correcting propagation speed based on estimated altitude.		
Path	Can be reduced by improving atmospheric model and by reducing separation of sensors.		
Survey	Extended surveying can reduce survey errors below 10cm.	5m	10m
Reference	Estimated	5ns	5m
Algorithm	Included in timing accuracy.	-	-
Multipath	Not yet known		
Total	RSS		52m

[a] – Converts worst case (top hat) distribution to a 1 SD level.

Propagation errors are considered systematic ones, occurring during the multilateration process when

the time to distance conversion is performed. This error is also associated with the propagation path and the propagation speed that is necessary to consider when modelling the signal.

Surveying errors are directly related to ground stations' position, and consequently to the creation of the hyperbolas.

Reference errors take place mainly at situations in which the system uses different tools to perform activities that are part of the multilateration process. One example of these activities is clock synchronisation, because when performing the wide area timing configuration the system executes clock synchronisation not through the ground station antenna, but through the GPS data [Err06].

There is one more error that has an environmental and geographical nature, and that can contribute to the increase of the errors associated with a signal, which is multipath. This is the most significant one when the signal is travelling at 1 090 MHz, corresponding to the transponder reply, because depending on the environment in which the ground station is located, the signal can suffer reflections what affect TOA.

So adapting these findings to (3.2) the following results are achieved [Gav15]:

$$\sqrt{\left(x_{[\mathrm{m}]}-x_{i_{[\mathrm{m}]}}\right)^2+\left(y_{[\mathrm{m}]}-y_{i_{[\mathrm{m}]}}\right)^2+\left(z_{[\mathrm{m}]}-z_{i_{[\mathrm{m}]}}\right)^2}-\sqrt{\left(x_{[\mathrm{m}]}-x_{1_{[\mathrm{m}]}}\right)^2+\left(y_{[\mathrm{m}]}-y_{1_{[\mathrm{m}]}}\right)^2+\left(z_{[\mathrm{m}]}-z_{1_{[\mathrm{m}]}}\right)^2}$$

$$+\,n_{i,1_{[\mathrm{m}]}}=\;D_{i\,[m]}-\;D_{1\,[m]}+\;n_{i,1_{[\mathrm{m}]}}=\;c_{[\mathrm{m/s}]}.\left(t_{i[\mathrm{s}]}-\;t_{1[\mathrm{s}]}\right)+\;n_{i,1_{[\mathrm{m}]}},\;i\in\{2,3,4,\ldots,n_{gs}\}\qquad(3.4)$$

where:

- $n_{i,1}$: Quantified error.

The introduction of the error in a multilateration system, Figure 3.2, results in the increase of the number of hyperbolas, which are named boundaries, and also that the airplane is surrounded by an area that is considered to be the one in which the airplane achieves the maximum error position.

3.1.3 Difference between WAM and ADS-B routes

The difference between WAM and ADS-B systems, and the way that the results for each of the systems are obtained, have already been explained in Chapter 2. By having all the readings from all the airplane's positions using the WAM system, it is possible to have the complete route that the airplane is executing. At the same time, the GPS system installed in the airplane is also collecting data for each position that the airplane is taking.

Both these readings result on the route of the airplane, but with some differences, and these differences can be analysed by calculating the distance between the WAM route and the ADS-B one. This task is accomplished by calculating the distance between a point and a line, (3.5), the point being at the WAM route and the line at the ADS-B one, [Mat16], Figure 3.3:

$$d_{[m]}=\frac{\left|(y_{n+1}-y_n).x_1+\;(x_{n+1}-x_n).y_1+\;x_{n+1}.y_n-\;y_{n+1}.x_n\right|}{\sqrt{(y_{n+1}-y_n)^2+\;(x_{n+1}-x_n)^2}}\qquad(3.5)$$

where:

- x_1 and y_1 are the coordinates of point, P,
- x_n, y_n, x_{n+1} and y_{n+1} are the coordinates of points, Q_n and Q_{n+1}, on the line,
- d corresponds to the distance between the point and the line.

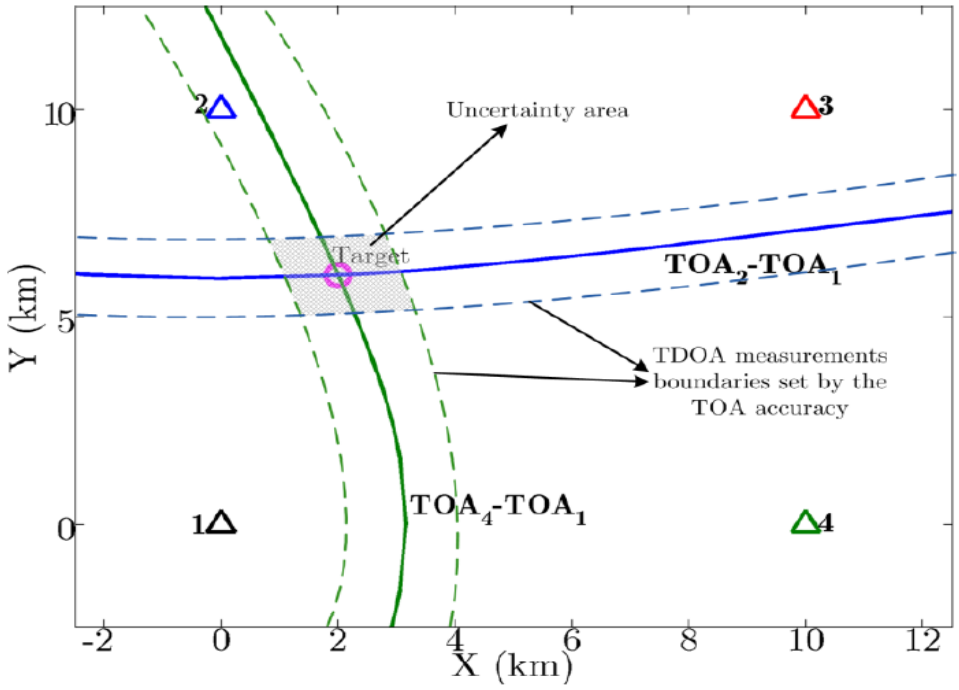

Figure 3.2 – Airplane inside the uncertainty area (extracted from [Gav15]).

3.2 Algorithm Development

3.2.1 Initial considerations

In order to achieve the goal of this thesis, one has used the divide and conquer method. The first step was to divide the main problem into two different types of analysis: one in which the difference between WAM and ADS-B routes is calculated, from now on called route difference analysis, and another in which the maximum error that an airplane's position can take is calculated, designated by error position analysis.

The error position analysis is applied in two different scenarios: Scenario 1, in which all the information related to the used ground stations and the airplane routes from WAM and ADS-B systems are available, Figure 3.4, and Scenario 2, in which the only information available is the ADS-B route, Figure 3.5, hence, being an analysis of the set of ground stations that can be used to minimise the location error.

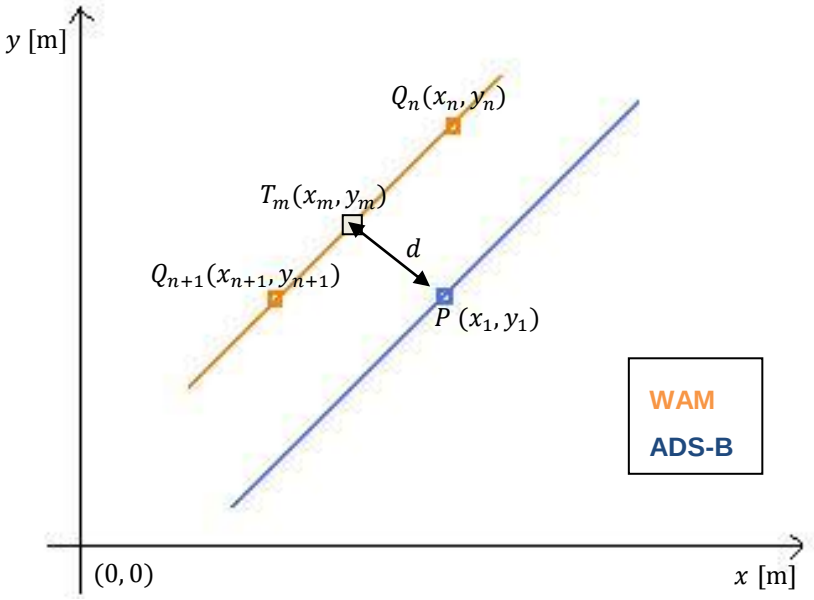

Figure 3.3 – Distance between a line and a point.

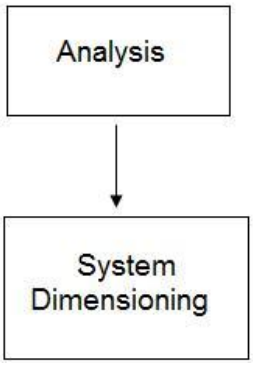

Figure 3.4 – Main structure of Scenario 1 analysis.

To perform route difference analysis, it is necessary to know the airplane route provided by the WAM and the ADS-B systems. Even though both routes report to the same airplane route, their origin is different, thus the difference between them, and this difference is one of the parameters that contributes to evaluate system's accuracy.

One should note that the route information provided by the WAM system also contains the set of ground stations that is used in each of the airplane's positions in order to calculate the maximum error.

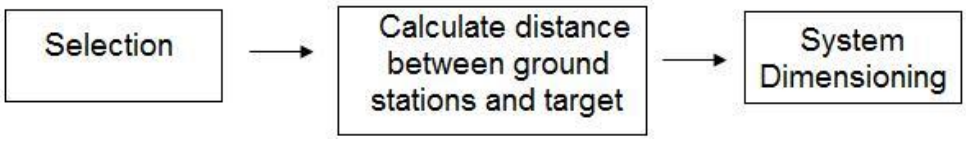

Figure 3.5 – Main structure of Scenario 2 analysis.

3.2.2 Difference between WAM and ADS-B routes

The flowchart for the analysis of the difference between WAM and ADS-B routes is shown in Figure 3.6. WAM and ADS-B routes must be selected, and from the WAM route information one knows the initial airplane's position, P_{targ}. Then, a search on the ADS-B route information is performed, in order to find the coordinates that are above and below the airplane position, Q_m and Q_{m+1}, respectively. After collecting this information, it becomes a distance between point and line problem, P_{targ} being the point, and Q_m and Q_{m+1} the two points defining the line.

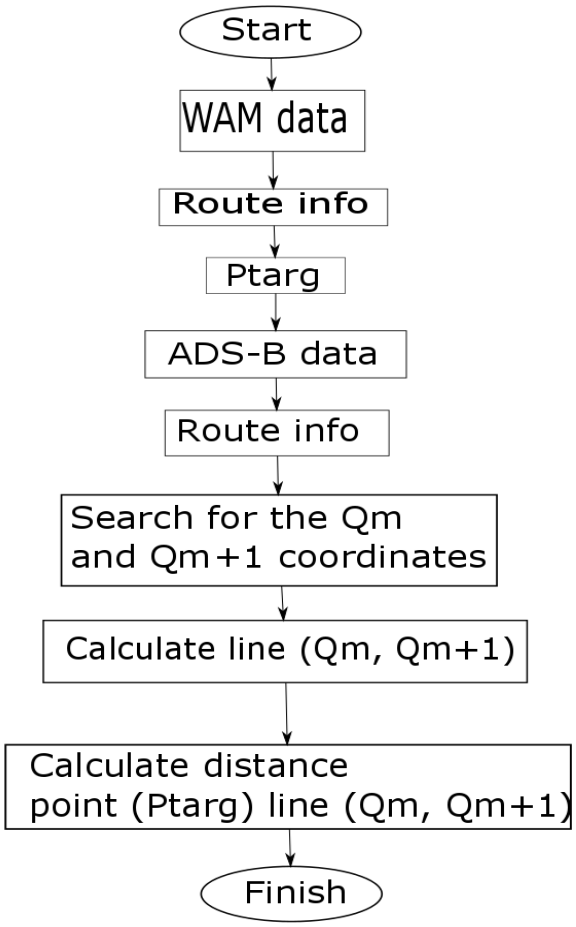

Figure 3.6 – Difference between WAM and ADS-B routes.

Finally, after computing this distance problem using (3.5), one obtains the expected result, the difference between both routes. One should note that this result is useful when evaluating the influence that the airplane's approximation to the ground stations has on the system.

3.2.3 Analysis and System Dimensioning Algorithm

In order to determinate the maximum error of an airplane's position, two fundamental steps to achieve this goal are the analysis and system dimensioning, in Figure 3.7 and Figure 3.8, respectively.

Figure 3.7 shows the flowchart of the steps necessary to load all the information needed to build the hyperbolas. First, the WAM route is loaded and the information related to the route and the set of

ground stations that is used for each route position is extracted. Then, a similar process is done to the ADS-B data. ADS-B data are more reliable, because this information is given by the airplane´s GPS, the difference in between WAM and ADS-B routes being calculated in order to obtain the coordinates of the point that is the new target position, T_m, Figure 3.3.

All the collected information is used to calculate the distance between the airplane and every ground station, and the distances in between all ground stations using (3.1). These results are used to create the hyperbolas that allow the determination of the maximum error that an airplane's position can take.

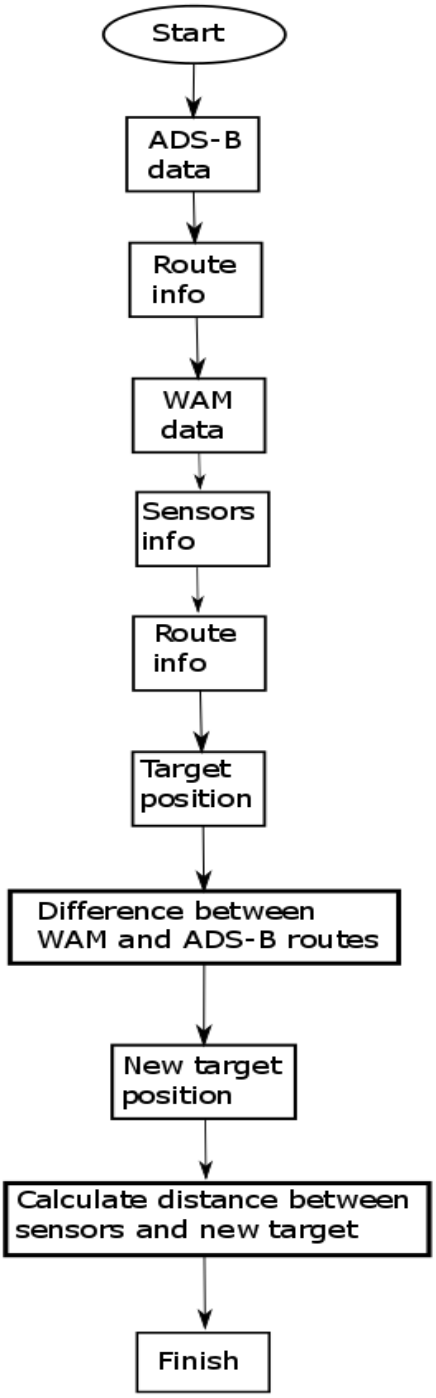

Figure 3.7 – Analysis – information loading.

In order to complete the process of error determination, it is necessary to build the hyperbolas, Figure 3.8: for each pair of different ground stations a hyperbola is created, and then an error to the hyperbolas is applied. This error generates two situations: one in which the error is equal to zero and then all the hyperbolas intersect in one point, that point being the airplane's position, implying that the multilateration system is well implemented in the simulator; another in which the error assumes a non-zero value, and then the different pairs of hyperbolas associated with the error intersect and create an area similar to the one seen in Figure 3.2, and from the points that form this area the one that is the farthest from the airplane is considered to be the maximum error that the airplane's position takes.

One should note that, in Figure 3.8, the S variable represents the set of ground stations that is used in each position of the route and the N one represents the number of ground stations.

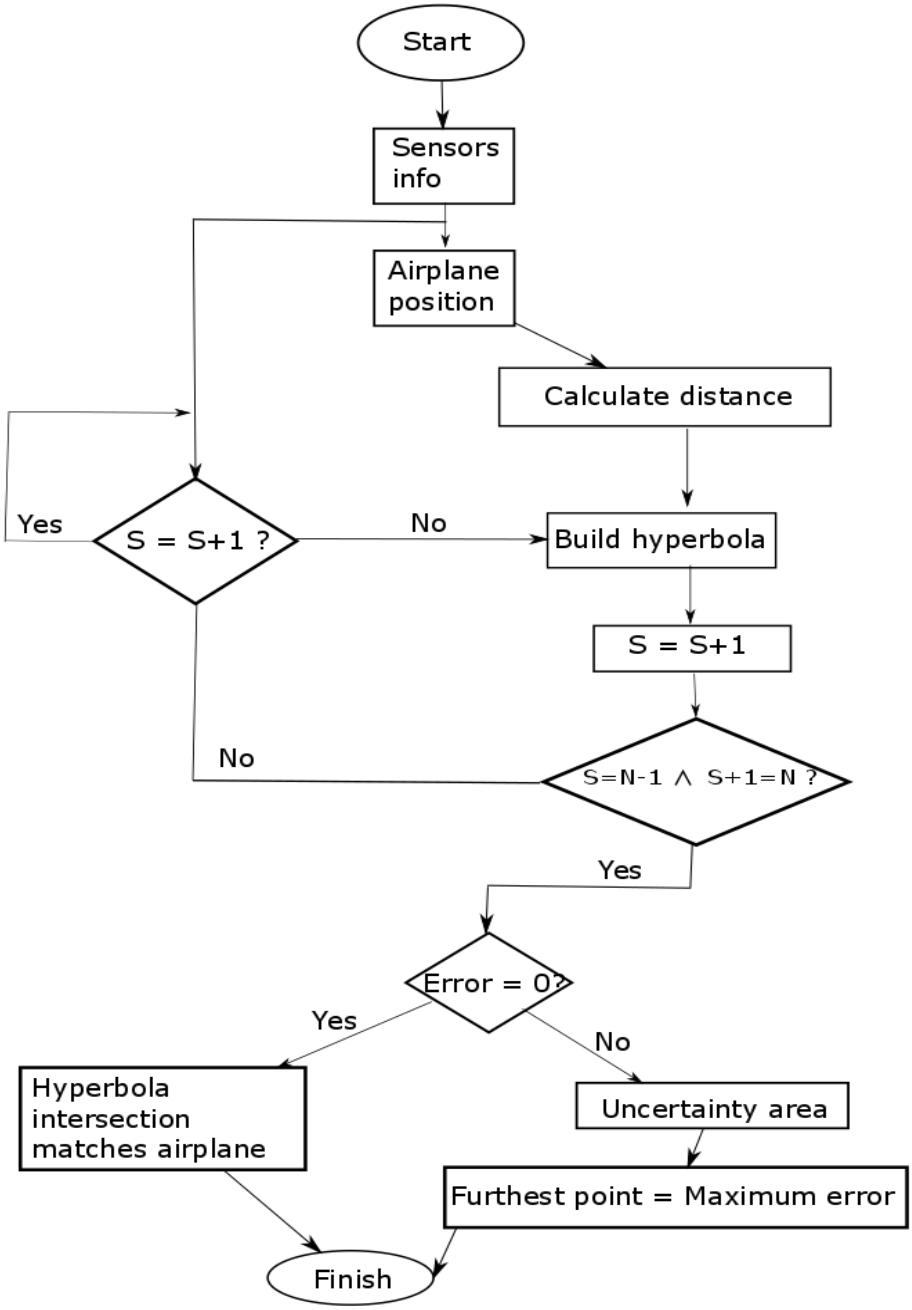

Figure 3.8 – System dimensioning – hyperbola building.

3.2.4 Selection Algorithm

The selection algorithm is used in situations where the WAM route information is not available, and therefore the set of ground stations that are used for each airplane's position is not known. In these situations, the ADS-B route data are the only available information, Figure 3.9.

First, an ADS-B route must be selected and loaded, where all ground stations positions must be known and loaded. After collecting this crucial information, it becomes a combination problem. For each airplane's position, the distance between all ground stations and the airplane is calculated using (3.1), then the m ground stations that are closer to the airplane are the ones selected to be taken into the combination problem.

Combinatorial analysis was chosen to find all the different sets of ground stations that can provide a minimum error associated with a given airplane's position, combinations being [Mor10]:

$$C_k^m = \binom{m}{k} = \frac{m!}{k!(m-k)!} \tag{3.6}$$

where:

- m represents the total of ground stations that will be taken;
- k represents the number of ground stations that the combination will have, this value varying between a minimum and a maximum, the latter being m.

The result of the combinatorial analysis is a set of subsets of k distinct elements of m. Each subset represents a possible combination of ground stations, therefore, for each of the subsets the system dimensioning will be applied. Finally, the error associated with each of the ground stations combination is obtained, and then the one that presents the minimum value is the combination of ground stations that should be used on the MLAT system for that particular airplane's position.

3.3 Model Implementation

3.3.1 Main Simulator Structure

This section describes the implementation of the models and algorithms described in Section 3.1 and Section 3.2. A simulator using Matlab2013b was developed, enabling to analyse the different scenarios presented in Section 3.2.

The main structure of the simulator is presented in Figure 3.10, and although there are different scenarios being simulated, implying that different algorithms are used, the general structure of the simulator does not change.

First, the ground stations and airplane routes are described, and then the models and algorithms from Section 3.2 are applied.

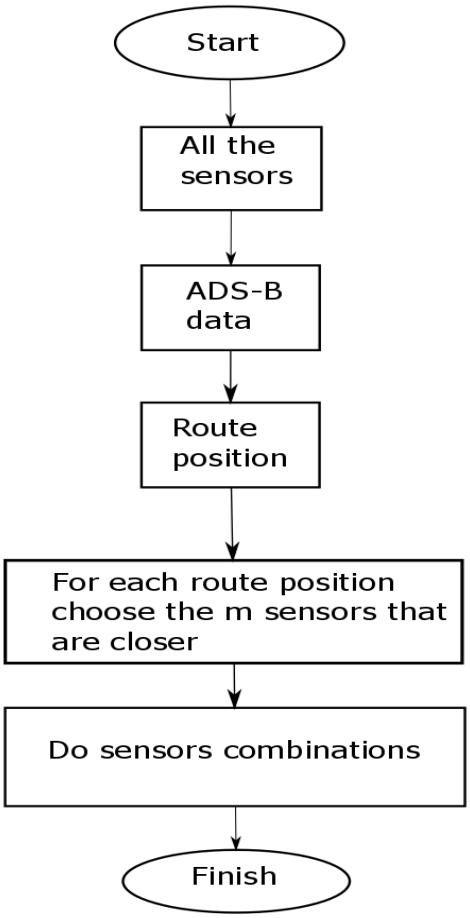

Figure 3.9 – Selection of the ground stations.

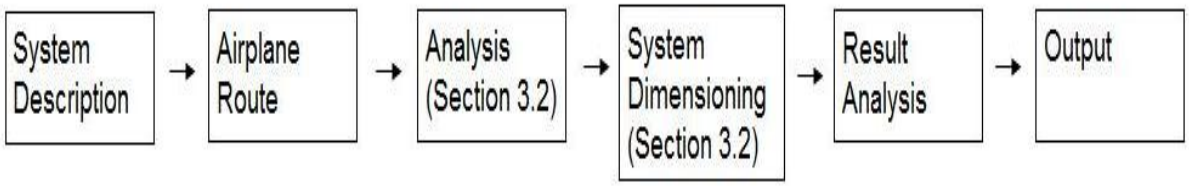

Figure 3.10 – Main structure of the simulator.

After obtaining the results, these are analysed in two different ways: in the first one, the purpose is to observe the error evolution throughout the airplane's route, and if possible to validate some of the hypotheses of this thesis; in the second one, the goal is to compare the experimental measurements and the real values of the airplane's routes.

In order to calculate the comparison in between routes, one takes a statistical perspective, it is necessary to obtain the Probability Density Function (PDF) that better describes the variation in the number of measurements. In order to validate the results presented by the PDF, it is crucial to check the goodness-to-fit statistics using some parametric models defined in [Mat15a]:

- Coefficient of Determination (R-square): it measures how successful the fit is in explaining the variation of the data. This parameter is the square of the correlation in between the response

values and the predicted ones, and it is also defined as the ratio between the sum of squares of the regression and the total sum of squares. It can take on any value between 0 and 1, with a value closer to 1 indicating that a greater proportion of variance is accounted for by the model.

The R-square is defined by [Mat15a]:

$$R^2 = \frac{\sum_{i=1}^{n} w_i \times (\hat{y}_i - \mu_y)^2}{\sum_{i=1}^{n} w_i \times (y_i - \mu_y)^2} \quad (3.7)$$

where:

- y_i : observation i.
- $\hat{y}_i$: estimated or predicted value of y_i.
- μ_y : average of the observations of variable y.
- n : number of observations.

- Adjusted R-square: it uses the R-square parameter defined above, and adjusts it based on the residual degrees of freedom. It can take on any value less than or equal to 1, with a value closer to 1 indicating a better fit. Negative values can occur when the model contains terms that do not help to predict the response.
- Root Mean Squared Error (RMSE): it is also known as the fit standard error and the standard error of regression. It is an estimate of the standard deviation of the deviation of the random component in the data. An RMSE value close to 0 indicates a fit that is more useful for prediction.

The RMSE is obtained via [Mat15a]:

$$\sqrt{\overline{\varepsilon^2}} = \sqrt{\frac{\sum_{i=1}^{n} (y_i - \hat{y}_i)^2}{n}} \quad (3.8)$$

The parametric models used to evaluate the goodness-of-fit are the direct result of a Matlab tool, the Matlab *Curve Fitting* Tool [Mat15b].

Finally the output is written in an Excel file (*.xlxs) that contains in each line the error associated with one airplane's position.

3.3.2 Maximum error of an airplane position simulator

To calculate the maximum error of an airplane's position as explained in Section 3.2, it is necessary to implement the analysis and system dimensioning algorithms, but more computations are required, Figure 3.11.

For Scenario 1, all the information related to the ground stations used and the airplane's routes from WAM and ADS-B systems are available, and the simulator starts by reading and loading the input files that contain all this information.

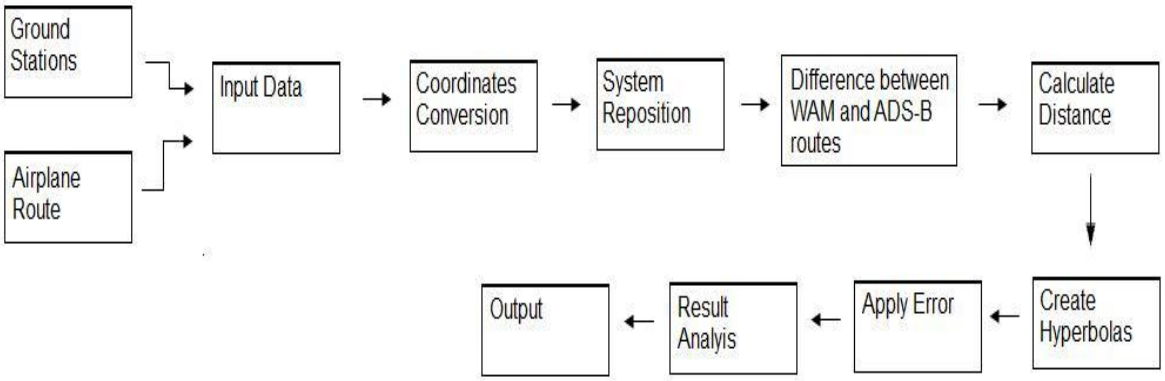

Figure 3.11 – Detailed main structure.

From the files with the WAM and ADS-B routes, some more crucial information is extracted in order to execute the simulation. In the WAM route Excel file, each line represents an airplane's position, being extracted:

- Geographical coordinates (latitude and longitude).
- Flight level.
- Time stamp.
- Set of ground stations that are used to implement the TDOA measurements.

From the ADS-B route file, one also extracts the same information, except the set of ground stations, because this information does not exist for this system.

In this stage, the simulator converts the geographical coordinates into UTM (Universal Transverse Mercator) ones. One should note that the set of ground stations is presented in hexadecimal, so is necessary to convert it to binary in order to identify the used ground stations. Then, it is assumed that one of the ground stations is the reference one in the system, meaning that this ground station takes the coordinates (0, 0), and all the other elements in the system are repositioned in relation to the reference. The difference between WAM and ADS-B routes algorithm is applied, and the new airplane's position is obtained. In order to perform the TDOA measurements, it is required to calculate the distances in between the airplane's position and the all ground stations, and distances in between all ground stations. These distances are critical when creating the hyperbolas, which were based in a developed function *hyperbol*, which has as input:

- Error value.
- Distance between ground stations A and B.
- Position of airplane.
- Position of ground station A.
- Position of ground station B.

This *hyperbol* function is applied to every pair of ground stations. Then, depending on the value of the error, the system has two different results: if the error is equal to zero, a set of hyperbolas intersecting only in one point in the system is obtained, that point being the airplane position, Figure 3.12; if the error is not zero, the hyperbolas are not all intersecting in one point, instead an area that surrounds

the target, called uncertainty area, being create, Figure 3.2.

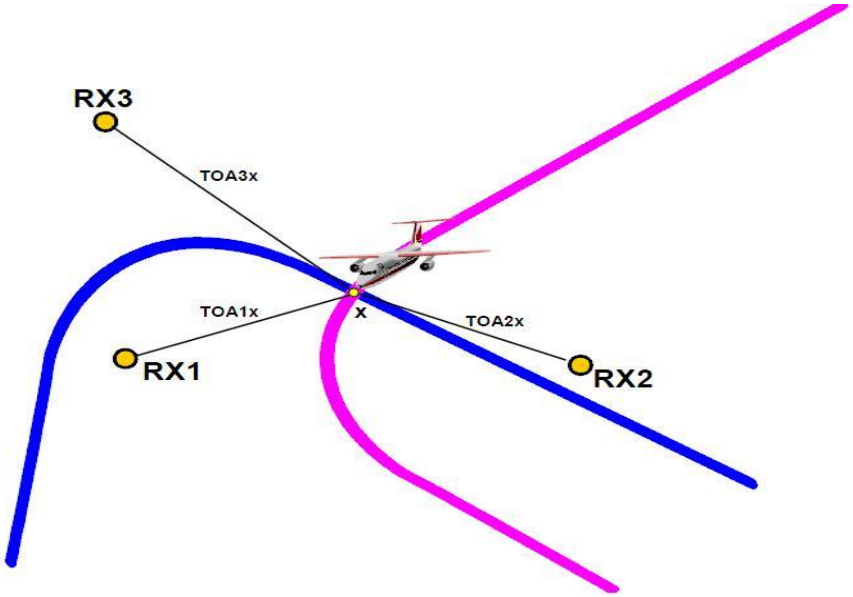

Figure 3.12 – Hyperbolas intersection in a 3 ground stations scenario (extracted from [Air07]).

In order to analyse the uncertainty area, the first step is to obtain all the hyperbolas' intersections that exist, and to calculate the distance in between the target and all intersections. Because not all intersections are relevant for the uncertainty area, a decision was made to consider only the relevant number of intersections, $N_{intersect}$, the ones that are closer to the target. Then, from the remaining set of intersections, all possible combinations of $N_{intersect}$ taking N_{choos} at a time are done, by using the *nchoosek* function from Matlab2013b.

From the result of the intersections' combinations, polygons with N_{choos} vertices are created, and then a verification to check in which of the polygons the target is inside is made; for the polygons that verify this condition their perimeter is calculated. For the points that belong to the polygon that presents the smallest perimeter the distances from the target to those points are calculated. Finally, the distance between the farthest point and the target is considered to be the maximum error that an airplane's position can assume.

When analysing Scenario 2, the initial part of the simulator is different, but after obtaining the ground stations' combinations, it repeats the simulation for Scenario 1. For Scenario 2, the available information are the ground stations coordinates and the airplane's route from the ADS-B system. The simulator begins by reading and loading the input files that contain the coordinates of the ground stations and the ADS-B route, being extracted from the latter:

- Geographical coordinates (latitude and longitude).
- Flight level.
- Time stamp.

As in Scenario 1, geographical coordinates are converted to UTM ones. Because the ADS-B system

does not have a set of ground stations, the selection algorithm is applied, Section 3.2, to find all the possible ground stations combinations. From this point on, all combinations of ground stations go through the same simulation done for Scenario 1. In the end, and as an output for each of the combinations, an error value is calculated. Afterwards, from the output data a simple search is made in order to find the minimal error value, this value and the respective ground stations combination provide the ideal solution for a certain airplane's position.

3.4 Model Assessment

In this section, the simulator, described in Section 3.3, is assessed in order to validate the implemented models. The models verification is done through the analysis of the output results.

The flight routes and ground stations considered as input data for the simulator were provided by NAV. This information has to check some criteria, because of the way that the simulator is developed, and the flight routes have to follow the headers in Table 3.2 for WAM and in Table 3.3 for ADS-B, and the same goes for ground stations files, Table 3.4.

Table 3.2 - Header for WAM routes (extracted from [Fil15a]).

lat_WGS84	lng_WGS84	Tod	trkNr	modeS	csn	modeC	lat	lng	X	y	mH	vx	vy	Trp

ts	caf	dopX	dopy	dopCxy	sdX	sdY	sdCxy	sdLat	sdLng	sdCII	vel	hdg	ru

Table 3.3 - Header for ADS-B route (extracted from [Fil15b]).

lat_WGS84	lng_WGS84	tmrp	modeS	modeA	lat	lng	modeC	Csn	fom	ec	trp	lti	ts

Table 3.4 - Header for ground stations (extracted from [Fil15c]).

Latitude			Longitude			Height
Degree	Minutes	Seconds	Degree	Minutes	Seconds	

A tool was used to verify the correct positions of simulator's input data, i.e., Google Earth. By comparing the maps provided by Google Earth with the simulator results, it was possible to check if the implemented input was correct. Another important assessment, which has several impacts on the

implemented models, is the distance between ground stations. These distances were confirmed by using Microsoft Excel tools, Google Earth features, or scientific calculator.

Also when assessing the difference between WAM and ADS-B routes, it was possible to validate the results, because the determination of distance between point to line could be checked by using a scientific calculator, assuming that all the points in analysis are correct.

When introducing the error in the hyperbola formation stage with error equal to zero if all hyperbolas intersect in one point, and if that point corresponds to the airplane's position, then it is safe to claim that the model is correctly implemented and the simulator provides the expected results.

A set of decisions were made regarding the implementation of the simulator, because of the computer processor capacity, particularly in the system dimensioning analysis. Because the *nchoosek* MATLAB command has an associated time limitation, it is not possible to perform combinations with all the hyperbolas intersections, so a decision was taken to include only 20 of the intersections, the ones that are closer to the airplane's position. When using *nchoosek,* the combination takes 8 items from 20 intersections, this decision being the number of vertices of the formed polygons. By using the *inpolygon* MATLAB command, it is possible to verify which of the polygons includes the target, Figure 3.2. This *inpolygon* command returns a logical 1 (true) if the query point is inside or on the edge of the polygon area, and logical 0 (false) otherwise.

The system dimensioning analysis is the most time consuming section of the simulator, making the total time per simulation 2 hours.

Chapter 4

Analysis of Results

This chapter presents the different scenarios description, the simulations results and their analysis. At the end of the chapter, a set of recommendations is proposed, regarding the set of ground stations to be used for one of the scenarios.

4.1 Scenarios Description

4.1.1 Initial Considerations

In this section, the different scenarios to be analysed are presented, as well as the different flight routes that are considered in the simulations. Subsections 4.1.2 to 4.1.4 present the scenarios corresponding to the MLAT systems of Lisbon, Azores and Porto airports, respectively.

4.1.2 Lisbon Region Scenario

Figure 4.1 shows the locations of the ground stations in two different scenarios: one that represents the real positions, presented in Google Earth's graphics, and another, with the same information, but represented in the environment created by the simulator.

The maximum error calculation associated with the WAM system at the Lisbon airport fits the situation in which all the information related to the used ground stations and the flight routes from WAM and ADS-B systems are available, as explained in Chapter 3.

The WAM system in Lisbon is composed of 8 ground stations, Table 4.1, their positions being presented in Figure 4.1. The Caparica ground station is considered to be the reference one.

Table 4.1 – Lisbon WAM ground stations description.

Ground Station (GS) ID	Location	Latitude [DDºMM'SS.SS'']	Longitude [DDºMM'SS.SS'']	Height [m]
GS01	Caparica	38º38'32.20''N	9º13'17.77''W	8
GS02	Arruda	38º59'39.52''N	9º02'25.29''W	20
GS03	Arrábida	38º29'33.25''N	8º57'44.01''W	15
GS04	Montargil	39º04'38.00''N	8º11'14.93''W	10
GS05	Fanhões	38º53'16.00''N	9º09'45.23''W	6
GS06	Espichel	38º25'27.17''N	9º11'08.97''W	3
GS07	Montejunto	39º10'25.98''N	9º03'13.59''W	8
GS08	Monte Gordo	38º57'43.97''N	8º59'36.76''W	15

The flight routes used for the simulation are shown in Figure 4.2, for both WAM and ADS-B routes.

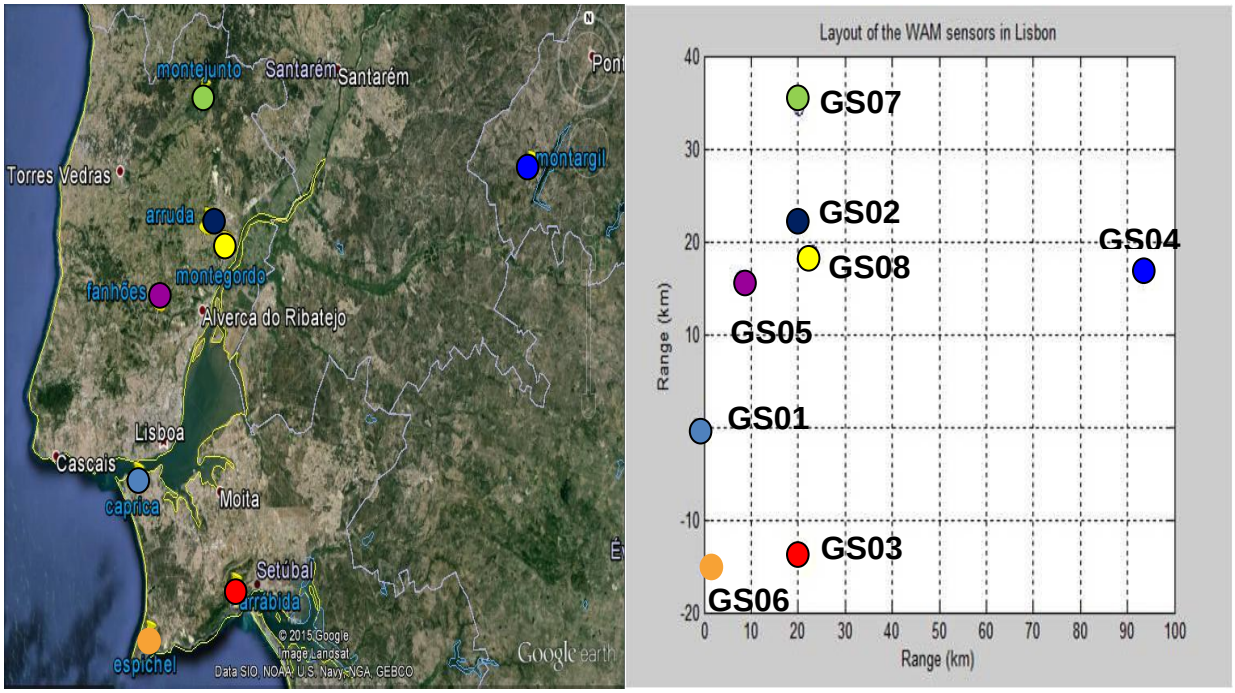

(a) Google Earth (b) Simulation

Figure 4.1 – Lisbon WAM ground stations locations (extracted from [Google Earth]).

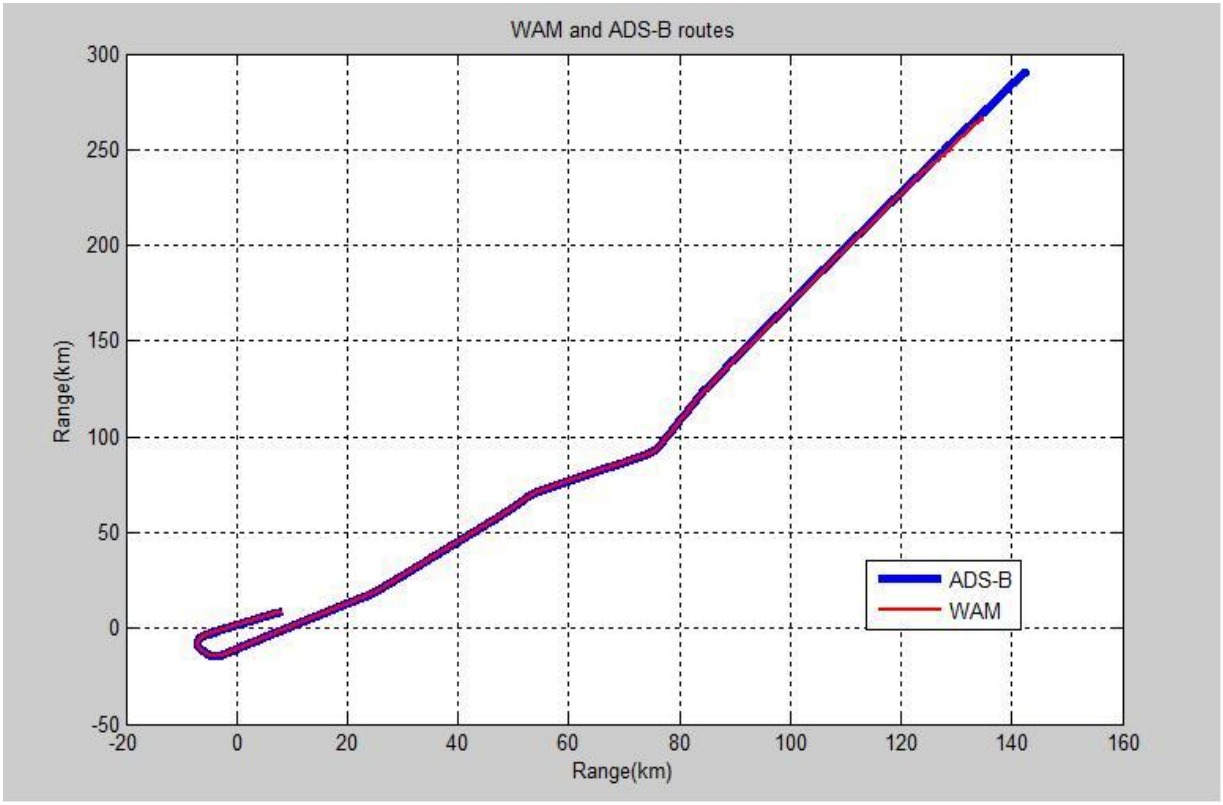

Figure 4.2 – WAM and ADS-B routes for Lisbon scenario.

4.1.3 Azores Region Scenario

The Azores region scenario analysis is done under the same conditions as the Lisbon one, i.e., information regarding all ground stations and the WAM and ADS-B routes are available.

The WAM system of the Azores region is composed of 17 ground stations, Table 4.2, their positions being presented in Figure 4.3. The GS00 ground station is the reference one.

Table 4.2 - Azores WAM ground stations description.

Ground Station ID	Location	Island	Latitude [DDºMM'SS.SS'']	Longitude [DDºMM'SS.SS'']	Height [m]
GS 00	Cabeço Gordo	Faial	38º34'33.20''N	28º42'47.50''W	35
GS 01	VOR VFL	Faial	38º31'11.73''N	28º37'24.60''W	6
GS 02	Estação GSM. TMN Candelária	Pico	38º27'58.86''N	28º30'40.90''W	40
GS 03	Estação GSM. TMN Aeroporto	Pico	38º31'52.25''N	28°26'27.31"W	40
GS 04	Parque Eólico – Terras do canto	Pico	38°27'45.33"N	28°15'49.14"W	14
GS 05	Communications Station Barroca	São Jorge	38°42'33.16"N	28°12'04.46"W	25
GS 06	Parque Eólico 2	São Jorge	38º36'01.02"N	27º55'56.32"W	8
GS 07	GSM Estação 1	São Jorge	38°32'58.13"N	27°46'06.17"W	45
GS 08	Parque Eólico 1	Graciosa	39°02'09.60"N	28°01'45.10"W	30
GS 09	Serra Santa Bárbara	Terceira	38°43'48.50"N	27°19'09.30"W	29
GS 10	GSM Estação 2	São Jorge	38°36'02.96"N	27°59'18.15"W	45
GS 11	Estação EDA	Corvo	39º40'37.45''N	31º06'24.21''W	10
GS 12	Torre de Antenas GSM	Corvo	39º40'24.09''N	31º06'47.31''W	10
GS 13	Morro Alto	Flores	39º27'48.28''N	31º13'11.68''W	20
GS 14	Monte das Cruzes	Flores	39º27'06.03''N	31º08'10.15''W	25
GS 15	Parque Eólico	Flores	39º25'23.76''N	31º10'59.10''W	20
GS16	Rocha do Touro	Flores	39º24'34.58''N	31º09'20.32''W	20

Figure 4.4 shows the corresponding WAM and ADS-B routes.

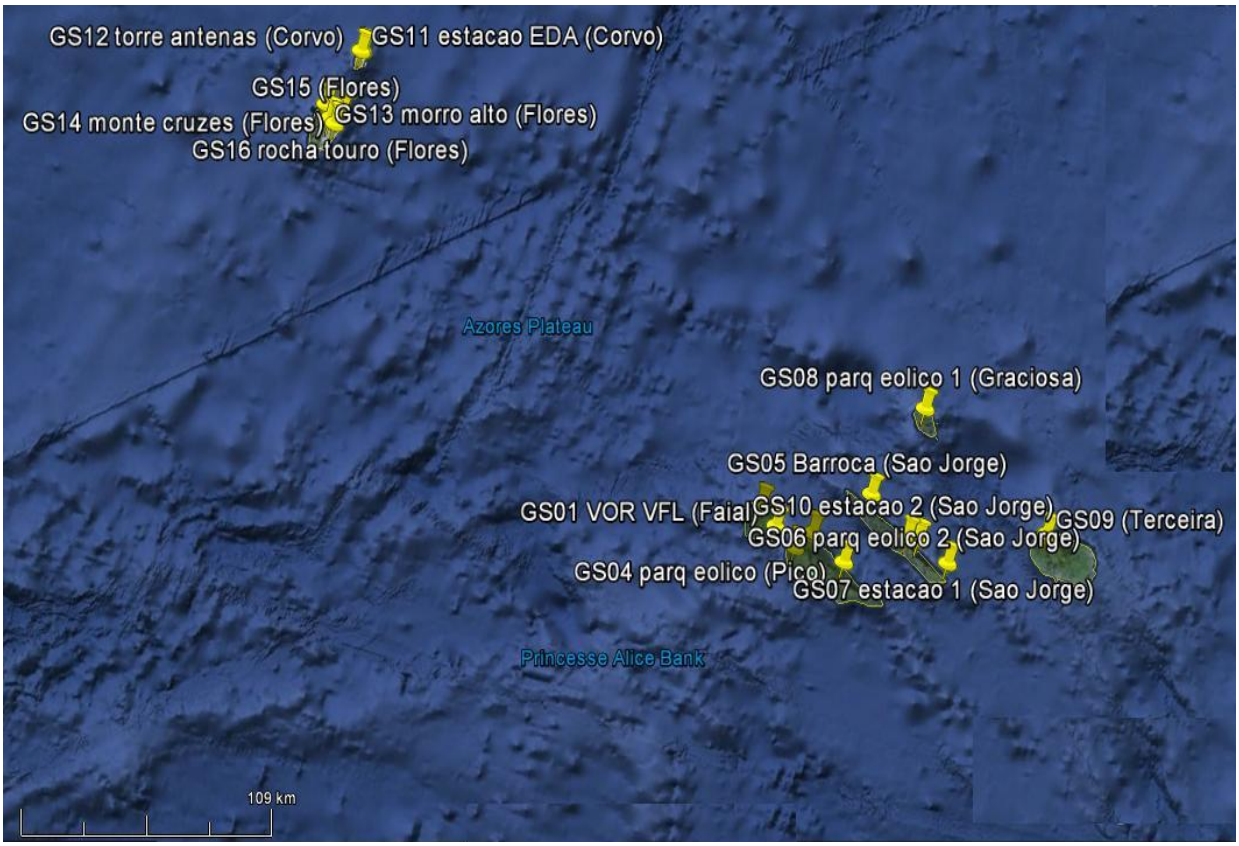

(a) Google Earth

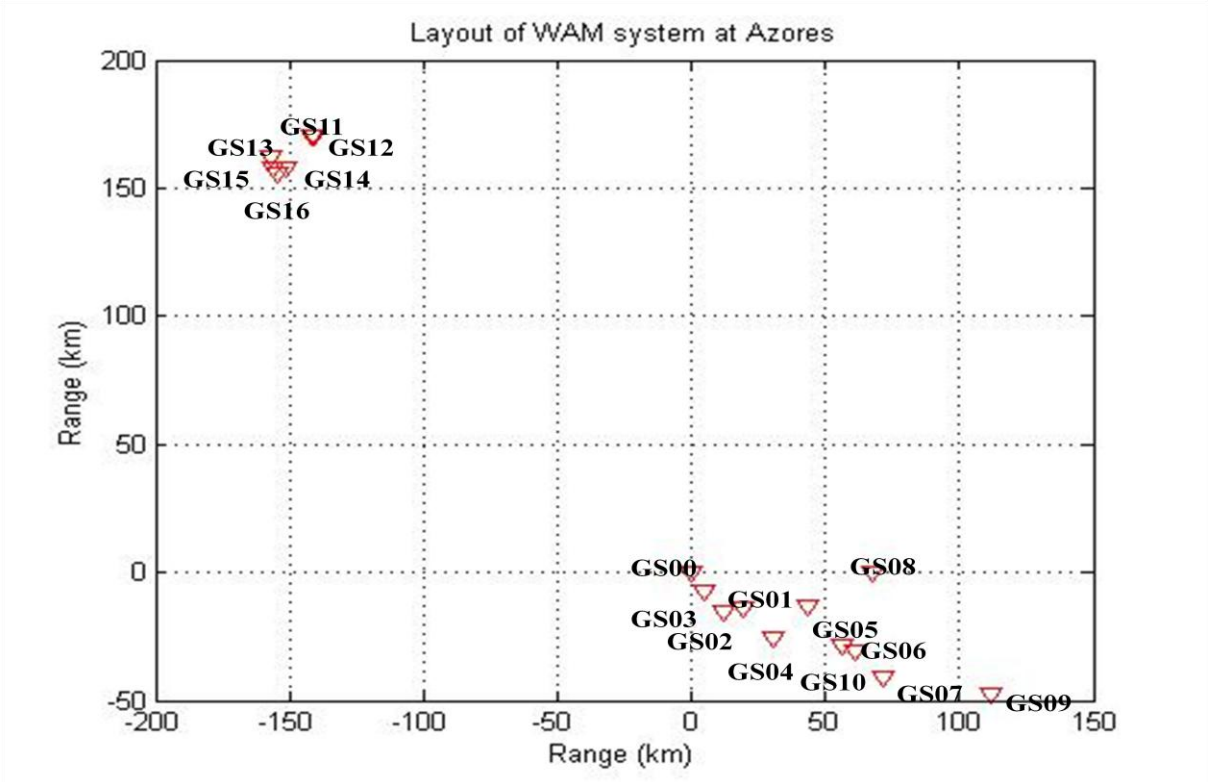

(b) Simulation

Figure 4.3 - Azores WAM ground stations locations.

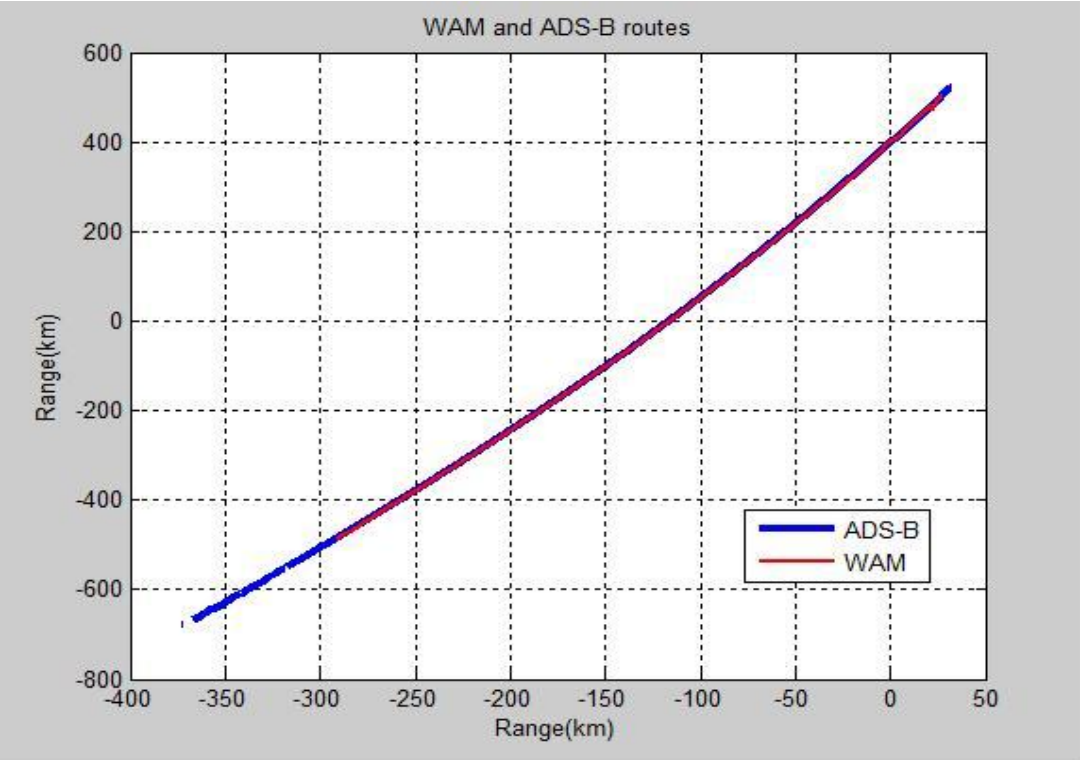

Figure 4.4 - WAM and ADS-B routes for Azores scenario.

4.1.4 Porto Region Scenario

The Porto region scenario fits the situation, described in Chapter 3, in which the only information available is the ADS-B flight route, Figure 4.6, and the ground stations positions, Figure 4.5. Because the WAM system is not fully operational, the goal for the Porto region scenario analysis was to determine the set of ground stations that provide the minimum system error, this information being useful to building the actual WAM system under deployment.

The Porto scenario is composed of 12 ground stations, Table 4.3, their positions being presented in Figure 4.5. The locations of the ground stations are presented in two different ways: one with the real positions in Google Earth's graphics, and another represented in the simulator environment.

Although there are 12 ground stations, two of them, RU07 and RU10, have the same location so for simulation purposes only one of them is considered. The RU01 ground station is considered to be the reference one.

4.2 Difference between WAM and ADS-B routes analysis

This section presents the results of the Lisbon and Azores regions simulations. One presents the

difference between the WAM and ADS-B routes, hence, being possible to verify that as an airplane gets closer to the ground stations the difference between the routes decreases.

In the Lisbon scenario, one knows that the MLAT system has a range of 30 NM (i.e. 55.6 km), meaning that the system is designed to ensure airspace surveillance under a 30 NM radius, with the centre at the Lisbon airport.

Table 4.3 – Porto ground stations description.

Ground Station ID	Latitude [DDºMM'SS.SS'']	Longitude [DDºMM'SS.SS'']	Height [m]
RU01	41º20'52.90''N	08º42'29.34''W	20
RU02	41º14'19.64''N	08º40'18.44''W	20
RU03	41º33'41.47''N	07º30'59.18''W	20
RU04	41º43'10.81''N	06º51'11.59''W	25
RU05	40º46'33.64''N	07º20'55.07''W	30
RU06	41º43'53.11''N	07º38'51.00''W	20
RU07	41º14'55.68''N	07º53'10.68''W	20
RU08	42º02'31.31''N	08º21'19.80''W	22
RU09	41º01'31.94''N	08º20'45.46''W	25
RU10	41º14'55.68''N	07º53'10.68''W	20
RU11	41º48'46.84''N	08º11'42.68''W	25
RU12	41º47'55.03''N	08º42'36.54''W	25

The results for the Lisbon region, Figure 4.8, show that the difference between routes decreases when the airplane is closer to the ground stations. One should note that around the 55 km (30 NM) red mark system requirements are satisfied, since the error is mostly less than 100 m.

For the Azores region, a similar analysis was performed, but with different requirements, since the two MLAT systems are not equal. Figure 4.9 presents the simulations results for Azores, and, as expected, the conclusions are the same, i.e., as the distance between the airplane and the reference ground station gets smaller, the difference in between the WAM and ADS-B routes also gets smaller. The reference value for the error in the Azores scenario is around 300 m, and in the area in which the airplane is closest to the reference ground station, this value is accomplished, since around that area the error is mostly less than 300m, showing that the implemented system is meeting the requirements and technical specifications set for it.

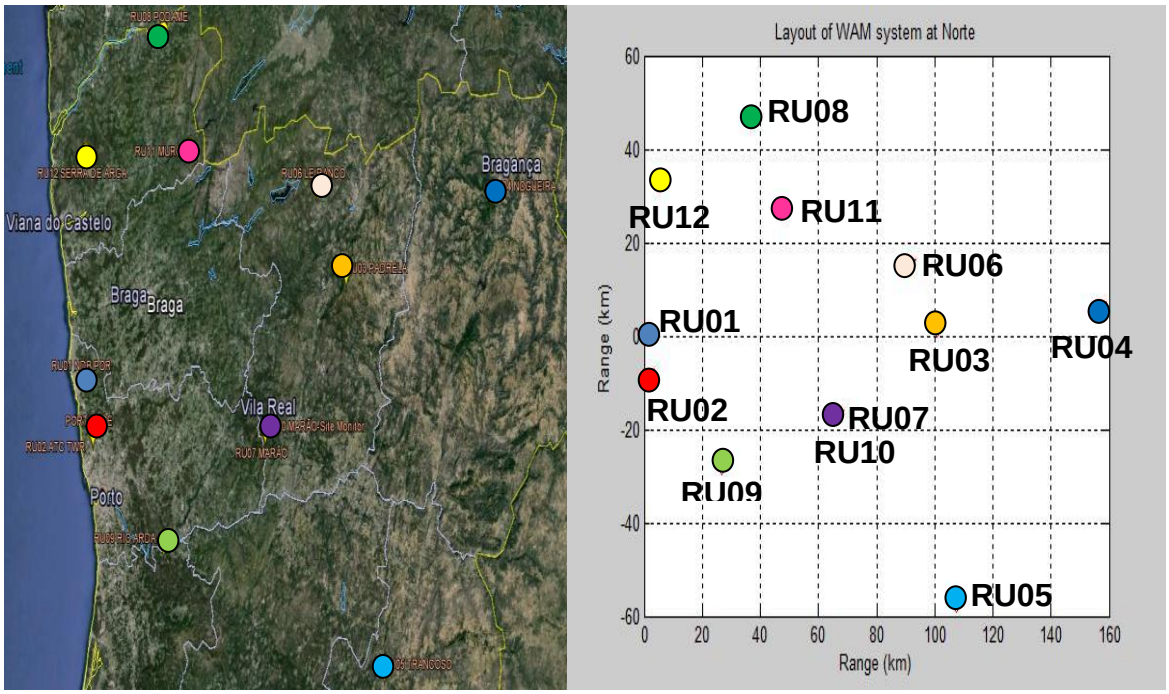

(a) Google Earth (b) Simulation

Figure 4.5 – Porto WAM ground stations locations (extracted from [Google Earth]).

Figure 4.6 shows the ADS-B route.

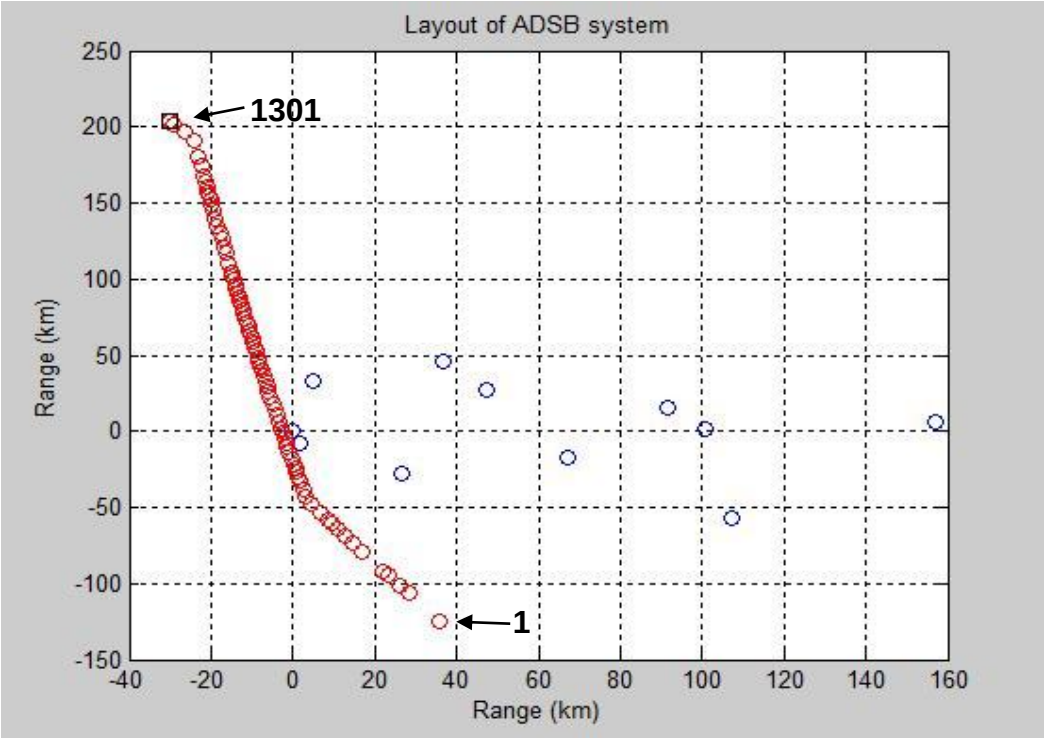

Figure 4.6 – Porto ADS-B route and ground stations.

Figure 4.7 shows that in fact the WAM and ADS-B routes do not overlap.

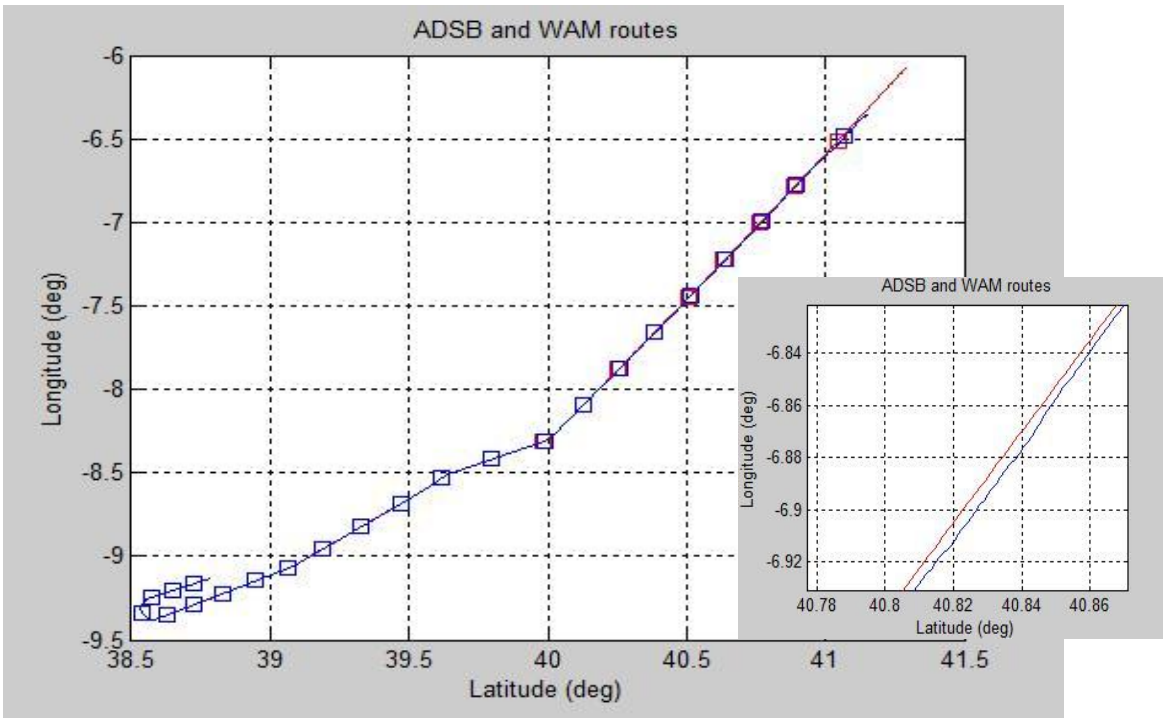

Figure 4.7 – Difference between WAM (blue) and ADS-B (red) routes.

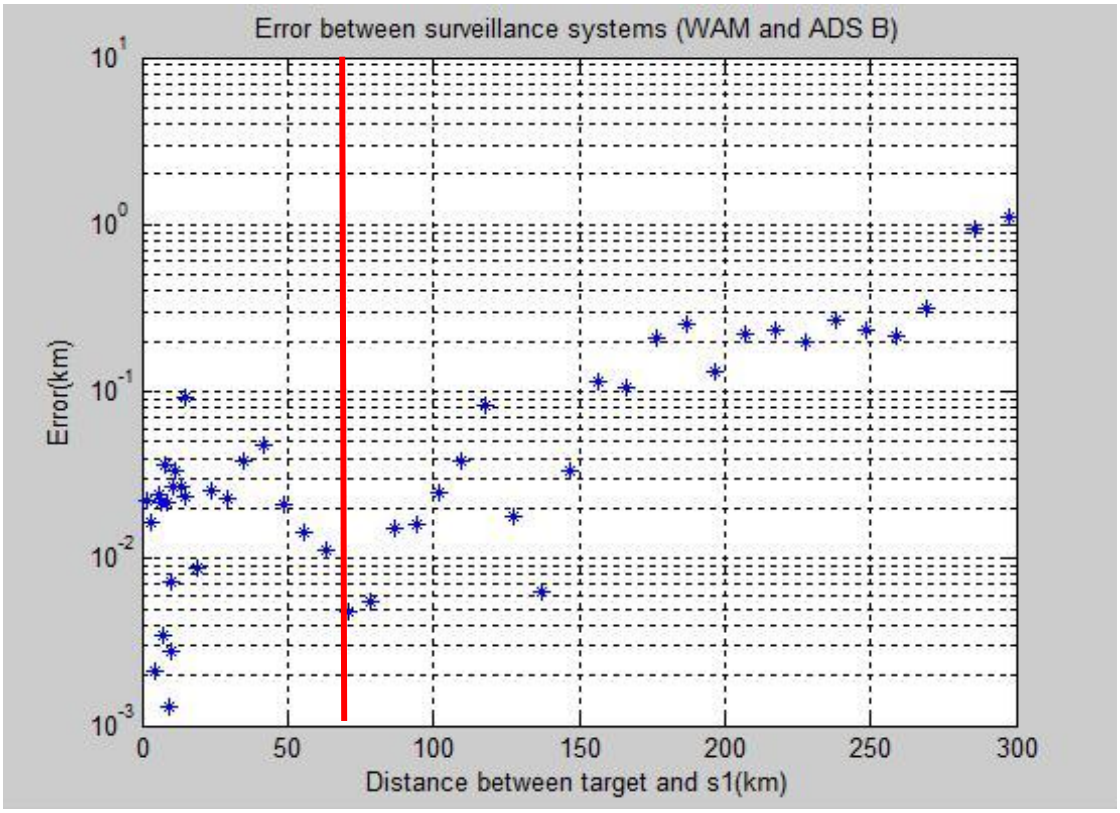

Figure 4.8 – Difference between WAM and ADS-B routes for Lisbon.

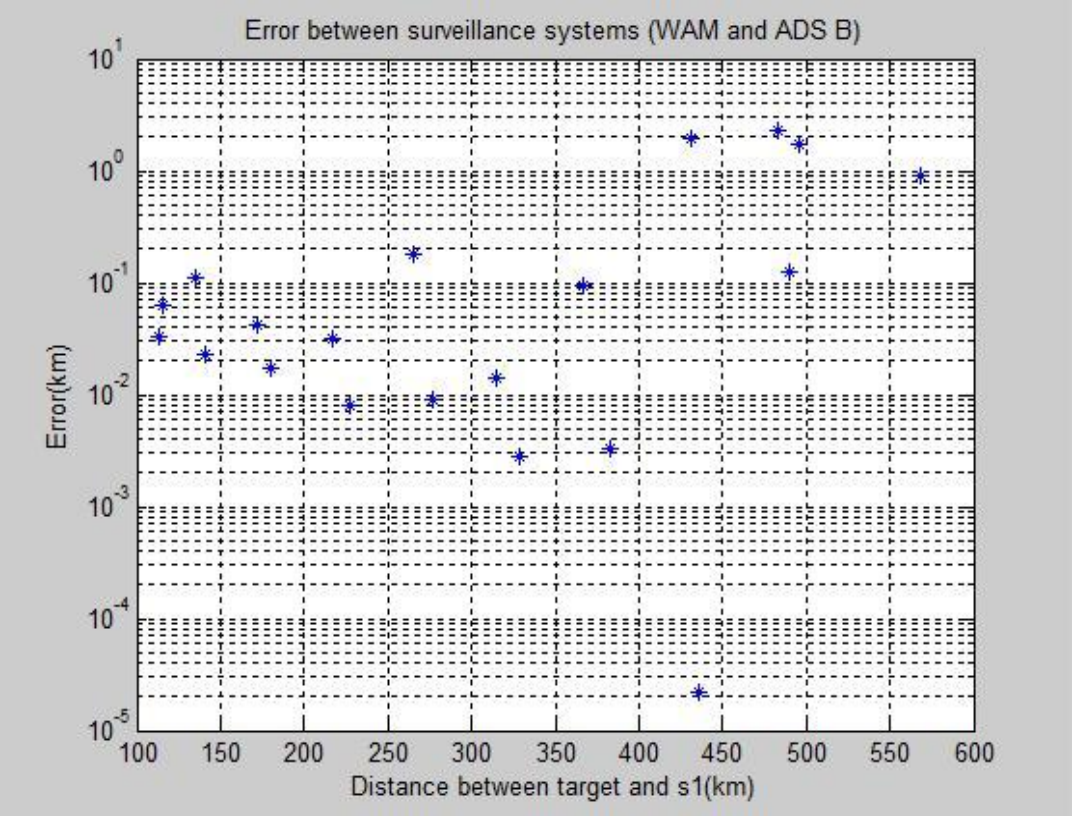

Figure 4.9 - Difference between WAM and ADS-B routes for Azores.

A statistical analysis to the Lisbon and Azores results was performed by using the *Curve Fitting Toolbox* of Matlab R2013b. After initially analysing the results, both Exponential and Normal Distribution were considered as possible best fits, but after computing the fitting distribution analysis, the Exponential distribution was chosen. The results for the goodness-of-fit parameters for the analysis of the difference between WAM and ADS-B routes results, for Lisbon and Azores regions, are presented in Table 4.4.

Table 4.4 - Comparison between Normal and Exponential distributions.

	Lisbon	Azores
Distribution	Normal	Normal
R-square	0.9466	0.8911
Adjusted R-square	0.9444	0.8888
RMSE [km]	0.0367	0.5362
Distribution	Exponential	Exponential
R-square	0.9381	0.8999
Adjusted R-square	0.9368	0.8979
RMSE [km]	0.0391	0.0469

The samples that were introduced in the *Curve Fitting Toolbox,* are presented in Figure 4.11 and Figure 4.12 respectively for the Lisbon and Azores regions. Most of the results presented in Table 4.4 came from these set of samples, Figure 4.11 and Figure 4.12, except the results for the Azores region for the Normal distribution; since in this case, the way that the samples were taken had to be rearranged, in order to become possible to compute with the Normal distribution: a mirrored version of

the initial sample was taken, Figure 4.10.

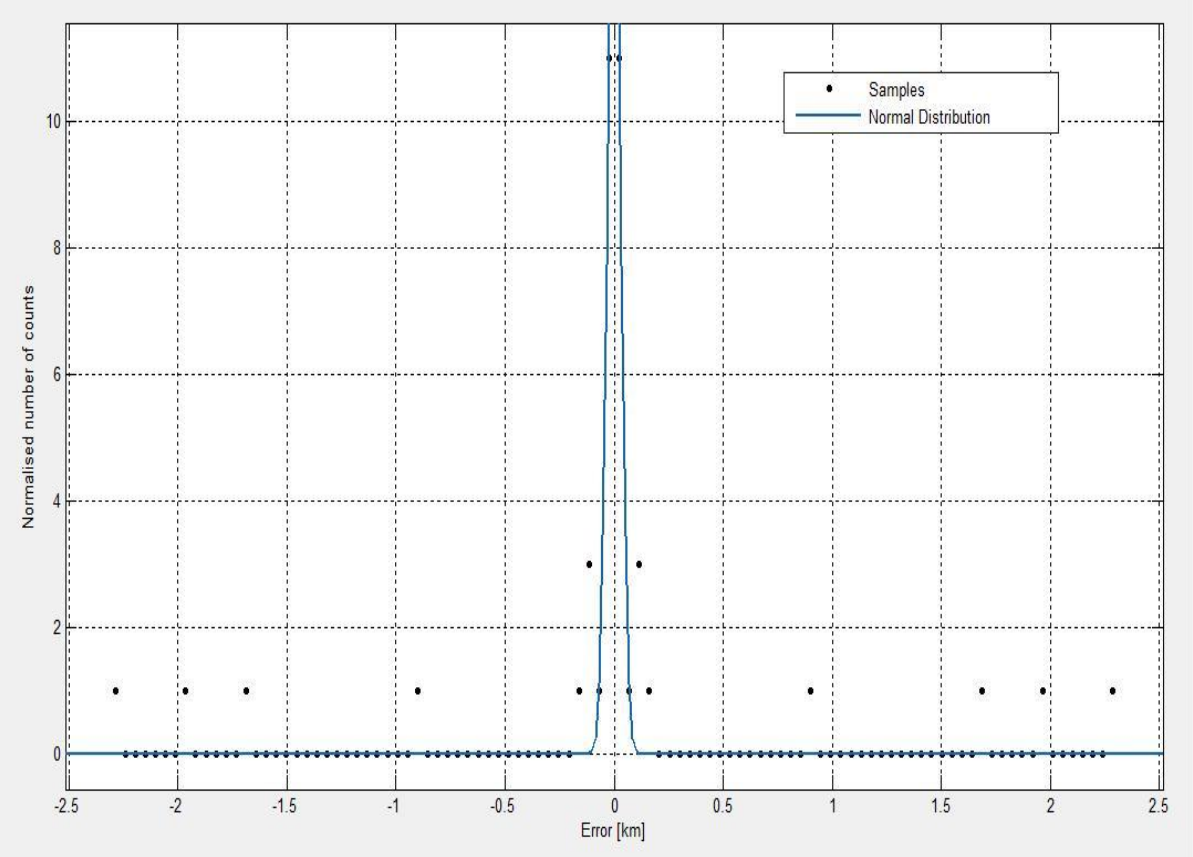

Figure 4.10 - Normalised number of measurements fitted with normal distribution for the Azores scenario.

After analysing the results from Table 4.4, it is possible to conclude that the Exponential distribution provides the best fitting results, being over all the best option for the fitting distribution to be used. Since the RMSE parameter, also known as the fit standard error, is an estimation of the standard deviation of the random component of the data [Mat15a], presenting a value not close to 0 in the Azores region and Normal distribution analysis, when comparing with the other results, is possible to say that the Exponential distribution is the best fit.

The information from Figure 4.8 and Figure 4.9 act as sample of experimental measurements that enter as input into the *Curve Fitting Toolbox*, then the normalised number of measurements is plotted, and in the end it is possible to analyse the variation of these values and obtain the best PDF.

By using the *Curve Fitting Toolbox* of Matlab R2013b to fit the samples with an Exponential distribution, it is possible to obtain the curve provided by (4.1), Figure 4.11 for Lisbon and Figure 4.12 for Azores [Mor10].

$$N(x) = \lambda \times e^{-\lambda x} \tag{4.1}$$

where:

- N : normalised number of measurements.
- λ : rate parameter.

- x : value of the samples.

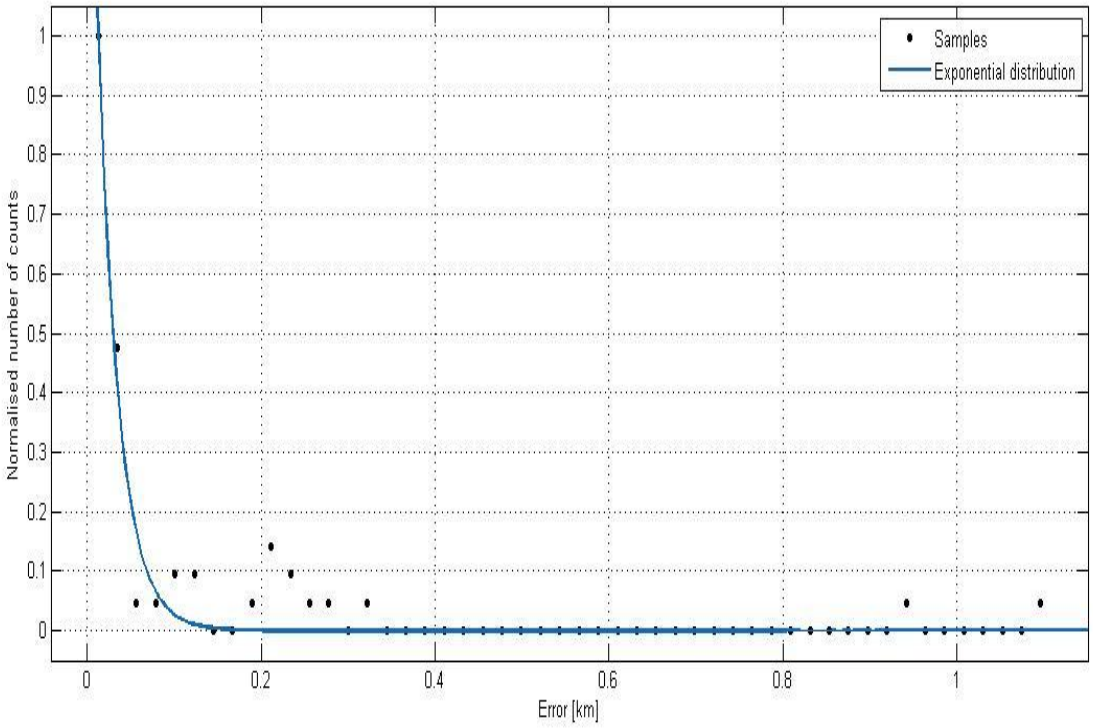

Figure 4.11 – Normalised number of measurements fitted with an exponential distribution for the Lisbon scenario.

As mentioned in Chapter 3, in order to validate the fittings presented in Figure 4.11 and Figure 4.12, it is necessary to check the goodness-of-fit statistics using the parametric models already defined in Section 3.3.1. By using the *Curve Fitting Toolbox* of Matlab R2013b, it is possible to obtain the results regarding the parametric models as in Table 4.5.

Table 4.5 – Goodness-of-fit parameters for Lisbon and Azores.

	Lisbon	Azores
R-square	0.9381	0.8999
Adjusted R-square	0.9368	0.8979
RMSE [km]	0.0391	0.0469

For both situations, it is valid to say that the R-square and the adjusted R-square present values close to 1 and a RMSE value very close to 0. These results mean that the fitting is appropriate to the set of samples. The fitting model applied to the Lisbon scenario explains 93.8% of the total variation in the data, and since the RMSE value is so close to 0, this indicates that the fit is useful for prediction. The fitting model applied to the Azores scenario explains 90.0% of the total variation in the data, and again the RMSE value being close to 0 indicates that the fitting is useful for prediction.

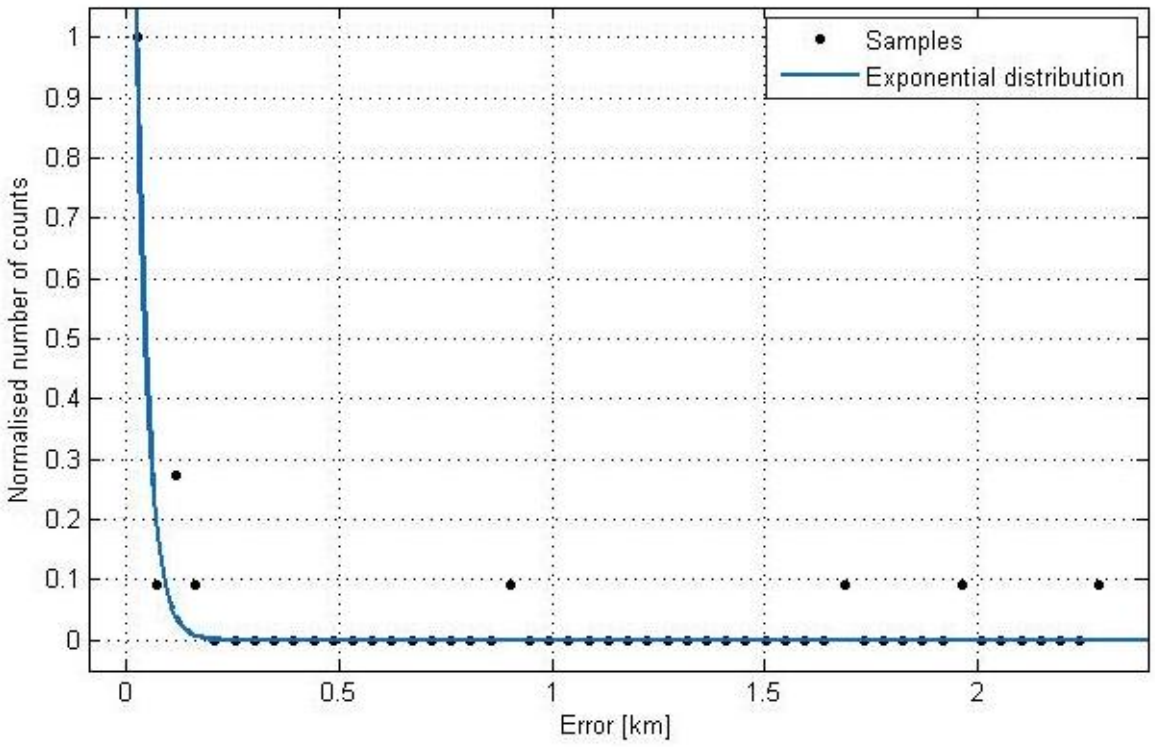

Figure 4.12 - Normalised number of measurements fitted with an exponential distribution for the Azores scenario.

4.3 Set of ground stations

From the results presented in this section, it is possible to observe the variation of the number of ground stations that belong to the set selected to determine an airplane's position.

After analysing the Lisbon route and the number ground stations used throughout the flight route, the results are presented in Figure 4.13.

A MLAT system works with a minimum of 3 ground stations in order to obtain a bidimensional location of an airplane [Air07], this situation occurs when an airplane is circulating on the ground. If the airplane is in navigation mode, that is circulating in airspace, the system requirements change, in order to the MLAT system perform is necessary to have a minimum of 4 ground stations to generate a tridimensional position of the airplane [Air07]. But to execute the MLAT system in the most accurately way the number of ground stations necessary is usually greater than 4. The number of ground stations used is related to the accuracy and reliability of the system. That said the number of ground stations increases as is required from the system to achieve higher performance values.

From the results presented in Figure 4.13, it is possible to observe that for this Lisbon route, when the airplane navigates at distances above 100 km from the reference point, the number of used ground stations varies in between 4 and 6, in the majority of the cases. When this distance decreases to the

interval [25, 100] km, the number of ground stations varies mostly in between 6 and 8. Finally, when the airplane is approaching the reference ground station, the number of ground stations varies mostly, from 4 to 8.

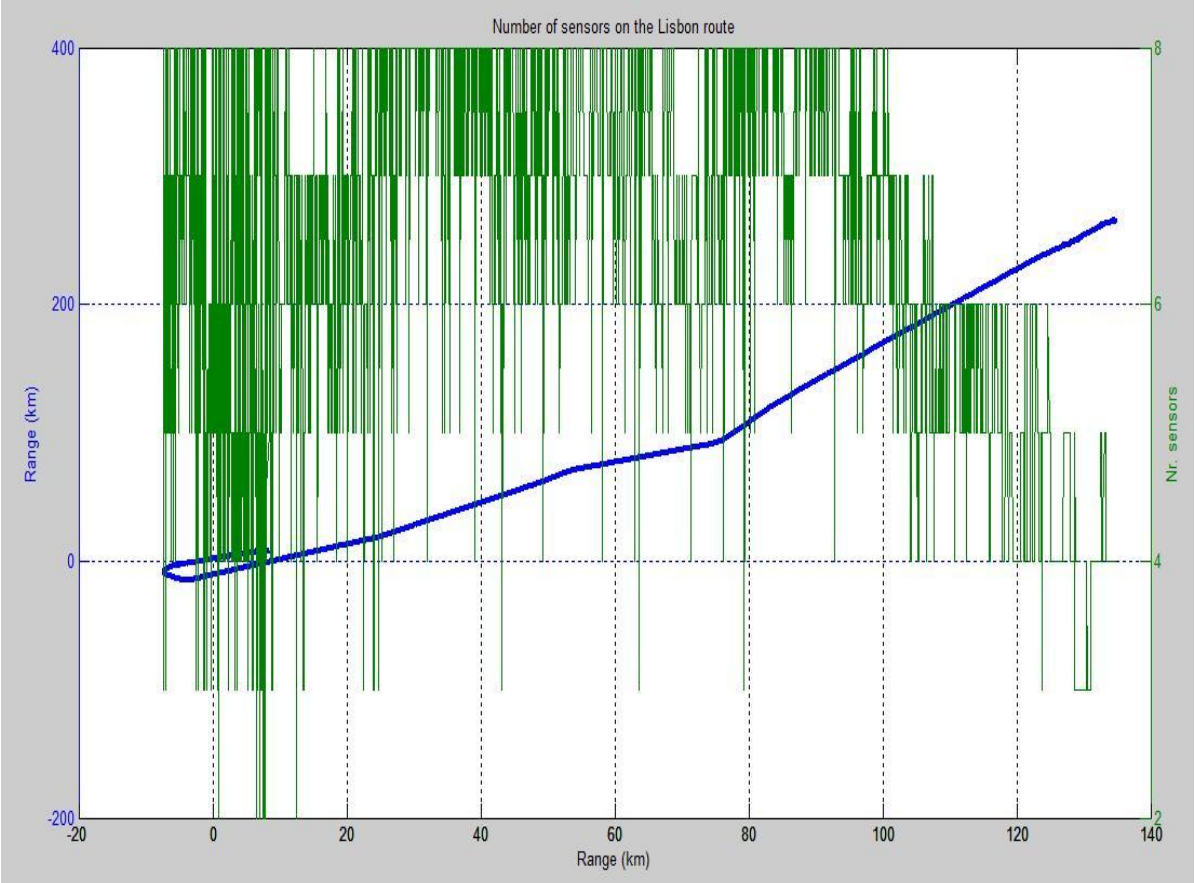

Figure 4.13 – Number ground stations used throughout Lisbon route.

Since the Lisbon system is designed to perform on a 30NM radius, under this 55km radius it is possible to observe, Figure 4.13, that as the airplane navigates in the interval [25, 55] km, the number of ground stations varies between 6 and 8 confirming that more ground stations are necessary to achieve higher performance values. And as the airplane approaches the reference ground station, and therefore gets closer to the airport ground, the number of ground stations needed to perform the TDOA algorithm decreases confirming that when an airplane circulates near the ground less ground stations are needed for the system to perform. This confirms that the simulations results are validated by the theoretical results.

In Figure 4.14, a similar analysis is performed, taking the number of ground stations used to determine an airplane's position versus the distance from that airplane position to the reference ground station. It is possible to observe a trend in the results, the number of ground stations used to implement the TDOA algorithm increasing as the distance between the airplane and the reference ground stations decreases. When the airplane assumes a distance from the reference equal or greater than 200 km, the number of ground stations varies between 4 and 6, in most of the cases, but when this distance assumes values between 50 km and 150 km, the number of ground stations varies between 6 and 8, and when it is below 50 km the number of ground stations can be from 4 to 8.

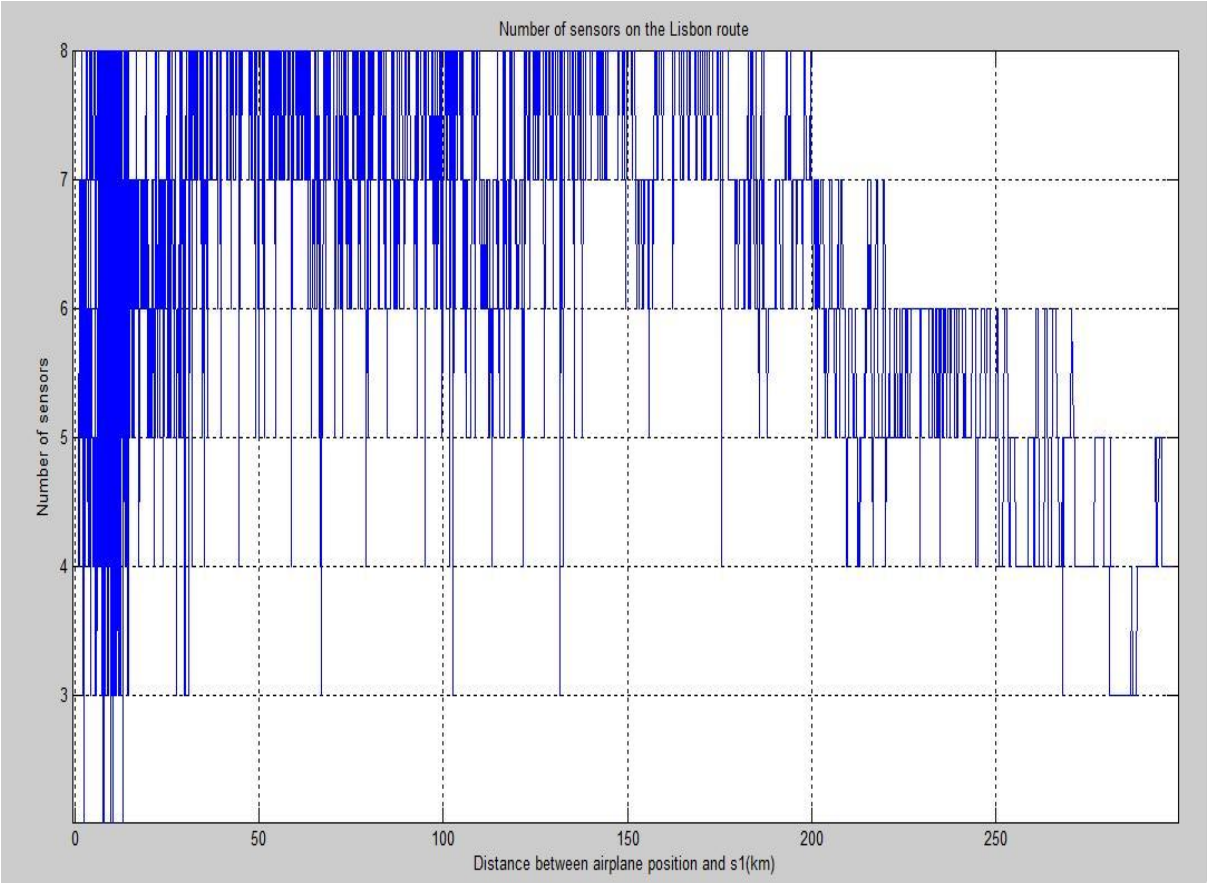

Figure 4.14 – Number of ground stations versus distance between airplane and reference ground station, Lisbon scenario.

Since the information regarding the set of ground stations used in the MLAT process is provided by the WAM route file, the same type of analysis was performed for the Azores scenario, the results being presented in Figure 4.15: from left to right, one can see that in the interval [250, 300] km, the interval in which the airplane is the farthest from the reference ground station, the number of ground stations varies from 4 to 5: in [200, 200] km, this number values between 5 and 10; when the airplane gets closer to the ground stations, in [50, 200] km, the number of ground stations increases to vary between 10 and 15: and finally, towards the end of the flight route, in [0, 50] km, the number of ground stations decreases to vary from 5 to 10. In conclusion, when the airplane navigates towards the reference ground station, the number of ground stations used increases.

In Figure 4.16 a similar analysis is performed, on the number of ground stations used to determine an airplane's position versus the distance from that airplane to the reference ground station. It is possible to observe a trend in the results, the number of ground stations used to implement the TDOA algorithm increasing as the distance between the airplane and the reference ground stations decreases. When the airplane assumes a distance from the reference equal or greater than 500 km the number of ground stations varies between 4 and 5, in most of the cases; when this distance assumes values between 350 km and 550 km, this number varies between 4 and 10, while when this distance assumes values between 150 km and 300 km, the number varies between 9 and 12, and when it is below 150 km the number ranges between 12 to 15.

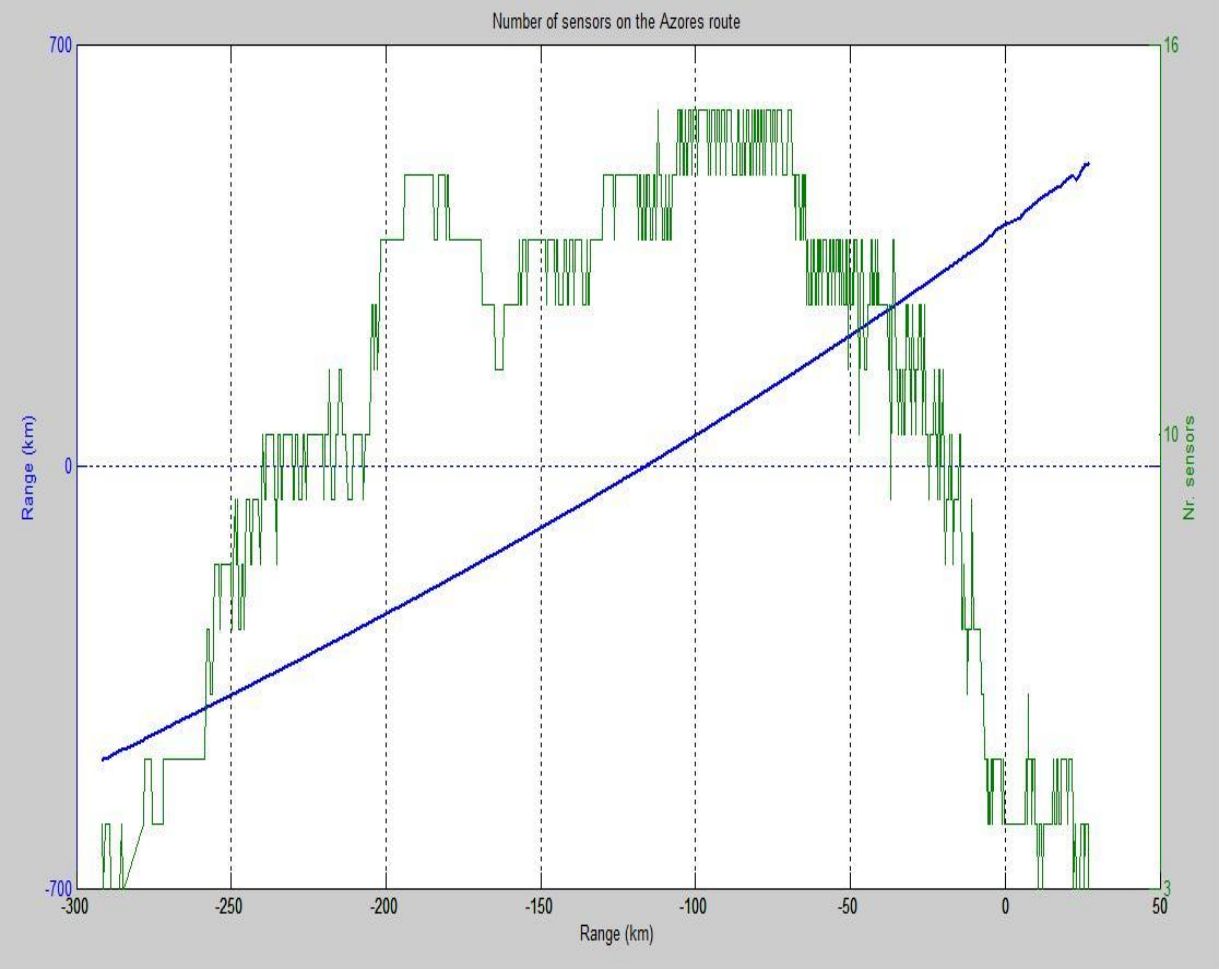

Figure 4.15 - Number ground stations used throughout Azores route.

After analysing the results for the Lisbon and Azores, the same conclusions are reached. As the distance between the airplane position and the respective reference ground station decreases, the number of used ground stations increases, and when the airplane reaches the minimum distance, the maximum number of used ground stations is reached.

4.4 Error analysis

This section is dedicated to the analysis of the maximum error achieved when calculating an airplane position, as explained in Section 3.2.

In this section, one presents results for Lisbon and Azores. In order to correctly determine and analyse the evolution of the error throughout the considered routes, it is necessary to know the set of ground stations used in each route position, Figure 4.17.

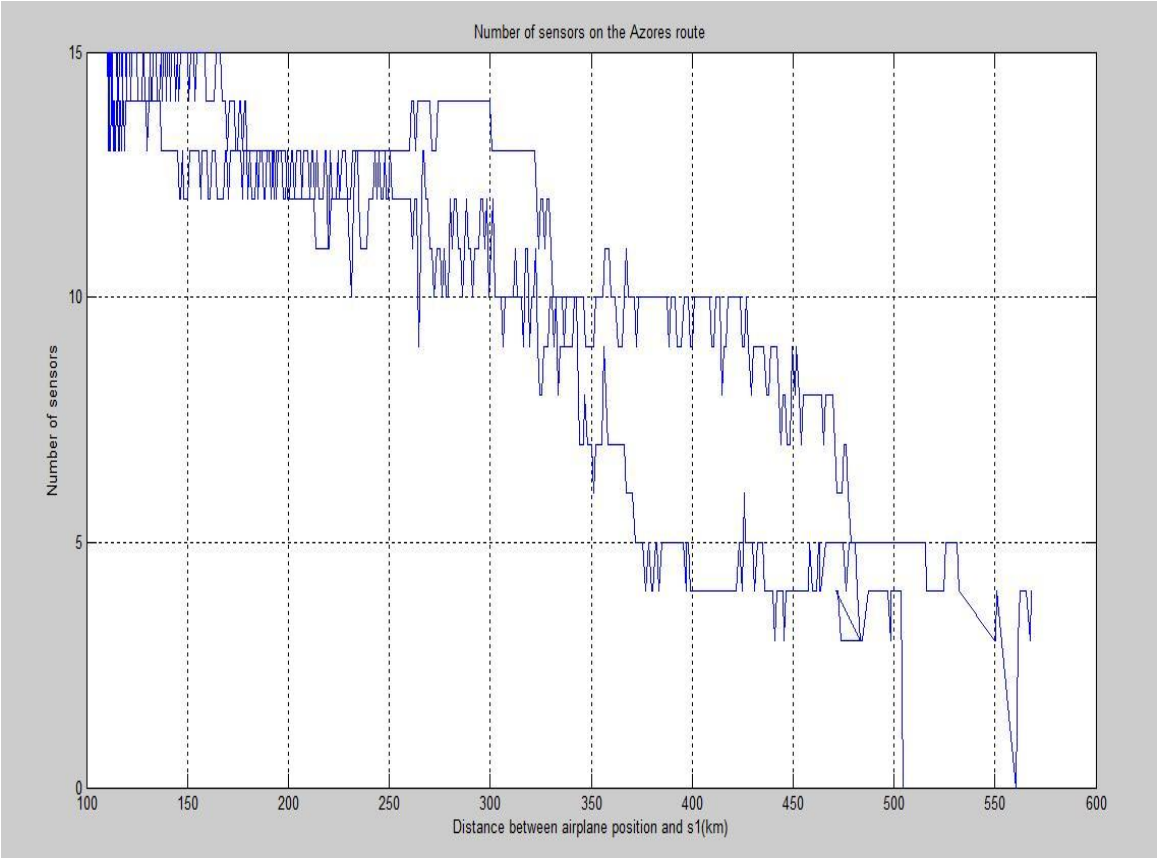

Figure 4.16 - Number of ground stations versus distance between airplane and reference ground station, Azores scenario.

In Figure 4.17, one of the first stages of the simulation results is represented, where it is possible to find the flight route that has been loaded to execute the simulation, all the ground stations that belong to Lisbon, the airplane position that has been taken under analysis, and the set of ground stations used to perform the TDOA algorithm for that airplane's position.

In Figure 4.18, the positions marked in Figure 4.17 are put into evidence, in order to facilitate the visualisation of the hyperbolas that are formed next.

From the set of ground stations information, the hyperbolas are formed, but depending on the error value applied to the hyperbolas, two different outcomes are possible: on the one hand, if the error is equal to zero, all hyperbolas should intersect in one point, which corresponds to the airplane's position, validating that the simulator is well developed, Figure 4.19; on the other hand, if the error is not equal to zero, the hyperbolas intersection results in an area, Figure 4.20, similar to the one in Figure 3.2.

In Figure 4.20, it is possible to determine the uncertainty area and, consequently, the point of this area that is the farthest from the airplane's position, which is the one considered to be the maximum error that the airplane's position can reach. In order to evaluate the variation of the maximum error throughout Lisbon's and Azores' routes, measurements were made.

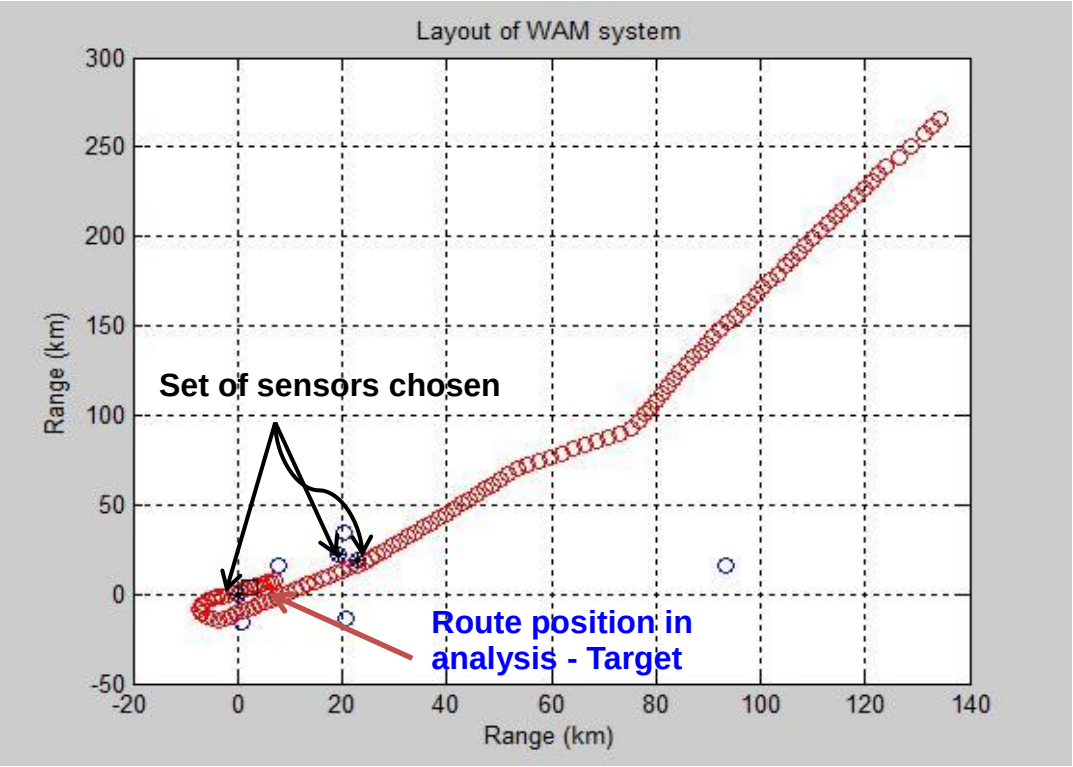

Figure 4.17 – Selection of ground stations for one route position, Lisbon.

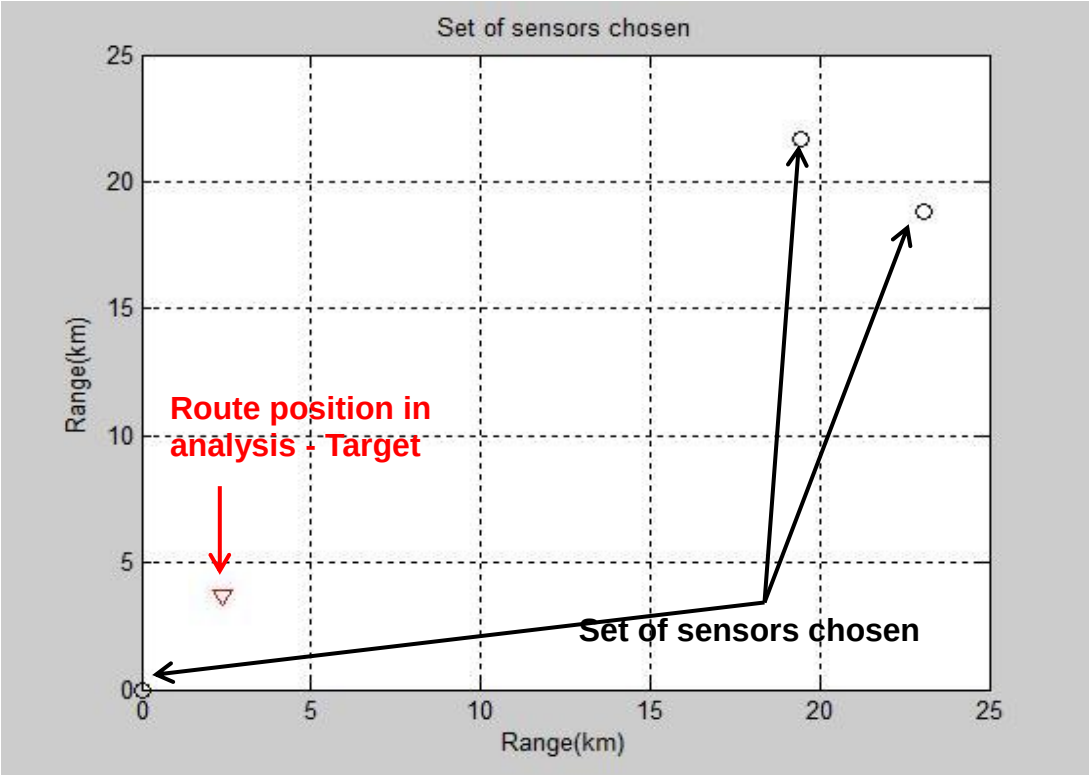

Figure 4.18 – Ground stations selected to determine the airplane's position, Lisbon.

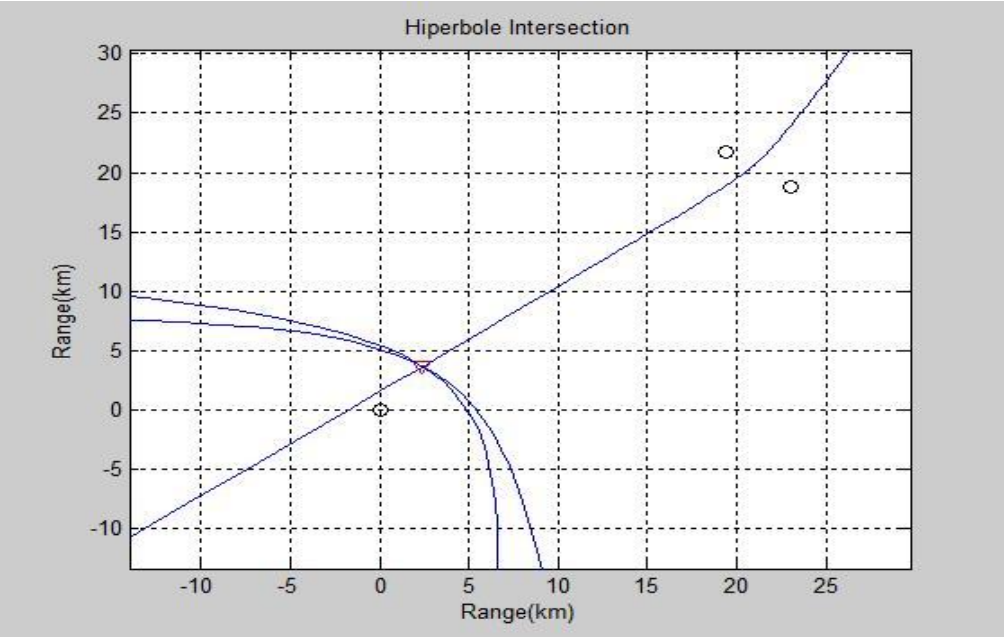

Figure 4.19 – Hyperbolas intersection with error equal to zero.

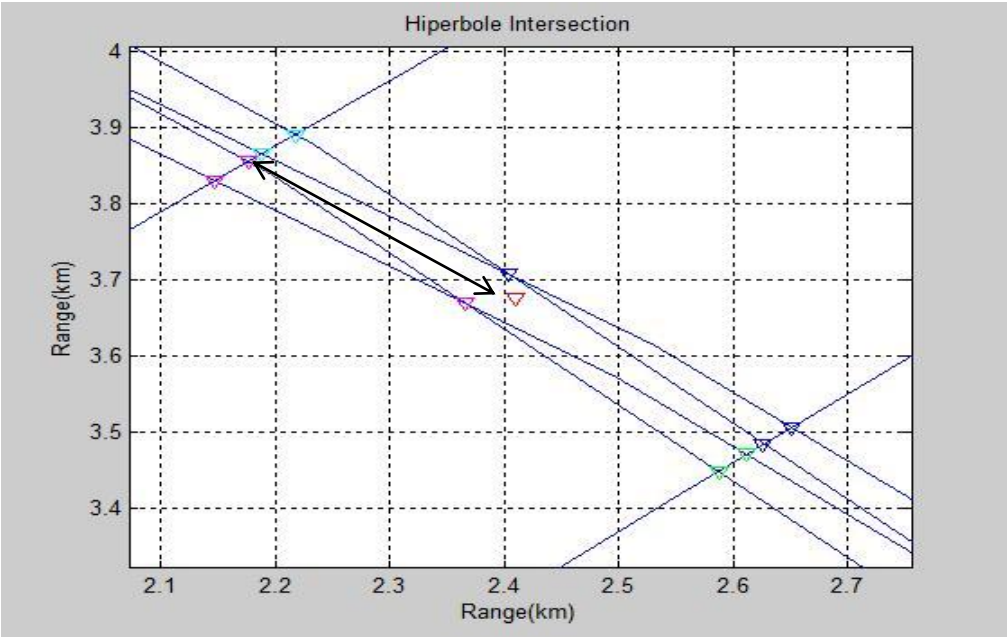

Figure 4.20 – Uncertainty area.

Table 3.1 presents the types of errors in detail, and all their contributions to the total value of the error. The summation makes up the final value of 52 m [Err06], but following a NAV's recommendation, the value considered in the simulator was half of the original, meaning that for the calculations regarding the error from this point forward, the value of the error is 25 m. It was necessary to adjust the value of the error, because after performing the first set of simulations with the Lisbon route and error equal to 52 m the results were not as expected, therefore, an adjustment was made to the error value. This adjustment happens because the true value used by the MLAT system manufacturer is not available, so corrections were made in order to achieve the results known from the actual system.

In Figure 4.21, it is possible to observe the variation of the maximum error with an error value equal to 52 m and 25 m. The error decreases as the airplane gets closer to the ground stations. And as the boundaries, i.e., hyperbolas that result from the error introduction (Figure 3.2) get smaller due to the transition from 52 m to 25 m, the result for the maximum error also decreases.

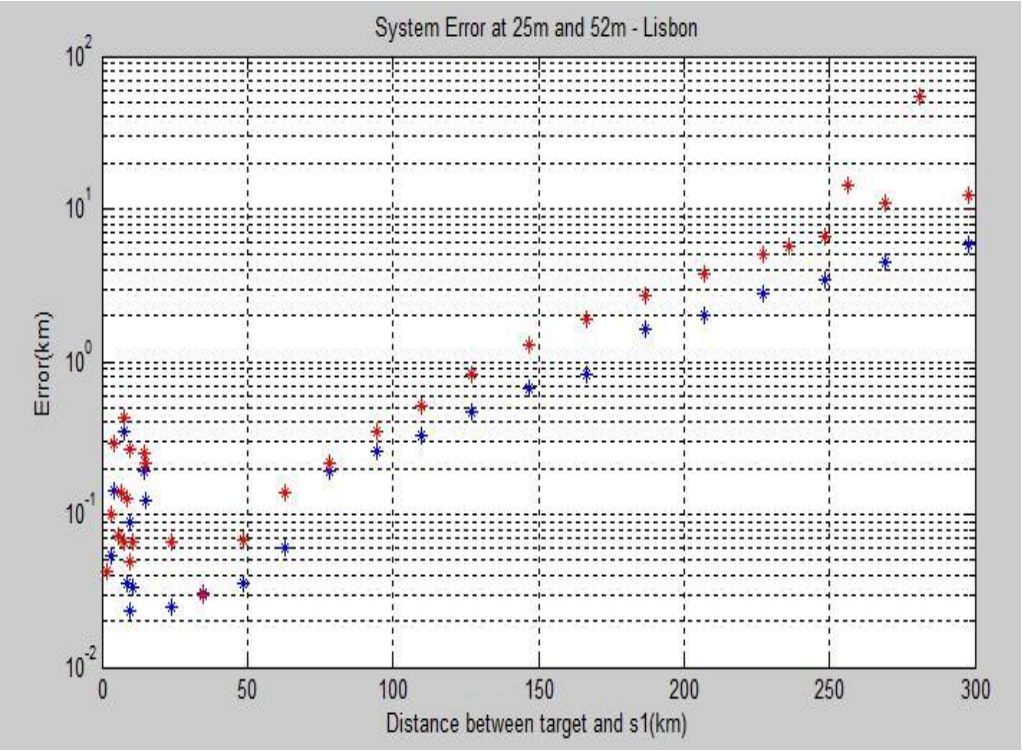

Figure 4.21 – Comparison of results applying different error values, 25 m (blue) and 52 m (red), for the Lisbon scenario.

Figure 4.22 presents the simulation results for the Lisbon scenario using an error value of 25 m and Figure 4.23 the ones for the Azores, under the same conditions. In both scenarios, Lisbon and Azores, it is possible to verify, Figure 4.22 and Figure 4.23, respectively, that the error position results follow the same trend. As the distance between airplane and reference ground station get smaller, the values of the airplane's position error also decrease. Corresponding the minimum error value to the minimum distance between airplane and reference ground station.

In figure 4.22 it is possible to observe that in the interval between [0, 50] km, the results for the error associated to the airplane's position suffers a slight elevation. This results from the curvature that the Lisbon's route takes in this interval, Figure 4.2.

In Figure 4.23 it is clear to observe the decrease of error's value as the airplane navigates towards the ground stations. Assuming at the minimum distance between airplane and reference ground station, the error values are less than 100 m.

As in Section 4.2, a statistical analysis is done, by using the *Curve Fitting Toolbox*, to the results obtained and presented in Figure 4.22 and Figure 4.23. As previously, the Exponential distribution was used, PDF and the fitting curve being shown in Figure 4.24 for Lisbon and in Figure 4.25 for the Azores.

As mentioned before, in order to validate the fittings presented it is necessary to check the goodness-of-fit statistics using the parametric models already defined in Section 3.3.1. By using the *Curve Fitting Toolbox* of Matlab R2013b, it is possible to obtain the results regarding the parametric models, Table 4.6.

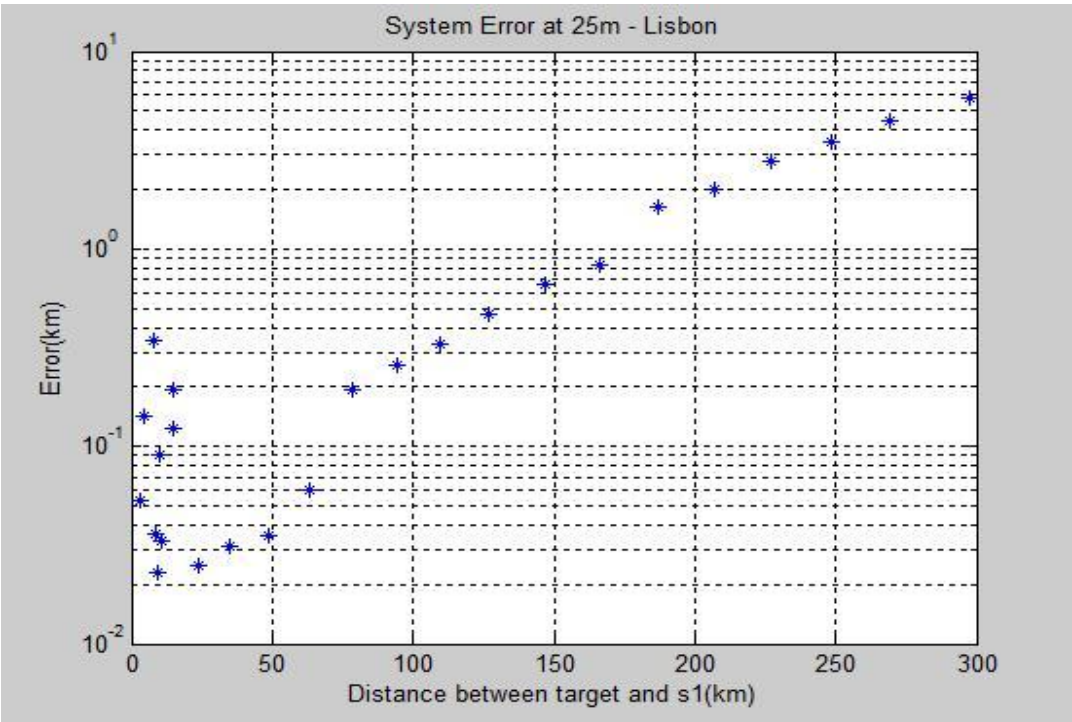

Figure 4.22 – Lisbon simulation results with error at 25 m.

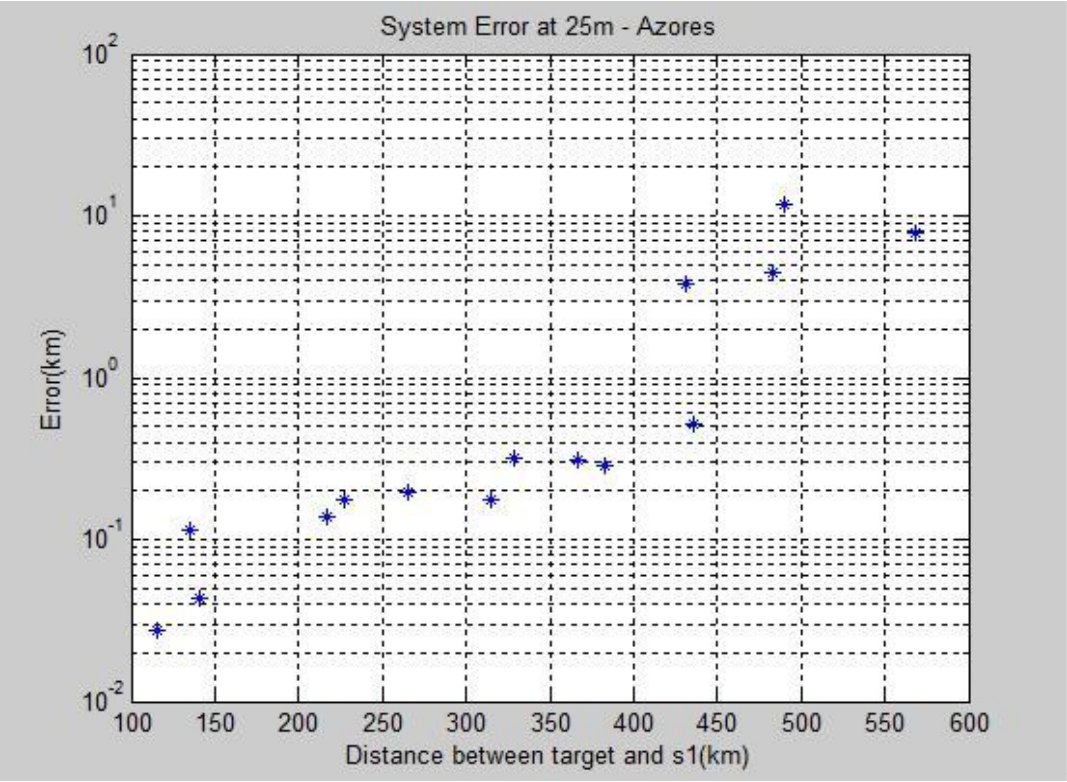

Figure 4.23 - Azores simulation results with error at 25 m.

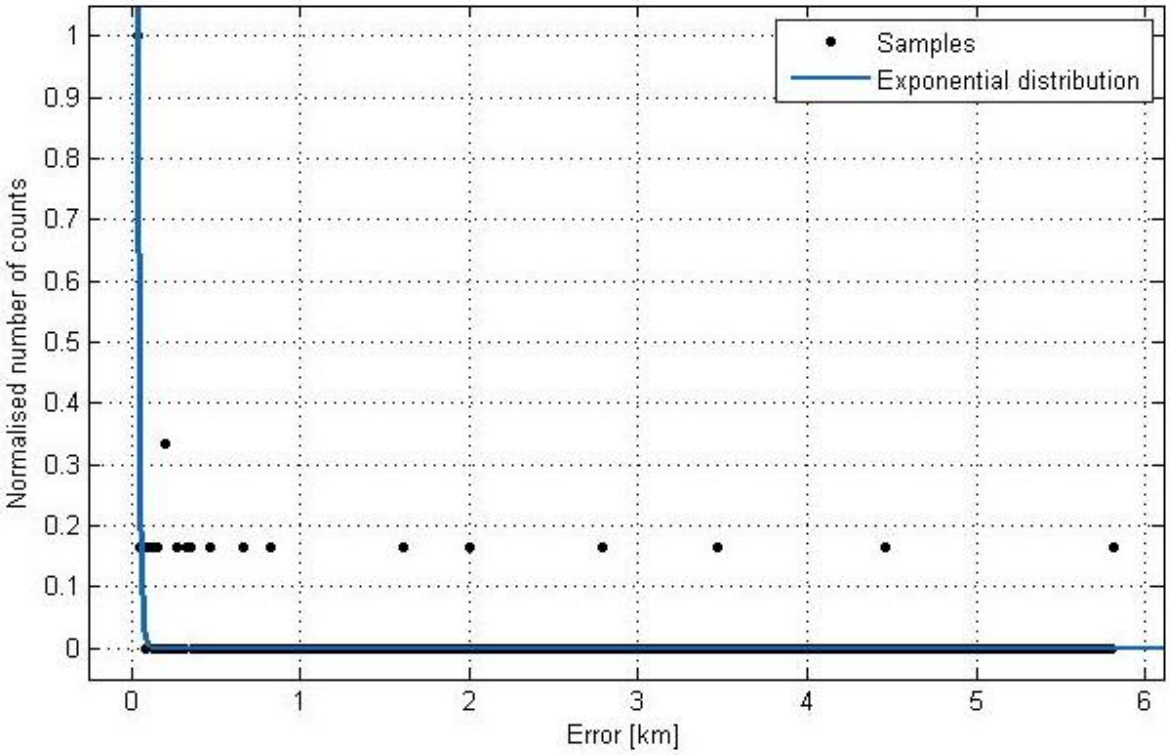

Figure 4.24 – Lisbon results with error equal 25 m.

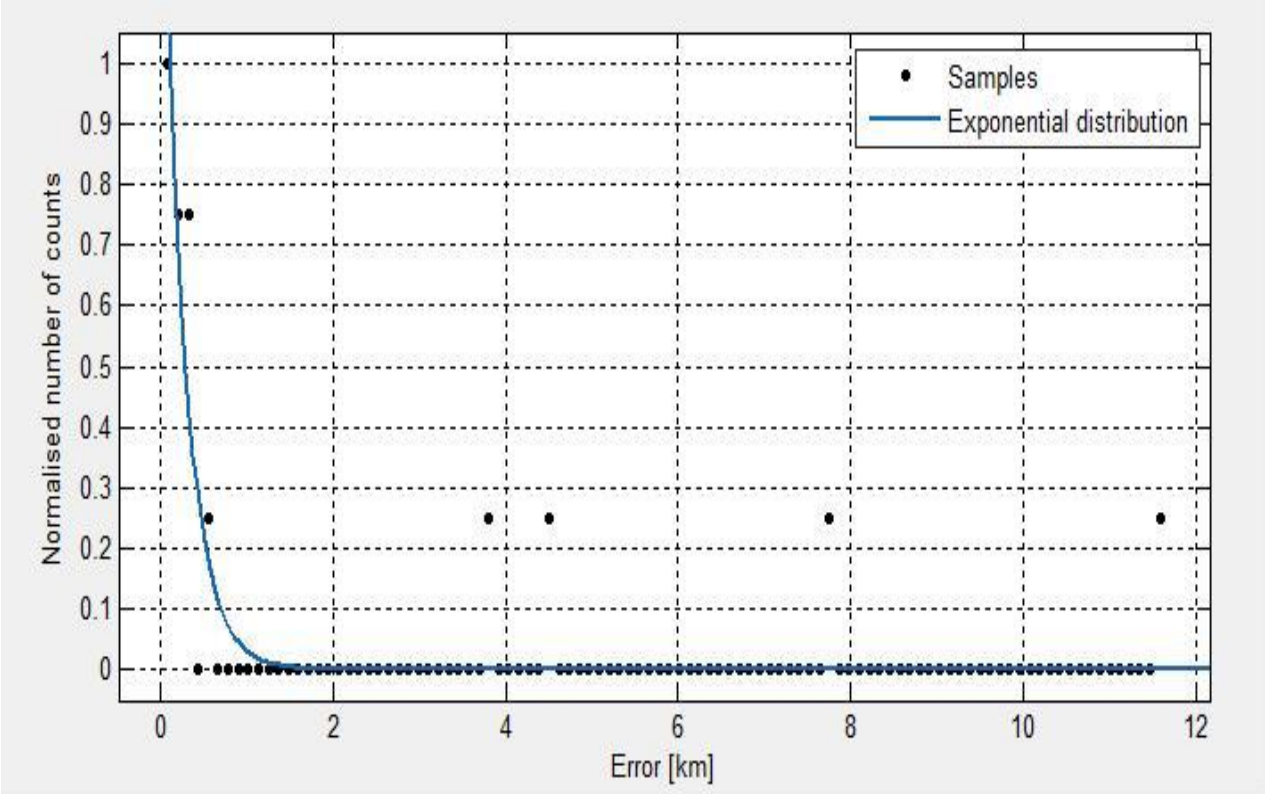

Figure 4.25 - Azores results with error equal 25 m.

Table 4.6 - Goodness-of-fit parameters for the error analysis with error equal to 25 m.

	Lisbon	Azores
R-square	0.6455	0.7988
Adjusted R-square	0.6445	0.7967
RMSE [km]	0.0395	0.0686

The fitting model applied to Lisbon scenario explains 64.6% of the total variation in the data, and when applied to the Azores it explains 79.9%; since the RMSE value is so closer to 0, this indicates that the fitting is useful for prediction.

4.5 Porto analysis

Since the WAM system for the Porto region is not fully implemented, the goal of this section is to determine the set of ground stations that provide the best result for each of the airplane's position in the route under analysis, as explained in Section 3.2.2.

Following a NAV recommendation for the Porto region analysis, for each airplane's position in the ADS-B route, the distance between all ground stations and the airplane's position was calculated via (3.1), and the 6 ground stations that are closer to the airplane's position were selected. Finally, from this 6 ground stations, the set that provides the best solution was chosen.

In order to achieve this goal, a set of different combinations using (3.6) was taken, resulting in a series of subsets of k distinct elements of the selected 6 ground stations, k assuming a value from 4 to 6, resulting in a total of 22 possible combinations:

- $C_4^6 = \binom{6}{4}$ results in 15 possible combinations of 4 elements taken 6 ground stations at a time.
- $C_5^6 = \binom{6}{5}$ results in 6 possible combinations of 5 elements taken 6 ground stations at a time.
- $C_6^6 = \binom{6}{6}$ results in 1 possible combinations of 6 elements taken 6 ground stations at a time.

For each of the 22 possible ground stations combinations, the maximum error that an airplane's position can achieve was calculated. Finally, the combination that presents the minimum error value is considered to be the set of ground stations to be recommended to be used for the WAM system for that particular airplane's position.

In Figure 4.26, it is possible to observe the results achieved for the minimum error and in Figure 4.27 the number of ground stations that provides that optimum result. As expected, as the distance between the airplane and the ground stations gets smaller, the error associated with the airplane's position decreases. After collecting the information from the results presented in Figure 4.26 and

Figure 4.27, it is possible to obtain the recommendations for the Porto WAM system, Table 4.7.

Table 4.7 – Combinations of ground stations chosen.

Minimum Error		
Number of ground stations	Ground stations combination	Airplane position in route
5	RU01 RU03 RU05 RU07 RU09	1
5	RU02 RU05 RU07 RU09 RU11	101
5	RU01 RU07 RU09 RU11 RU12	201
5	RU02 RU07 RU09 RU11 RU12	301
6	RU01 RU02 RU07 RU09 RU11 RU12	401
6	RU01 RU02 RU08 RU09 RU11 RU12	501
5	RU01 RU02 RU08 RU11 RU12	701
4	RU01 RU02 RU11 RU12	901
5	RU01 RU08 RU09 RU11 RU12	1001
5	RU01 RU06 RU08 RU11 RU12	1301

In Figure 4.6 it is possible to identify where the airplane positions mentioned in Table 4.7 are located in the Porto flight route.

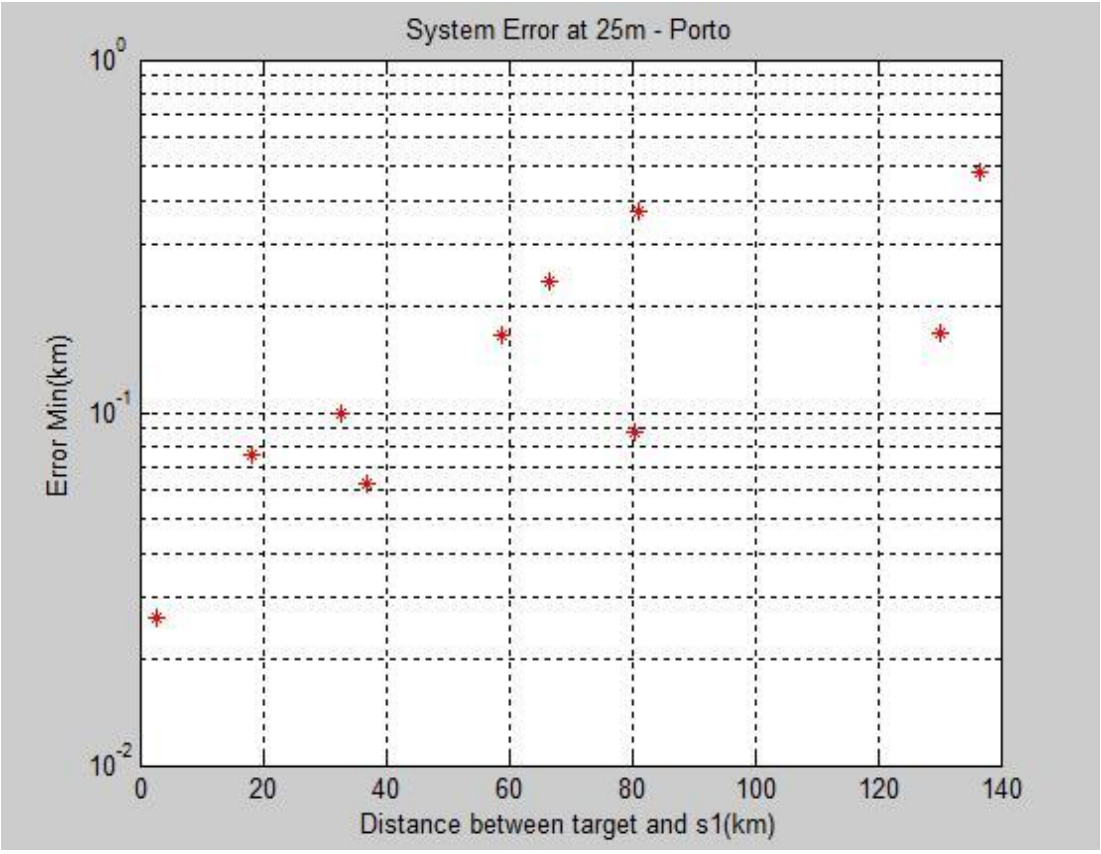

Figure 4.26 – Minimum error associated with each airplane's position.

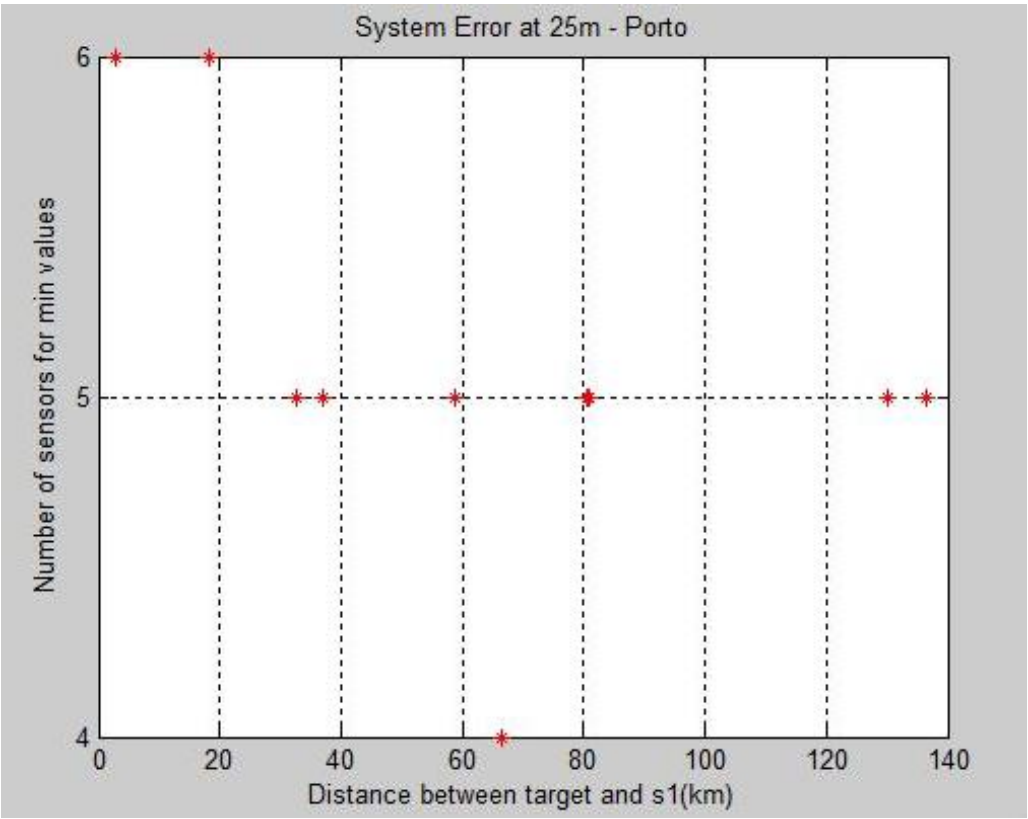

Figure 4.27 – Number of ground stations that provide the minimum error.

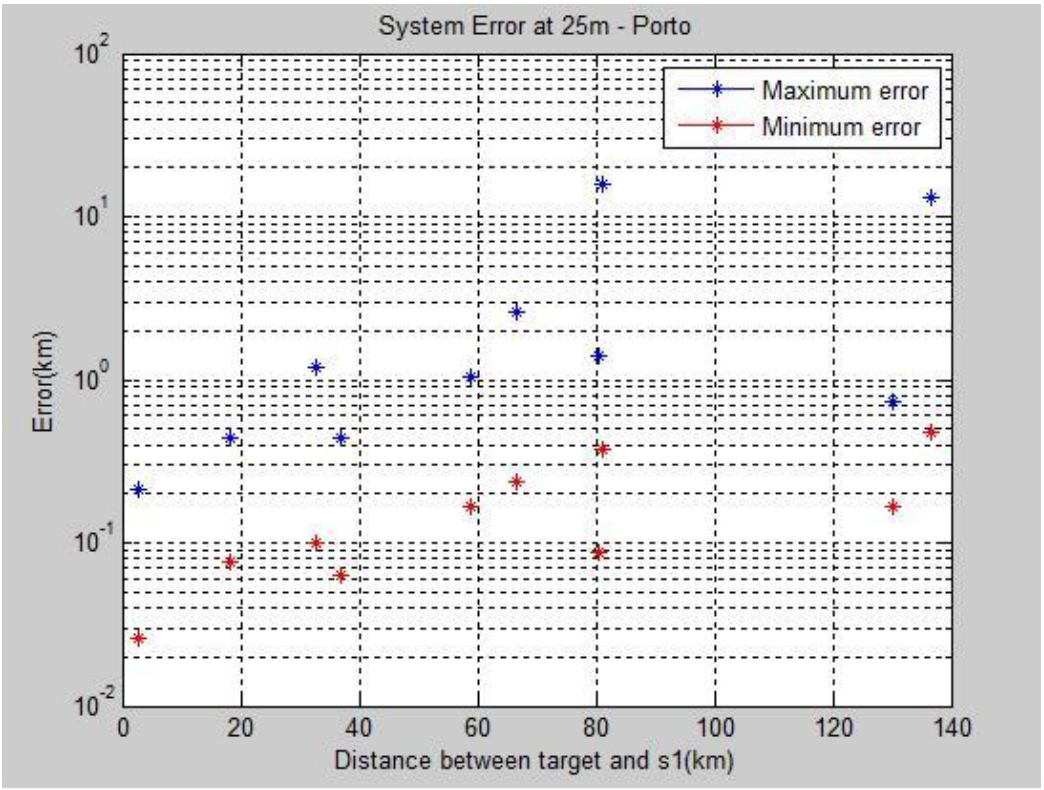

Figure 4.28 – Comparison of results regarding the maximum and minimum error associated with each airplane's position.

From Figure 4.28, it is possible to perform the comparison of results between the minimum and the maximum error associated with an airplane's position when analysing the Porto route provided for simulation. As presented in Figure 4.27, a similar analysis was done in order to obtain the number of ground stations that provide the maximum error, Figure 4.29. It is possible to observe that this results always in a combination of 4 ground stations, because, as expected, this number of intersecting hyperbolas increases the uncertainty area, so if the goal is to find the maximum error, it is crucial to find the largest areas, therefore, the area formed by the smallest number of hyperbolas and, consequently, the smallest number of ground stations.

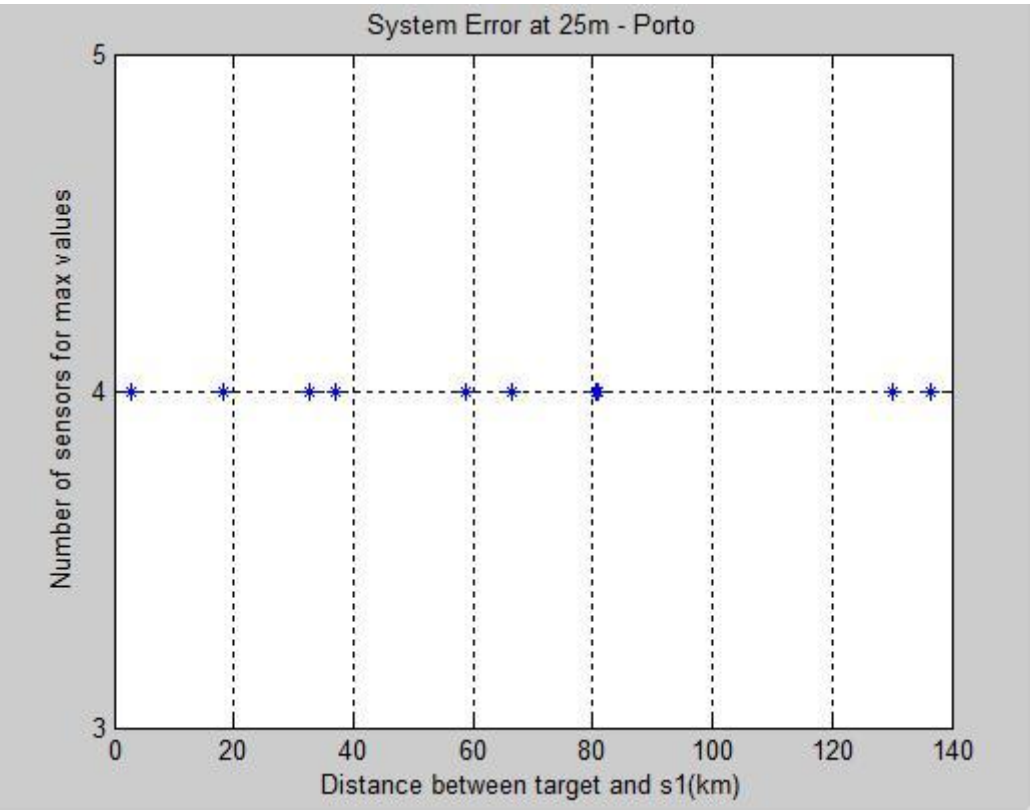

Figure 4.29 - Number of ground stations that provide the maximum error.

As mentioned in Chapter 3, the total time to execute a single simulation is around 2 hours. Since the developed simulator is divided in 6 main blocks, Figure 3.10, the system description block, the airplane route block, the analysis block and the result analysis block have a simulation time less than 5 minutes, and the remaining blocks, i.e., the system dimensioning block, has a simulation time around 2 hours.

Chapter 5

Conclusions

This chapter finalises this work, summarising conclusions and pointing out aspects to be developed in future work.

The main goal of this thesis was the study of multilateration systems, focusing on the assessment of the performance of the systems installed in Portugal, in Lisbon and Azores, and some design recommendations for the Porto WAM system.

In the first chapter, a description of the different types of surveillance technologies available and the evolution of this technology throughout the years is provided. It is followed by an explanation about the motivation and contents of this thesis.

Chapter 2 addresses 4 different subjects: different types of air surveillance using radar, multilateration systems, requirements and specifications of spatial and temporal resolution, and state of art. The differences, advantages and limitations, which are associated with the PSR, SSR and ADS surveillance systems, are presented. The description of the technology and the algorithms used on the MLAT system application, from the frequency in which the messages are received to the different types of clock synchronisation systems available, are presented. Finally, on the spatial and temporal resolution section, the requirements of the MLAT system are described, followed by a brief state of the art.

In Chapter 3, the mathematical formulation and implementation of the models are explained in detail. The models allow the determination of the airplane´s position, the determination of the uncertainty area of an airplane's position that translates into the error associated with that position, the disclosure of the errors that interfere with the MLAT system performance, and to calculate the difference between WAM and ADS-B routes.

The developed models and algorithms are used to analyse two different situations. One in which the difference between WAM and ADS-B routes is calculated, and another in which the maximum error that an airplane's position can take is calculated. This second analysis is applied in two different scenarios, One in which all the information related to the used ground stations and the airplane's routes from WAM and ADS-B systems are available, and another in which the only information available is the airplane ADS-B route, and because of that, the analysis is a dimensional one of the set of ground stations that is used in order to minimise the system's error.

The analysis and system dimensioning algorithms are fundamental to perform the error analysis and consequently to study system performance. The analysis algorithm was developed to load and select the necessary information to build the hyperbolas, the WAM and ADS-B routes being the input and as output one gets the distances between all ground stations and the airplane's position. The dimensioning algorithm was developed to build the hyperbolas necessary to determine the uncertainty area and to complement the analysis algorithm, being possible to complete the process of error determination. The dimensioning algorithm has as input the ground stations information and the airplane's position, from which the hyperbolas are created, and finally a certain error is applied to the hyperbolas. This error can be equal to or different from 0: if it is equal to 0, all the hyperbolas intersect in one point, which is the airplane's position, implying that the multilateration system is well implemented in the simulator; if it is different from 0, all the different pairs of hyperbolas associated with the error intersect and create an uncertainty area, in which the maximum error that an airplane

can have at that particularly moment is found.

Finally, the selection algorithm is used when the WAM route information is not available, and therefore the set of ground stations that are used for each airplane's position is not known. The ADS-B route being data the only information available, the goal is to find through combinatorial analysis the different sets of ground stations that can provide a minimum error associated with a given airplane's position.

Through the developed algorithms, i.e., the difference between WAM and ADS-B routes algorithm, analysis and system dimensioning algorithms, and selection algorithm, it was possible to implement the described models in a logical way. Having all the necessary pieces to assemble the simulator, the simulator was developed and prepared to provide the output results for each of the different scenarios and situations to be analysed. From this simulator, it is possible to obtain results for the maximum error of an airplane's position throughout the flight route and the differences between WAM and ADS-B routes.

In Chapter 4, the results for the Lisbon, Azores and Porto scenarios are presented. For each scenario, the flight route under analysis, the number of ground stations, and the locations of the ground stations are different. For example, the Lisbon scenario has 8 ground stations, Azores has 17, and Porto 12.

A more detailed analysis of each conclusion follows:

- From the difference between WAM and ADS-B routes and the Lisbon and Azores scenarios analysis, it is possible to achieve the same set of conclusions: as the airplane gets closer to the ground stations, the difference between the routes decreases. After using the *Curve Fitting Toolbox*, it is safe to say that the Exponential distribution provides a good fitting, since for Lisbon the R-square is equal to 0.938 and for Azores it is 0.900.
- Regarding the set of ground stations analysis for the Lisbon and the Azores scenarios, it is possible to conclude that the number of ground stations used for the implementation of the TDOA algorithm varies throughout the flight route, but this variation follows the same trend: the number of ground stations increases as the distance between the airplane and the reference ground station deceases.
- When evaluating the results of the maximum error that an airplane can achieve for Lisbon and Azores, the conclusions are the same. In both scenarios, the value of the error added to the system is equal to 25 m, and under these conditions the obtained results are satisfactory. The error associated with Lisbon decreases as the airplane navigates towards the reference ground station, and when analysing the area under the 30 NM radius, the error presents values under 100 m. A similar analysis for the Azores leads to the same conclusions, but under a different radius area, this time a 100 NM radius, the error presents values under 300 m. In both cases, the results obtained from the simulator meet the margins recommended by NAV. After using the Curve Fitting Toolbox, the Exponential distribution provides a fitting model that explains 64.6% of the total variation in the data for Lisbon and 79.9% for the Azores.
- The results of the analysis for Porto are different, because the goal was to determine the set

of ground stations that provide the best result for each of the airplane's positions in the route under analysis. It is possible to conclude that the number of ground stations has a direct influence on the size of the uncertainty area, since as the number of ground stations increases the size of the uncertainty area decreases. As expected, as the distance between the airplane and the reference ground station decreases the error value also decreases.

Regarding the values of the error, 25 m, used for simulation purposes, it is not that accurate, since it was not possible to obtain the real value used by the manufacturer of the MLAT system used by NAV, rather being obtained through a trial and error process.

After analysing all the results, it is possible to validate some of the initial hypotheses:

- The bigger the number of ground stations, the wider the range of the system and the smaller the error associated with it.
- The terrain typology, the building surrounding the airports, the mountainous areas are all factors that influence system's performance and add to its error.
- Is necessary to use more ground stations as the airplane gets closer to the reference ground station, due to the spatial resolution problem. As the distance gets smaller, the 'opening' of the angle of the ground stations also gets smaller creating the necessity to use more ground stations.

In order to complete the study set up for this thesis the same type of analysis made for the Porto scenario should be done for the Madeira airport and for the South of Portugal, because these two areas are under the same conditions as the Porto airport, the WAM system not being fully implemented. These two analyses represent the future work that needs to be developed.

References

[Air07] Aires,A.P., *MLAT - Multilateration*, NAV, Lisbon, Portugal, Jan. 2013.

[Air15] https://www.thalesgroup.com/sites/default/files/asset/document/Global%20Surveillance%20Solution%20Booklet.pdf, Mar. 2015.

[Aue14] Auer,J., Kobelbauer,H., Schranz,H., Berndt,E., Langhaus,W., ‘‘ATM system integration of a nationwide wide-area multilateration system: Integrating WAM into a state-of-the-art ATM system including an ARTAS tracker’’, in *Proc. of ESAV’14 - Enhanced Surveillance of Aircraft and Vehicles (Tyrrhenian International Workshop on Digital Communications)*, Rome, Italy, Sep. 2014.

[Corr13] Correia,L.M., *Mobile Communications Systems Lecture Notes*, IST-UL, Lisbon, Portugal, Feb. 2013.

[Era10] Creativerge*, Multilateration Executive Reference Guide*, Public Report, Era Corporation and Creativerge, Virginia, US, 2010 (http://www.multilateration.com/downloads/MLAT-ADS-B-Reference-Guide.pdf).

[Euro07] Berends,J., *European Surveillance Strategy - Surveillance Seminar for the NAM/CAR/SAM Regions*, Eurocontrol, Port of Spain, Republic of Trinidad and Tobago, Jun. 2007.

[Euro13] Eurocontrol, *Annual Report 2013,* European Organisation for the Safety of Air Navigation, Brussels, Belgium, July 2013.

[Err06] Leeson,M.J., *Error Analysis for a Wide Area Multilateration System,* Report QinetiQ/C&IS/ADC/520896/7/19, QinetiQ , Farnborough, UK, Aug. 2006.

[Fil15a] NAV, *WAM System Flight Route File*, NAV, Lisbon, Portugal, Nov. 2015.

[Fil15b] NAV, *ADS-B System Flight Route File*, NAV, Lisbon, Portugal, Nov. 2015.

[Fil15c] NAV, *Ground Stations Coordinates File*, NAV, Lisbon, Portugal, May 2015.

[Gal08] Galati,G., Leonardi,M., Tosti,M., ‘‘Multilateration (Local and Wide area) as a distributed sensor system: Lower bounds of accuracy’’, in *Proc. of* EuRAD - *European Radar Conference*, Amsterdam, Netherlands, Oct. 2008.

[Gav15] Gaviria,I.A.M., *New strategies to improve multilateration systems in the air traffic control*, Editorial Universitat Politécnica de Valência, Valencia, Spain, 2015.

[ICAO07a] International Civil Aviation Organisation Asia and Pacific, *Guidance Material on Comparison of Surveillance Technologies (GMTS)*, Edition 1.0, Sep. 2007

(http://www.icao.int/APAC/Documents/edocs/cns/gmst_technology.pdf).

[ICAO07b] International Civil Aviation Organisation Asia and Pacific, *Multilateration (MLAT) Concept of Use*, Edition 1.0, Sep. 2007 (http://www.icao.int/APAC/Documents/edocs/cns/mlat_concept.pdf).

[Kon08] Konchenko,I., ‘‘Availability analysis of multilateration surveillance system in Kiev (Boryspil) airport’’, in *Proc. of MRRS’08 - Microwaves, Radar and Remote Sensing Symposium*, Kiev, Ukraine, Sep. 2008.

[Leo15] Leonardi,M., Bellapanni,L., Galati,G., *Synchronisation of Wide Area Multilateration Systems by GNSS Common View Technologies*, Tor Vergata University, Rome, Italy, May 2015 (http://www.researchgate.net/profile/Mauro_Leonardi/publication/239949412_Synchronisation_of_wide_area_multilateration_systems_by_GNSS_common_view_techniques/links/0deec51c407ae7bd65000000.pdf).

[Mat15a] MathWorks, MATLAB *2015a Documentation – Evaluating Goodness of Fit*, United States, Dec. 2015 (http://www.mathworks.com/help/curvefit/evaluating-goodness-of-fit.html?s_tid=gn_loc_drop#bq_5kwr-3).

[Mat15b] MathWorks, MATLAB *2015b Documentation – Curve Fitting Toolbox*, United States, Dec. 2015 (http://www.mathworks.com/help/curvefit/index.html).

[Mat16] http://mathworld.wolfram.com/Point-LineDistance2-Dimensional.html, Fev. 2016.

[Man11] Mantilla-Gaviria,I.A., Leonardi,M., Galati,G., Balbastre-T,J.V., and Reyes,E.d.l., ‘‘Improvement of multilateration (MLAT) accuracy and coverage for airport surveillance’’, in *Proc. of ESAV’11 - Enhanced Surveillance of Aircraft and Vehicles* (*Tyrrhenian International Workshop on Digital Communications*), Capri, Italy, Sep. 2011.

[Mor10] Morais,M.C., *Notas de Apoio da Disciplina de Probabilidades e Estatística*, IST-TUL, Lisboa, Portugal, Set. 2010.

[Mun09] Munoz, D., Lara,F.B., Vargas,C., Enriquez-Caldeira,R., *Position Location Techniques and Applications*, Academic Press, United States, May 2009.

[Ncbi15] http://www.ncbi.nlm.nih.gov/pmc/articles/PMC3673074/ , May 2015.

[Nev05] Neven,W.H.L., Quilter,T.J., Weedon,R. and Hogendoorn,R.A., *Wide Area Multilateration-Report on EATMPTRS 131/04 V1.1*, Eurocontrol – Institute of Air Navigation Services, Brussels, Belgium, Aug. 2005.

[Nil15] http://www.faa.gov/about/office_org/headquarters_offices/ato/service_units/techops/navservices/gnss/library/documents/APNT/media/WAM_WhitePaperFINAL_MITRE_v2.pdf, May 2015.

[Sie08] Siewerdt,E., *Air Surveillance. Automatic Dependent Surveillance, Radiofusion and Multilateration Desmitification* (in portuguese), VII Simpósio de Transporte Aéreo (VII

SITRAER), Rio de Janeiro, Brazil, 2008 (http://www.tgl.ufrj.br/viisitraer/pdf/426.pdf).

[Sta13] Stanzel,S., ‘‘Development of new and modified methods for data performance analysis under standard test conditions of wide area multilateration systems’’, in *Radar Symposium* , IEEE, Vol. 2, June 2013, pp. 567-572.